Available online at www.sciencedirect.com
SCIENCE DIRECT
Coordination Chemistry Reviews 250 (2006) 2059–2092
COORDINATION CHEMISTRY REVIEWS
www.elsevier.com/locate/ccr

Review

Lanthanide chalcogenolate complexes: Syntheses, structures and applications in organic chemistry

Hong-Xi Li [a], Yan-Jun Zhu [a], Mei-Ling Cheng [a], Zhi-Gang Ren [a], Jian-Ping Lang [a,b,*], Qi Shen [a]

[a] *Key Laboratory of Organic Synthesis of Jiangsu Province, School of Chemistry and Engineering, Suzhou University, Suzhou 215123, Jiangsu, PR China*
[b] *State Key Laboratory of Coordination Chemistry, Nanjing University, Nanjing 210093, Jiangsu, PR China*

Received 18 October 2005; accepted 9 February 2006
Available online 23 February 2006

Contents

Abbreviations: 2,2′-bipy, 2,2-bipyridine; 18c6, 18-crown-6; C_5H_4NOS, 1-hydroxy-2(1H)-pyridine thionato; C_8H_8, cyclooctatetraenyl; ε-CL, ε-caprolactone; C_5Me_5, 1,2,3,4,5-pentamethylcyclopentadienyl; Cp, cyclopentadienyl; dddt, 5,6-dihydro-1,4-dithiin-2,3-dithiolate; DME, dimethyloxyethane; dmit, 2-thioxo-1,3-dithiole-4,5-dithiolate; DMPE, $Me_2PCH_2CH_2PMe_2$; DMSO, dimethylsulfoxide; DTC, 2,2-dimethyltrimethylene carbonate; ETMA, ethylthiomaltolato; HMPA, hexamethylphosphoric amide; Ln, any of the following elements: scandium, yttrium, lanthanum or the lanthanides; Ph, phenyl; phen, 1,10-phenanthroline; py, pyridine; ROP, ring opening polymerization; SC_4H_5N, 2-thiopyridyl; SC_7H_4NS, benzothiazole-2-thiolate; THF, tetrahydrofuran; TMA, thiomaltolato; TMEDA, $Me_2NCH_2CH_2NMe_2$; $Tp^{Me,Me}$, tri-3,5-dimethylpyrazolyborate; $Tp^{Me,Me,4\text{-}Et}$, tri-(3,5-dimethyl-4-ethyl)pyrazolyborate

* Corresponding author. Tel.: +86 512 65882865; fax: +86 512 65880089.
E-mail address: jplang@suda.edu.cn (J.-P. Lang).

0010-8545/$ – see front matter
doi:10.1016/j.ccr.2006.02.005

Abstract

The chemistry of lanthanide chalcogenolate complexes has expanded dramatically in the recent years. This review summarized the syntheses and crystal structures of the lanthanide chalcogenolate complexes and their applications in organic chemistry. Four methods for the synthesis of lanthanide chalcogenolate complexes were outlined: protonolysis, metathesis, oxidation–reduction, and insertion reaction. The lanthanide chalcogenolate complexes were classified according to the ancillary ligands coordinated to lanthanide atoms and the number of lanthanide atoms, and some specific structures were briefly described. The reactivity and catalytical property of some lanthanide chalcogenolate complexes in organic and polymer synthesis along with their luminescent properties are highlighted.

Keywords: Lanthanide complex; Chalcogenolate complex; Synthesis; Structure; Reactivity; Catalysis

1. Introduction

Lanthanide chalcogenolate complexes continue to attract considerable attention due to their fascinating structural chemistry [1–5] and their potential applications in the preparation of organic or organolanthanide complexes [6–11], new advanced materials [12–24], and catalysis [25–36]. It is a challenge to synthesize lanthanide chalcogenolates due to the nature of the bonding between these electropositive lanthanide metal ions and the less electronegative chalcogenolates. In the past decades, some synthetic approaches to lanthanide chalcogenolates have been developed. Most lanthanide chalcogenolates were prepared by oxidative reactions of REER with lanthanide(II) complexes [37–54] or lanthanide metals in the presence of a catalyst [55–76], or by reactions of lanthanide chalcogenolates with elemental E (E = S, Se, Te) or cleavage reactions of the C–Se bond [77–87], or by protonolysis reactions of preformed lanthanide complexes with thiols/selenols/tellurols REH (E = S, Se, Te) [88–107], or by salt metathesis reactions of a lanthanide halide with an alkali metal chalcogenolate [108–130], or by insertion reactions of E into the Ln–C bond [131–137]. A large number of monomeric, oligomeric and polymeric lanthanide chalcogenolates have been isolated based on the methods mentioned above. In 1998, Nief gave a full account of complexes containing Ln–E bonds [1]. Therefore, the present review mainly concentrates on the developments of lanthanide chalcogenolate complexes during the 1998–2005 period. In this paper, we summarize general routes to lanthanide chalcogenolate compounds and outline their pertinent structural characteristics. Although many chalcogen-rich lanthanide clusters containing only E^{2-} and EE^{2-} species [138–144] have been reported, we will not include them because of the scope and the length of this review. However, we incorporate those containing both chalcogenolates and chalcogenides into this paper when necessary. The reactivity and catalytic properties of lanthanide chalcogenolate compounds in the syntheses of some organic and polymeric complexes are introduced. The luminescent properties of lanthanide chalcogenolate compounds are briefly outlined. Those related to the utilization of lanthanide chalcogenolates as precursors to new lanthanide chalcogenides [8,64,70,75,79,80,87,103–105,117,118] are omitted, although they are certainly very important subjects.

2. Methods of preparation

There are four typical methods for the synthesis of lanthanide chalcogenolate complexes that have been isolated: protonolysis reaction, metathesis reaction, oxidation–reduction reaction, and insertion reaction. In the following subsections, we describe the characteristics of each method.

2.1. Protonolysis reaction

The protonolysis reaction is a useful approach to prepare lanthanide chalcogenolate complexes, which may be difficult to prepare by routine methods. As shown in Eqs. (1)–(3), interaction of $LnCp_3$ with thiol HSR afforded organolanthanide thiolate complexes such as $[(Cp)_2Ln(\mu\text{-}SR)]_2$ (R = Pr^n, Bu^n, Ln = Dy, Yb; R = Et, Ln = Y, Yb, Er, Sm; R = $C_6H_4(NH_2)$-2, Ln = Yb), $[(C_5H_4Me)_2Ce(\mu\text{-}SBu^t)]_2$, $[(C_5H_4Bu^t)_2Ce(\mu\text{-}SR)]_2$ (R = Pr^i, Ph), $[(C_5H_4Me)_2Ln(\mu\text{-}SPh)(THF)]_2$ (Ln = La, Nd, Sm) [8,9,35,91–94]. In the case of bulky thiols, a similar procedure yielded only monomeric organolanthanide thiolates. For instance, treatment of $YbCp_3$ with $HSC_6H_2(CF_3)_3$-2,4,6 resulted in the formation of $(THF)Yb(Cp)_2SC_6H_2(CF_3)_3$-2,4,6 [95]. Complexes $(THF)Yb(Cp)_2[SC_6H_4(NH_2)$-4] and $(THF)Ln(Cp)_2(SC_7H_4S)$ (Ln = Y, Sm, Tm, Yb, Dy) (Eq. (4)) [96,97] were prepared by reactions of $LnCp_3$ with chelating thiol ligands $HSC_6H_4(NH_2)$-4 or HSC_7H_4S. Compounds $Cp_2Ln(NEPPh_2)_2$ (Ln = Y, La, Gd, Er, Yb, E = Se; Ln = Y, Yb, E = S) [98,99] could be readily formed by reactions of Cp_3Ln

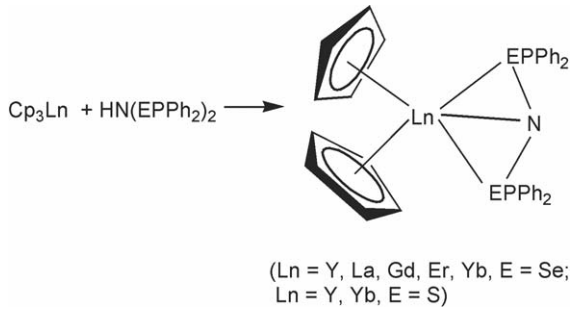

Scheme 1.

with $HN(EPPh_2)_2$ (Scheme 1):

$$(Cp)_3Ln + HSR \rightarrow [(Cp)_2Ln(\mu\text{-}SR)]_2 \quad (R = Pr^n, Bu^n, Ln = Dy, Yb; \quad R = Et, \quad Ln = Y, Yb, Er, Sm; \quad R = C_6H_4(H_2N)\text{-}2, \quad Ln = Yb) \tag{1}$$

$$(C_5H_4R)_3Ce + HSR' \rightarrow [(C_5H_4Me)_2Ce(\mu\text{-}SBu^t)]_2 \quad (R = Me, \quad R' = Bu^t; \quad R = Bu^t, \quad R' = Pr^i, Ph) \tag{2}$$

$$(C_5H_4Me)_3Ln + HSPh \rightarrow [(C_5H_4Me)_2Ln(\mu\text{-}SPh)(THF)]_2 \quad (Ln = La, Nd, Sm) \tag{3}$$

$$(Cp)_3Ln + HSR \rightarrow (Cp)_2Ln(SR)(THF) \quad (Ln = Yb, SR = SC_6H_2(CF_3)_3\text{-}2, 4, 6, SC_6H_4(H_2N)\text{-}4; \quad Ln = Y, Sm, Tm, Yb, Dy) \tag{4}$$

Mixing amidolanthanide complexes $Ln[N(SiMe_3)_2]_3$ with thiols also gave insoluble lanthanide thiolate polymeric materials at room temperature. For example, interaction of $Ln[N(SiMe_3)_2]_3$ (Ln = Ce, Pr, Nd, Eu, Yb, Y) with 3 equiv. of $HSBu^t$ in toluene led to the rapid formation of an insoluble polymeric material [101]. There are some ways to tackle this problem to avoid the formation of insoluble phases. At low temperature (e.g. −23 °C), addition of equimolar $HSBu^t$ to a solution of $Eu[N(SiMe_3)_2]_3$ in toluene/THF produced an aminolanthanoid thiolate complex $[\{(Me_3Si)_2N\}_2Eu(\mu\text{-}SBu^t)]_2$ [107]. In the presence of strong donor ligand (2,2′-bipy), interaction of 3 equiv. of $HSBu^t$ with a toluene solution of $Ln[N(SiMe_3)_2]_3$ afforded soluble complexes $[\{(2,2'\text{-bipy})Ln(SBu^t)_2\}(\mu\text{-}SBu^t)]_2$ (Ln = Yb, Y) (Eq. (5)) [101]. In the case of bulky thiols (e.g. $HSC_6H_2Bu^t_3$-2,4,6, or $HESi(SiMe_3)_3$ (E = Se, Te)), a similar reaction resulted in the formation of mononuclear complexes $Sm(SC_6H_2Bu^t_3\text{-}2,4,6)_3$, $(DME)_2Yb(SC_6H_2Bu^t_3\text{-}2,4,6)_2$ [102], $Ln[ESi(SiMe_3)_3]_3$ (E = Se, Ln = La, Y; E = Te, Ln = La, Ce), $(THF)_2Ln[SeSi(SiMe_3)_3]_2$ (Ln = La, Sm, Yb), and $Ln[ESi(SiMe_3)_3]_2$ (E = Se, Te; Ln = Sm, Eu, Yb) (Eqs. (6)–(11)) [103–105].

Using TMEDA or DMPE as strongly chelating ligands, a family of lanthanide selenolates and tellurolates with an empirical formula $(TMEDA)_2Ln[ESi(SiMe_3)_3]_2$ (Ln = Yb, Eu, Sm; E = Se, Te), $(DMPE)_2Ln[TeSi(SiMe_3)_3]_3$ (Ln = La, Ce, Y) (Eqs. (12) and (13)) and $[\{Eu(ESi(SiMe_3)_3)_2(DMPE)_2\}_2(\mu\text{-}DMPE)]$ (E = Se, Te) were prepared by protonolysis reactions of $Ln[N(SiMe_3)_2]_2$ or $Ln[N(SiMe_3)_2]_3$ with $HESi(SiMe_3)_3$ (E = Se, Te) (Scheme 2) [103–105]. Compounds $Ln_5Te_3[TeSi(SiMe_3)_3]$ (Ln = La, Ce) [104,105] were isolated from protolysis reaction of $Ln[N(SiMe_3)_2]_3$ and $HTeSi(SiMe_3)_3$ and the cleavage of the Te–Si bond of $TeSi(SiMe_3)_3$:

$$Yb[N(SiMe_3)_2]_3 + HSBu^t + bipy \rightarrow [Yb(SBu^t)_2(\mu\text{-}SBu^t)(bipy)]_2, \quad bipy = 2,2'\text{-bipyridine} \tag{5}$$

$$[Sm\{CH(SiMe_3)_2\}_3] + 3ArSH \rightarrow [Sm(SAr)_3] \tag{6}$$

$$(DME)_2Yb[N(SiMe_3)_2]_2 + 2ArSH \rightarrow [(DME)_2Yb(SAr)_2] \quad (Ar = C_6H_2Bu^t_3\text{-}2, 4, 6) \tag{7}$$

$$Ln[N(SiMe_3)_2]_3 + 3HSeSi(SiMe_3)_3 \rightarrow Ln[SeSi(SiMe_3)_3]_3 \quad (Ln = La, Y) \tag{8}$$

$$Ln[N(SiMe_3)_2]_3 + 3HSeSi(SiMe_3)_3 + 2THF \rightarrow (THF)_2Ln[SeSi(SiMe_3)_3]_3 \quad (Ln = La, Sm, Yb) \tag{9}$$

$$Ln[N(SiMe_3)_2]_3 + 3HTeSi(SiMe_3)_3 \rightarrow Ln[TeSi(SiMe_3)_3]_3 \quad (Ln = La, Ce) \tag{10}$$

$$Ln[N(SiMe_3)_2]_3 + 3HESi(SiMe_3)_3 \rightarrow Ln[ESi(SiMe_3)_3]_2 + 0.5\,[ESi(SiMe_3)_3]_2 \quad (E = Se, Te; \quad Ln = Sm, Eu, Yb) \tag{11}$$

$$(THF)_2Ln[N(SiMe_3)_2]_2 + 2HESi(SiMe_3)_3 \xrightarrow{TMEDA} (TMEDA)_2Ln[ESi(SiMe_3)_3]_2 \quad (E = Se, Te; \quad Ln = Yb, Eu, Sm) \tag{12}$$

$$Ln[N(SiMe_3)_2]_3 + 3HTeSi(SiMe_3)_3 + DMPE \rightarrow (DMPE)_2Ln[TeSi(SiMe_3)_3]_3 \quad (Ln = La, Ce, Y) \tag{13}$$

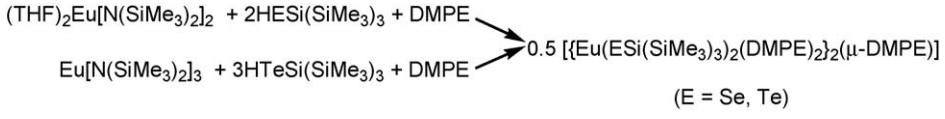

Scheme 2.

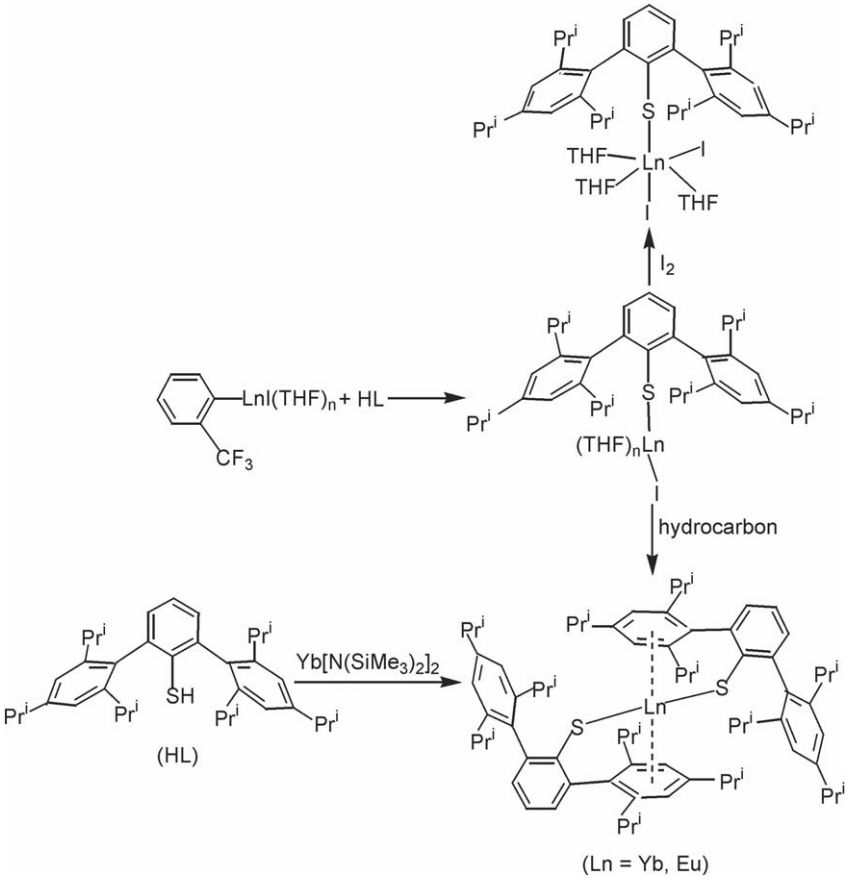

Scheme 3.

As shown in Scheme 3, treatment of $Yb[N(SiMe_3)_2]_2$ with the more bulky thiol $HSC_6H_3(C_6H_2Pr^i_3\text{-}2,4,6)_2\text{-}2,6$ yielded the purple ytterbium(II) thiolate compound $Yb[SC_6H_3(C_6H_2Pr^i_3\text{-}2,4,6)_2\text{-}2,6]_2$. This compound was further coordinated by two DME ligands to give a yellow compound $(DME)_2Yb[SC_6H_3(C_6H_2Pr^i_3\text{-}2,4,6)_2\text{-}2,6]_2$. The Grignard-analogous aryllanthanide(II) iodide compound $[C_6H_4(CF_3)\text{-}2]LnI$ was instantly protolysed by the thiol $HSC_6H_3(C_6H_2Pr^i_3\text{-}2,4,6)_2\text{-}2,6$ to produce a thiolatolanthanide(II) iodide $(THF)_nLn[SC_6H_3(C_6H_2Pr^i_3\text{-}2,4,6)_2\text{-}2,6]I$, which could be converted to $Ln[SC_6H_3(C_6H_2Pr^i_3\text{-}2,4,6)_2\text{-}2,6]_2$ (Ln = Yb, Eu) by removal of THF and iodine. Furthermore, the oxidation reaction of $(THF)_nYb[SC_6H_3(C_6H_2Pr^i_3\text{-}2,4,6)_2\text{-}2,6]I$ with I_2 generated a diiodo(thiolato)ytterbium(III) complex $(THF)_3YbI_2[SC_6H_3(C_6H_2Pr^i_3\text{-}2,4,6)_2\text{-}2,6]$ in a good yield [106].

As described in Eqs. (14)–(16), treatment of some lanthanide amide complexes containing a bridging Cl^- and a $[Li(THF)_3]^+$ unit, $[(Me_3Si)_2N]_3Ln(\mu\text{-}Cl)Li(THF)_3$ (Ln = Pr, Nd, Sm) with equimolar benzenthiol HSPh produced three soluble lanthanide thiolates $[\{(Me_3Si)_2N\}_2(\mu\text{-}SPh)Pr(\mu\text{-}SPh)Li(THF)_2]_\infty$, $Li[\{(Me_3Si)_2N\}_4(\mu_4\text{-}Cl)Nd_4(\mu\text{-}SPh)_8]$, and $[\{(Me_3Si)_2N\}_4(\mu_4\text{-}Cl)Sm_4(\mu\text{-}SPh)_4(\mu_3\text{-}Cl)_4Li(THF)]$ [36]. In these reactions, lithium and chloride ions were essential for the formation of soluble phases from thiolysis reactions with Ln silylamides:

$$[(Me_3Si)_2N]_3Pr(\mu\text{-}Cl)Li(THF)_3 + HSPh \rightarrow [\{(Me_3Si)_2N\}_2(\mu\text{-}SPh)Pr(\mu\text{-}SPh)Li(THF)_2]_n + [\{((Me_3Si)_2N)_2Pr(\mu'\text{-}Cl)Li(THF)_3\}(\mu\text{-}Cl)]_2 \quad (14)$$

$$[(Me_3Si)_2N]_3Nd(\mu\text{-}Cl)Li(THF)_3 + HSPh \rightarrow Li[\{(Me_3Si)_2N\}_4(\mu_4\text{-}Cl)Nd_4(\mu\text{-}SPh)_8] \quad (15)$$

$$[(Me_3Si)_2N]_3Sm(\mu\text{-}Cl)Li(THF)_3 + HSPh \rightarrow [\{(Me_3Si)_2N\}_4(\mu_4\text{-}Cl)Sm_4(\mu\text{-}SPh)_4(\mu_3\text{-}Cl)_4Li(THF)] + [\{((Me_3Si)_2N)_2Sm(\mu'\text{-}Cl)Li(THF)_2\}(\mu_3\text{-}Cl)]_2 \quad (16)$$

2.2. Salt metathesis reaction

Compound $[Li(TMEDA)_2][(Me_5C_5)_2Sm(\mu\text{-}SCCPh)_2]$ [108] was achieved by salt metathesis reaction of $(Me_5C_5)_2Sm(\mu\text{-}Cl)_2Li(Et_2O)_2$ with LiSCCPh (Eq. (17)). Treatment of $[Li(THF)_4]_2[(THF)_3LiE_2C_2B_{10}H_{10}Li(THF)]_2$ with $Cp'_2Ln(\mu\text{-}Cl)_2Li(THF)_2$ or $[Cp_2Ln(\mu\text{-}Cl)]_2$ in THF afforded the ionic binuclear *o*-carborane dichalcogenolate bridged complexes $[Li(THF)_4][Cp'_2LnE_2C_2B_{10}H_{10}]_2$ (E = S, Se; Ln = Nd, Gd, Dy, Er, Yb; Cp′ = Cp, $C_5H_4Bu^t$, $C_5H_3Bu^t_2$)

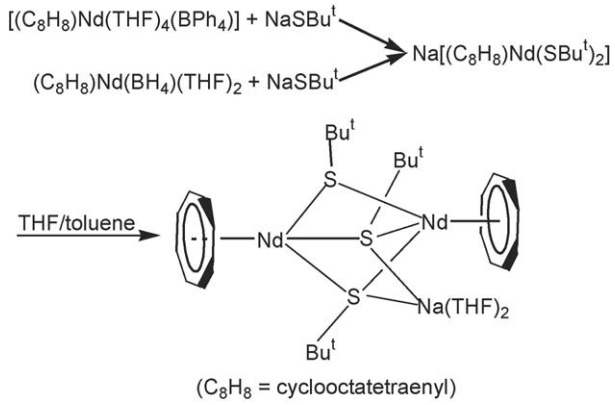

Scheme 4.

(Eq. (18)) [110–112]:

$$(Me_5C_5)_2Sm(\mu\text{-}Cl)Li(OEt_2)_2 \xrightarrow[THF]{LiSCCPh} \xrightarrow[Et_2O]{TMEDA} [Li(TMEDA)_2][(Me_5C_5)_2Sm(\mu\text{-}SCCPh)_2] \quad (17)$$

$$Cp'_2Ln(\mu\text{-}Cl)_2Li(THF)_2 \text{ or } [Cp_2Ln(\mu\text{-}Cl)]_2 + [(THF)_3LiE_2C_2B_{10}H_{10}Li(THF)]_2 \rightarrow [Li(THF)_4]_2[Cp'_2LnE_2C_2B_{10}H_{10}]_2$$
$$(E = S, Se; \quad Ln = Nd, Gd, Dy, Er, Yb; \quad Cp' = Cp, C_5H_4Bu^t, C_5H_3Bu^t_2) \quad (18)$$

Scheme 4 shows that the cyclooctatetraenyl neodymium thiolate compound $Na[(C_8H_8)Nd(SBu^t)_2]$ was prepared by treatment of $(C_8H_8)Nd(BH_4)(THF)_2$ or $[(C_8H_8)Nd(THF)_4(BPh_4)]$ with 2 equiv. of $NaSBu^t$ in THF. Crystallization of $Na[(C_8H_8)Nd(SBu^t)_2]$ from THF/toluene mixture formed pale green crystals of $[\{(C_8H_8)Nd\}_2(\mu\text{-}SBu^t)(\mu_3\text{-}SBu^t)_2Na(THF)_2]$ [115]. Complex $Sm(C_5H_4NOS)_3(DMSO)_3$ was obtained by reaction of $Sm(CH_3CO_2)_3$ with NaC_5H_4NOS (Eq. (19)) [123]:

$$Sm(CH_3CO_2)_3 + 3Na(C_5H_4NOS) \longrightarrow Sm(C_5H_4NOS)_3(DMSO)_3$$
(C_5H_4NOS = 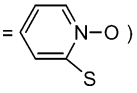) (19)

Recently, much attention has been drawn to the diversity of the main group and d-block transition metal complexes of dithiolene ligands, which exhibit interesting structural chemistry and behave as molecular precursors of conducting, magnetic, and optical materials [124,125]. Some dithiolene ligands have also been introduced into the chemistry of lanthanide chalcogenolates [126–129]. For example, addition of K_2dmit to $LnCl_3$ in the presence of phen gave the mono-(dithiolene) complexes $K_2[LnCl_3(dmit)(phen)_2]$ (Ln = La, Nd, Sm, Gd, Er, Y) (Eq. (20)) [126]. Compound $Gd_2(C_2S_4)_3$ was prepared by reaction of $GdCl_3$ and the tetraethylammonium salt of tetrathiooxalate [127]. According to Eq. (21), reaction of $[Ln(C_5Me_5)_2Cl_2K]$ with K_2dddt readily produced dimeric lanthanide complexes $[\{Ln(C_5Me_5)_2(dddt)K(THF)_2\}_2]$ (Ln = Ce, Nd), which could be transformed into salts $[K(15\text{-crown-}5)_2][Ln(C_5Me_5)_2(dddt)]$ (Ln = Ce, Nd) in the presence of 15-crown-5 [128]:

$$LnCl_3 + 1,10\text{-phenanthroline} + K_2dmit \xrightarrow{THF} K_2[LnCl_3(dmit)(phen)_2]$$
(Ln = La, Nd, Sm, Gd, Er, Y; $dimt^{2-}$ = 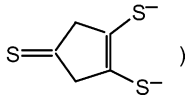) (20)

$$[Ln(C_5Me_5)_2Cl_2K] + K_2dddt \xrightarrow{THF} [\{Ln(C_5Me_5)_2(dddt)K(THF)_2\}_2] \xrightarrow[THF]{15\text{-crown-}5} [K(15\text{-crown-}5)_2][Ln(C_5Me_5)_2(dddt)]$$
(Ln = Ce Nd; $dddt^{2-}$ = 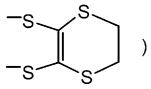) (21)

As shown in Scheme 5, reaction of $Nd(BH_4)_3(THF)_3$ with Na_2dddt and excess 18-crown-6 (18c6) in pyridine produced orange crystals of $[Na(18c6)(py)_2]_2[Na(18c6)(py)][Nd(dddt)_3(py)]$ and green crystals of $[\{Na(18c6)(py)_2\}_{0.5}\{Na(18c6)(py)_{1.5}\}\{Na_{1.5}Nd(dddt)_3\}]_\infty$. Compound $[Na_3(THF)_{1.5}Nd(dddt)_3]$ and 10 equiv. of 18-crown-6 were mixed in THF to afford a polymer $[\{Na_3(18c6)_{1.5}Nd(dddt)_3(THF)\}]_\infty$. The potassium salt of the dddt anion reacted with $Nd(BH_4)_3(THF)_3$ in THF to form a green powder. If the green powder was dissolved in pyridine in the presence of 3–10 equiv. of crown ether 18-crown-6, green crystals of $[K_3(18c6)_{1.5}Nd(dddt)_3(py)]_\infty$ were isolated. Mixing of $Ce(BH_4)_3(THF)_3$ with Na_2dddt in THF followed by addition of 3–10 equiv. of 18-crown-6 produced a polymer $[Na_2(18c6)Na(py)_2Ce(dddt)_3(py)]_\infty$ [129].

A family of lanthanide complexes with mixed O, S anionic ligands, e.g. $Ln(TMA)_3{\cdot}xH_2O$ (Ln = La, $x = 2$; Ln = Ho, $x = 1.5$), $Ln(ETMA)_3{\cdot}xH_2O$ (Ln = Pr, Sm, $x = 0.5$; Ln = La, $x = 1$; Ln = Nd, Ho, $x = 2$; Ln = Gd, $x = 2.5$), $LnL_2(OH){\cdot}H_2O$ (Ln = Pr, Nd, Gd, L = TMA; Ln = Sm, L = ETMA), and $Ln(TMA)_3$ (Ln = Sm, Lu) [130], were synthesized by reacting the respective metal perchlorates with two pyranthiones, HTMA and HETMA (Scheme 6), in the presence of NaOH in ethanol at room temperature.

2.3. Oxidation–reduction reaction

According to the nature of the starting lanthanide complexes, this method of preparation may be sub-classified into oxidation reaction of divalent lanthanocene, reaction of elemental lanthanide with REER, transmercuration reaction, reaction of elemental chalcogenide with lanthanide chalcogenolates, and cleavage reaction of Se–C bond.

2.3.1. Oxidation reaction of divalent lanthanocene complexes

The oxidation reaction of the divalent lanthanide complexes with organic dichalcogenides (REER) has proven to be a powerful method for the synthesis of a wide range

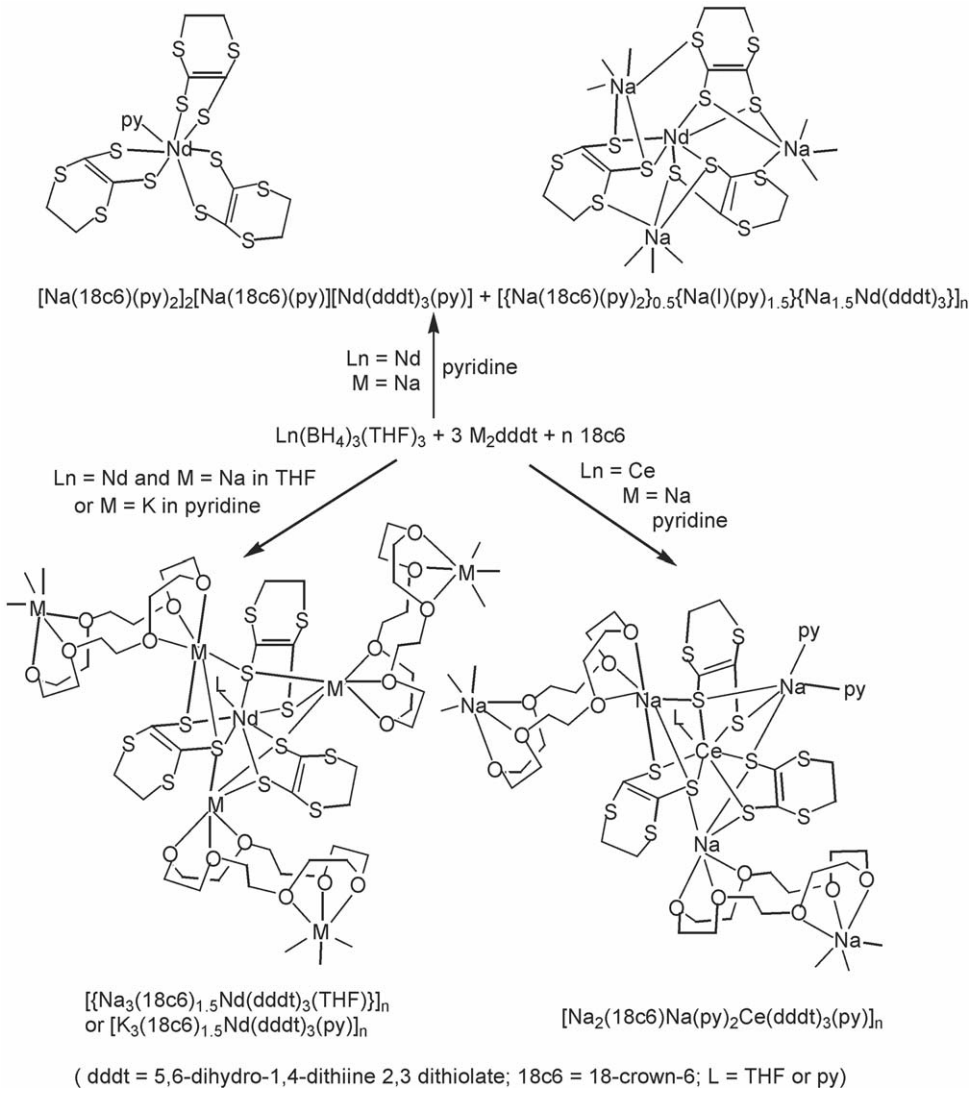

Scheme 5.

of organolanthanide chalcogenolate complexes. For example, some bis–Me_5C_5 monomeric samarium chalcogenlate complexes such as $(Me_5C_5)_2Sm(EPh)(THF)$ (E = S, Se, Te), were prepared from reactions of the solvated divalent lanthanide complexes $(Me_5C_5)_2Sm(THF)_2$ with PhEEPh (E = Se, Te) (Eq. (22)) [41]. The dimeric complexes $[(C_5Me_5)_2Sm(\mu\text{-}EPh)]_2$ (E = S, Se, Te) were obtained by reaction of $(C_5Me_5)_2Sm(II)$ with PhEEPh. The thiolate derivative $[(C_5Me_5)_2Sm(\mu\text{-}SPh)]_2$ was also prepared through reaction of $[(C_5Me_5)_2Sm][(Ph)_2BPh_2]$ and KSPh (Scheme 7) [41]:

$$(Me_5C_5)_2Sm(THF)_2 + Ph_2E_2 \rightarrow (Me_5C_5)_2Sm(EPh)(THF) \quad (E = S, Se, Te) \qquad (22)$$

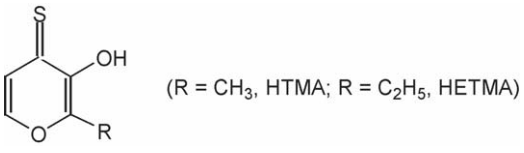

Scheme 6.

Bulky heteroallylic ligands such as benzamidinate anion $[RC_6H_4C(NSiMe_3)_2]^-$ have recently been established as useful alternatives to the cyclopentadienyl ligands [145–150]. Thus, the ytterbium(II) benzamidinate $[RC_6H_4C(NSiMe_3)_2]_2Yb(THF)_2$ may be regarded as an analogue of the metallocene complex $(Me_5C_5)_2Yb(OEt_2)_2$. As shown in Scheme 8, compounds $[PhC(NSiMe_3)_2]_2Yb(SeR)(THF)$ (R = Ph, $C_6H_2Me_3$-2,4,6) [43,44] were obtained by reactions of silylated Yb(II) benzamidinate $(THF)_2Yb[PhC(NSiMe_3)_2]_2$ with RSeSeR. The Yb(III) benzamidinate chalcogenolate complex $[4\text{-}MeOC_6H_4C(NMe)_2]_2Yb(TeC_6H_2Me_3\text{-}2,4,6)(THF)$ [44] could be obtained in a similar synthetic route.

The hydrotris(pyrazolyl)borate ligands are most useful nitrogen-based ligands, which are capable of stabilizing

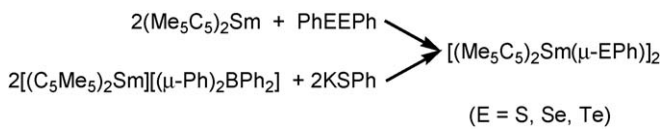

Scheme 7.

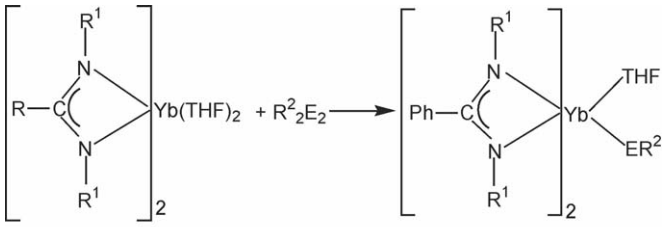

Scheme 8.

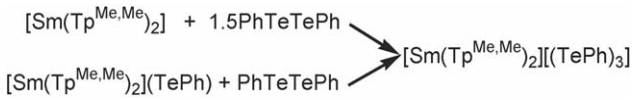

Scheme 9.

non-cyclopentadienyl lanthanide complexes [151–155]. The $Tp^{Me,Me}$ has been successfully employed in the synthesis of soluble and crystalline monomeric lanthanide chalcogenolates. The reductive cleavage of PhSSPh by samarium(II) with two pyrazolylborates as ancillary ligands $[Sm(Tp^{Me,Me})_2]$ led to the formation of $[Sm(Tp^{Me,Me})_2SPh]$. Other analogues $[Sm(Tp^{Me,Me})_2ER]$ (ER = SC_6H_4Me-4, SCH_2Ph, SePh, $SeC_6H_4Bu^t$-4, $SeCH_2Ph$, SeC_6H_4OMe-4, TePh) (Eqs. (23) and (24)) [45] and $[Sm(Tp^{Me,Me})_2(EC_5H_4N)]$ (E = S, Se) (Eq. (25)) [46] could be isolated in a similar way. Addition of a 1.5-fold excess of PhTeTePh to $[Sm(Tp^{Me,Me})_2]$ resulted in the formation of deep red complex $[Sm(Tp^{Me,Me})_2][(TePh)_3]$ [5]. This compound could also be prepared by addition of PhTeTePh to a solution of $[Sm(Tp^{Me,Me})_2TePh]$ (Scheme 9). Moreover, compounds $[Sm(Tp^{Me,Me,4\text{-}Et})_2ER]$ (ER = SPh, SCH_2Ph, $SeC_6H_4Bu^t$-4, TePh) were obtained in NMR-scale reactions starting from the toluene-soluble $[Sm(Tp^{Me,Me,4\text{-}Et})_2]$ and the corresponding REER ligands (Eq. (26)) [45,47]:

$$[Sm(Tp^{Me,Me})_2] + REER \rightarrow [Sm(Tp^{Me,Me})_2]ER$$
$$(E = S,\quad R = Ph,\ C_6H_4Me\text{-}4,\ CH_2Ph;\quad E = Se,$$
$$R = Ph,\ C_6H_4Bu^t\text{-}4,\ C_6H_4OMe\text{-}4,\ CH_2Ph) \qquad (23)$$

$$[Sm(Tp^{Me,Me})_2] + PhTeTePh \rightarrow [Sm(Tp^{Me,Me})_2TePh] \qquad (24)$$

$$[Sm(Tp^{Me,Me})_2] + [(C_5H_4N)E_2]$$
$$\rightarrow [Sm(Tp^{Me,Me})_2(EC_5H_4N)] \quad (E = S,\ Se) \qquad (25)$$

$$[Sm(Tp^{Me,Me,Et\text{-}4})_2] + REER \rightarrow [Sm(Tp^{Me,Me,Et\text{-}4})_2]ER$$
$$(E = S,\ R = Ph,\ CH_2Ph;\quad E = Se,\quad R = C_6H_4Bu^t\text{-}4;$$
$$E = Te,\quad R = Ph) \qquad (26)$$

As illustrated in Eq. (27), the dinuclear samarium(III) thiolate complexes $[(THF)_3I_2Sm(\mu\text{-}SR)]_2$ (R = Ph, $C_6H_4(Me_2N)$-4) [49] were obtained by direct reaction of SmI_2 in THF with two dialkyl disulfides in high yields:

$$SmI_2(THF)_2 + RSSR \rightarrow [(THF)_3I_2Sm(\mu\text{-}SR)]_2$$
$$(R = Ph,\ C_6H_4(Me_2N)\text{-}4) \qquad (27)$$

The divalent ytterbium compound $(C_5Me_5)_2Yb$ reacts with Ph_3PS, As_2S_3, or COS, Ph_3PSe, elemental Se, $Bu^n{}_3PTe$, or elemental Te, to give rise to the chalcogenide-bridged complexes $[(C_5Me_5)_2Yb]_2[\mu\text{-}E]$ (E = S, Se, or Te) [50]. A set of bis(pentamethylcyclopentadienyl)samarium sulfide or selenide or telluride complexes such as $[(C_5Me_5)_2Sm(THF)]_2(\mu\text{-}E)$ (E = S, Se, Te), $[(C_5Me_5)Sm]_2(E_3)(THF)$ (E = S, Se, Te), $[(C_5Me_5)_2Sm]_2(Se_aTe_b)(THF)$ ($a+b=3$), $[(C_5Me_5)_2Sm]_2(\mu\text{-}\eta^2\text{:}\eta^2\text{-}Te_2)$, and $[\{(C_5Me_5)Sm\}_6Se_{11}]$ were prepared by similar synthetic systems $(C_5Me_5)_2Sm/Te$, $(C_5Me_5)_2Sm/Se$ (or $Ph_3P=Se$), or $(C_5Me_5)_2Sm/S$ ($Ph_3P=S$) [51–53]. Reactions of $(C_5Me_5)_3Nd$ with $Ph_3P=Se$ resulted in the formation of $[(C_5Me_5)_2Nd]_2(\mu\text{-}\eta^2\text{:}\eta^2\text{-}Se_2)$ [54].

2.3.2. Reaction of elemental lanthanide and REER

It is difficult to prepare lanthanide chalcogenolates by direct reaction of elemental lanthanide with REER. In some related reactions, their activation could be achieved by the reversible complexation of the lanthanide metal to Ph_2CO [6], MeI [7], I_2 [55,56], or $HgCl_2$ [61].

The preparation of the dimeric mono(cyclooctatetraenyl)samarium(III) thiolate and selenolate complexes $[Sm(C_8H_8)(\mu\text{-}ER)(THF)_n]_2$ [58,59] was achieved by an approach similar to that shown in Scheme 10 using diaryl disulfides or diselennides REER as oxidizing agents instead of iodine. Such a reaction could be accelerated by activating the Sm metal surface with catalytic amounts of iodine in THF. The compound $[Sm(C_8H_8)(\mu\text{-}SPh)(THF)]_2$ was also prepared by reaction of $[Sm(C_8H_8)(THF)]_n$ with PhSSPh (Scheme 10). In the case of sterically demanding or potentially chelating thiolate ligands [60], a similar procedure was employed to make monomeric organosamarium thiolates. For example, mixing samarium metal, 1,3,5,7-cyclooctatetraene and $(C_6H_2Pr^i{}_3\text{-}2,4,6)_2S_2$ in HMPA resulted in the formation of the dark red thiolate compound $[(HMPA)_2Sm(C_8H_8)(SC_6H_2Pr^i{}_3\text{-}2,4,6)]$. In addition, the heterogeneous reaction of dipyridyl disulfide with Sm could also produce the red monomeric organosamarium thiolate compound $[(HMPA)_2Sm(C_8H_8)(SC_4H_5N)]$ (Scheme 11).

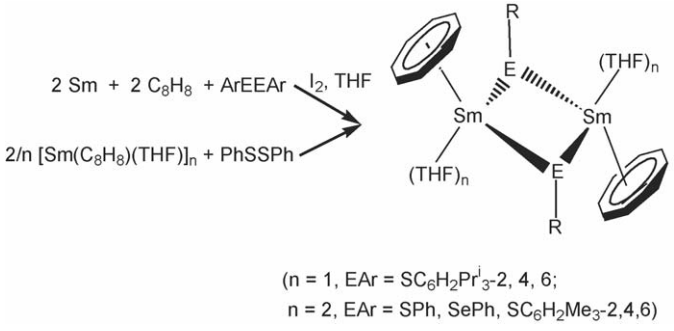

Scheme 10.

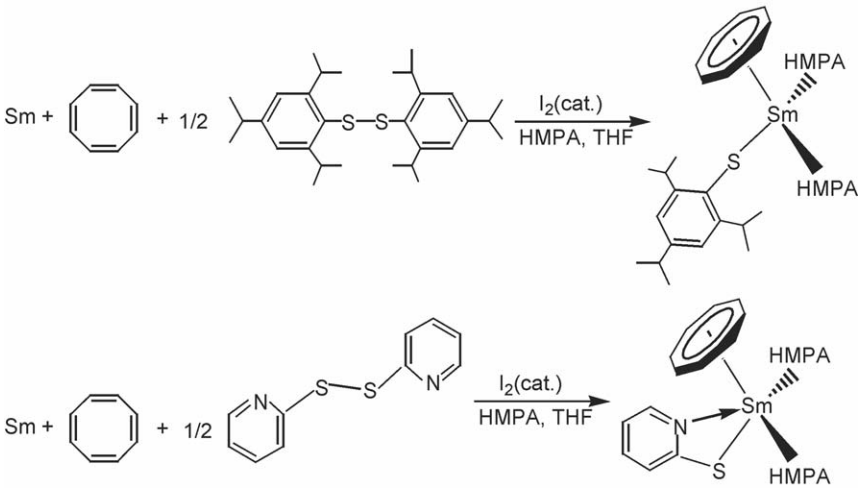

Scheme 11.

Using liquid ammonia as a solvent, reaction between Yb metal and PhEEPh (E = S, Se, Te) could form divalent ytterbium chalcogenolates, which could be isolated as the pyridine-coordinated complexes $(py)_4Yb(SPh)_2$, $(py)_4Yb(SePh)_2$, and $(py)_5Yb(TePh)_2$ (Eqs. (28) and (29)) [62]. The latter could also be prepared by the salt elimination reaction of $YbCl_3$ with NaTePh. The tellurolate compound $(py)_5Sm(TePh)_2$ (Eq. (30)) was prepared in a good yield from direct reduction of PhTeTePh with Sm metal in pyridine [63]:

$$Yb + PhEEPh \xrightarrow{\text{liquid } NH_3} \xrightarrow{py} (py)_4Yb(EPh)_2 \quad (E = S, Se) \tag{28}$$

$$Yb + PhTeTePh \xrightarrow{\text{liquid } NH_3} \xrightarrow{py} (py)_5Yb(TePh)_2 \tag{29}$$

$$Sm + PhTeTePh \xrightarrow{py} (py)_5Sm(TePh)_2 \tag{30}$$

2.3.3. Reaction of Ln/M amalgam with REER and trans-metallation reaction

A family of lanthanide benzenechalcogenolate complexes $(py)_4Yb(SPh)_2$, $(py)_4Yb(SePh)_2$, $(py)_3Yb(SPh)_3$ $(THF)_3Ln(SePh)_3$ (Ln = Tm, Ho, Er), $[(py)_3Ln(SPh)_3]_2$ (Ln = Ho, Tm), $[(py)_3Ln(SePh)_3]_2$ (Ln = Sm, Ho, Tm, Yb), and $[(THF)_4Ln_3(SePh)_9]_n$ (Ln = Pr, Nd, Sm) [62,64,65] could be isolated from the reactions of PhEEPh (E = S, Se) with Ln/Hg amalgam or elemental Ln in the presence of a catalytic amount of Hg (Eqs. (31)–(33)):

$$Yb/Hg + PhEEPh \xrightarrow{py} (py)_4Yb(EPh)_2 \quad (E = S, Se) \tag{31}$$

$$Yb/Hg + PhSSPh \xrightarrow{py} (py)_4Yb(SPh)_3 \tag{32}$$

$$Ln/Hg + PhSeSePh \xrightarrow{py} [(py)_3Ln(SePh)_3]_2$$
$$(Ln = Sm, Ho, Tm, Yb) \tag{33}$$

In some cases, the reaction medium may influence the formation of products. For examples, reduction of PhSSPh with Sm/Hg in pyridine or THF produced tetrametallic complex $[(py)_2Sm(SPh)_3]_4$ and light yellow crystals $[(THF)Sm(SPh)_3]_{4n}$, respectively [65].

Lanthanide benzenefluorothiolate complexes (Eqs. (34)–(39)), e.g. monomers $(THF)_3Ln(SC_6F_5)_3$ (Ln = Ho, Er), $(py)_4Ln(SC_6F_5)_3$ (Ln = Sm, Yb), $(DME)_2Er(SC_6F_5)$, dimers $[(THF)_2Sm(SC_6F_5)_2(\mu\text{-}SC_6F_5)]_2$, $[(THF)_3Ce(SC_6F_5)_3]_2$ and polymer $[(THF)_2Eu(\mu\text{-}SC_6F_5)_2]_n$ [67,68], were obtained by transmercuration reactions of elemental lanthanide with mercury thiolates $Hg(SC_6F_5)_2$. As shown in Scheme 12, a set of lanthanide(III) benzenefluorothiolates $Ln(SC_6F_5)_3$ (Ln = La, Ce, Pr, Nd, Sm, Gd) reacted with $Hg(SC_6F_5)_2$ to form heterometallic compounds with the general formula $[(DME)_3Ln(SC_6F_5)_2]_2[Hg_2(SC_6F_5)_6]$ (Ln = La, Ce, Pr, Nd, Sm, Gd) [69]. These compounds could also be prepared either by mixing Ln and $Hg(SC_6F_5)_2$ in DME or by in situ generation of the Ln reagent in the presence of excess $Hg(SC_6F_5)_2$:

$$2Ln + 3Hg(SC_6F_5)_2 \xrightarrow{THF} 2(THF)_3Ln(SC_6F_5)_3$$
$$(Ln = Er, Ho) \tag{34}$$

$$2Ln + 3Hg(SC_6F_5)_2 \xrightarrow{py} 2(py)_4Ln(SC_6F_5)_3 \quad (Ln = Sm, Yb) \tag{35}$$

$$2Er + 3Hg(SC_6F_5)_2 \xrightarrow{DME} 2(DME)_3Er(SC_6F_5)_3 \tag{36}$$

$$2Sm + 3Hg(SC_6F_5)_2 \xrightarrow{THF} [(THF)_2Sm(SC_6F_5)_2(\mu\text{-}SC_6F_5)]_2 \tag{37}$$

$$2Ce + 6Hg(SC_6F_5)_2 \xrightarrow{THF} [(THF)_3Ce(SC_6F_5)_3]_2 \tag{38}$$

$$Eu + Hg(SC_6F_5)_2 \rightarrow [(THF)_2Eu(\mu\text{-}SC_6F_5)_2]_n \tag{39}$$

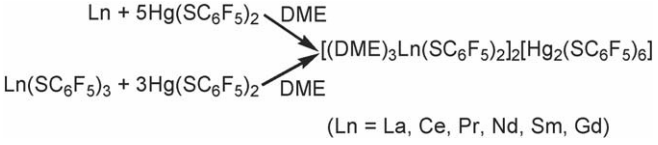

Scheme 12.

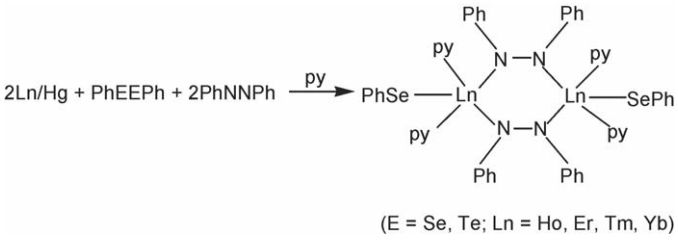

Scheme 13.

Reduction reactions of Ln/Hg metals with azobenzene and PhEEPh (E = Se or Te) in pyridine yielded the bimetallic compounds $[(py)_2Ln(EPh)(PhNNPh)]_2$ (E = Se, Ln = Ho, Er, Tm, Yb; E = Te, Ln = Ho, Er, Tm, Yb) (Scheme 13) [72].

2.3.4. Reactions of elemental chalcogens with lanthanide chalcogenolates and cleavage reactions of C–Se bond

The construction of polynuclear lanthanide chalcogenolate complexes has always attracted considerable attention because these compounds have potential applications in the new materials chemistry and exhibit a variety of fascinating structural patterns. The general synthetic approach to these compounds involves in the reduction of elemental E by $Ln(EPh)_3$, with concomitant oxidative elimination of PhEEPh. For example, the reduction of elemental S with $Yb(SPh)_3$ gave rise to a red hexanuclear ytterbium cluster $(py)_{10}Yb_6S_6(SPh)_6$ (Scheme 14) [77]. Further, a series of tetranuclear lathanide clusters $(THF)_6Ln_4E(EE)_4(SC_6F_5)_2$ (E = S, Ln = Yb; E = Se, Ln = Yb, Tm) were prepared in good yield by similar reactions of $Ln(SC_6F_5)_3$ and $Ln(EPh)_3$ (E = S, Se) with S (or Se) (Scheme 15) [78].

The molecular ytterbium selenolate $(py)_4Yb(SePh)_2$ could reduce elemental Se in pyridine to give the cubane-like cluster $(py)_8Yb_4Se_4(SePh)_4$ [77], which was isolated as deep red crystals in 73% yield. The selenium-rich Yb compound $(py)_8Yb_4Se(SeSe)_3(SeSeSePh)(Se_{0.38}SePh)$ [79] was formed at room temperature by reduction reaction of PhSeSePh and Se with Yb metal in pyridine. As shown in Scheme 16, the interconversion of the two clusters proved to be quite facile. The diselenide linkages in $(py)_8Yb_4(SeSe)_3Se(SeSeSePh)(Se_{0.38}SePh)$

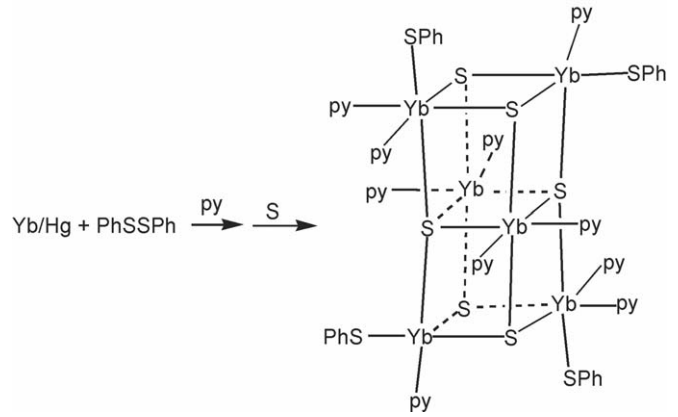

Scheme 14.

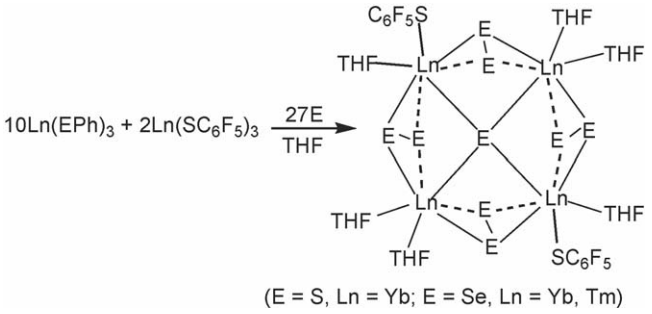

Scheme 15.

were readily reduced upon addition of $(py)_4Yb(SePh)_2$ to give a cubane-like cluster $(py)_8YbSe_4(SePh)_4$. Conversely, the same cluster $(py)_8Yb_4(SeSe)_3Se(SeSeSePh)(Se_{0.38}SePh)$ could also be regenerated by the reaction of the cubane $(py)_8YbSe_4(SePh)_4$ with elemental Se in pyridine at room temperature [79]. Reaction of PhTeTePh with Yb and Se produces the analogous Se-rich tellurolate derivative $(py)_8Yb_4(SeSe)_3Se(SeSeTePh)(SeTePh)$, whose structure is found to be isomorphous with that of $(py)_8Yb_4(SeSe)_3Se(SeSeSePh)(Se_{0.38}SePh)$. However, addition of PhSSPh into Yb and Se gave rise to a completely different tetrametallic cluster $(py)_8Yb_4(\mu_3\text{-}Se)_2(\mu_2\text{-}SeSe)_2(\mu_2\text{-}SPh)_2(SPh)_2$ (Scheme 17) [79].

As illuminated in Eqs. (40)–(42), lanthanide tellurido clusters $(py)_8Ln_4(\mu_4\text{-}Te)(\mu\text{-}TeTe)_2(\mu\text{-}\eta^2,\eta^2\text{-}Te_5Ph)(Te_{0.1}TePh)$ (Ln = Tb, Ho) can be isolated from the reactions of Ln metal with PhTeTePh and Te in pyridine. The samarium clusters $(py)_9Sm_4(\mu_4\text{-}Te)(\mu\text{-}TeTe)_2(\mu\text{-}TeTeTe(Ph)TeTe)(TePh)$ and $(py)_7Tm_4(\mu_4\text{-}Te)[(TeTe)_4TePh](Te_{0.6}TePh)$ [80] can also be

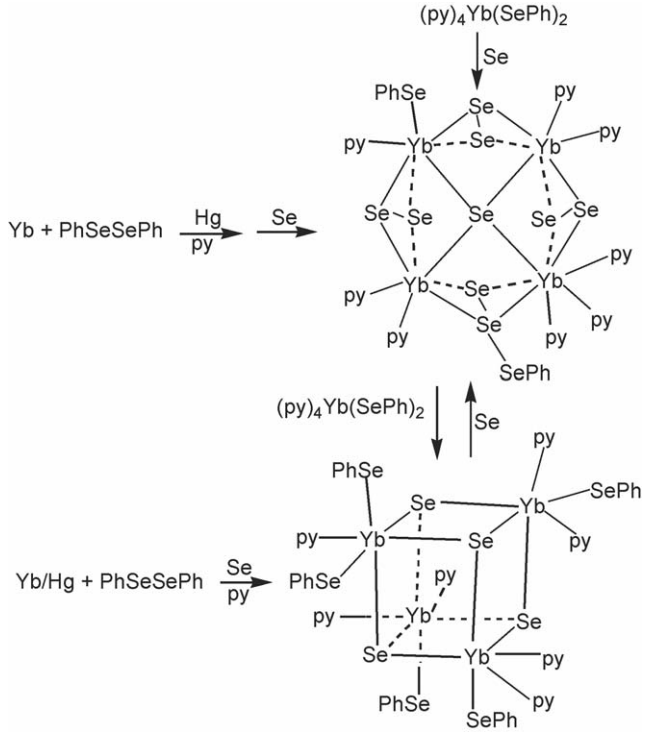

Scheme 16.

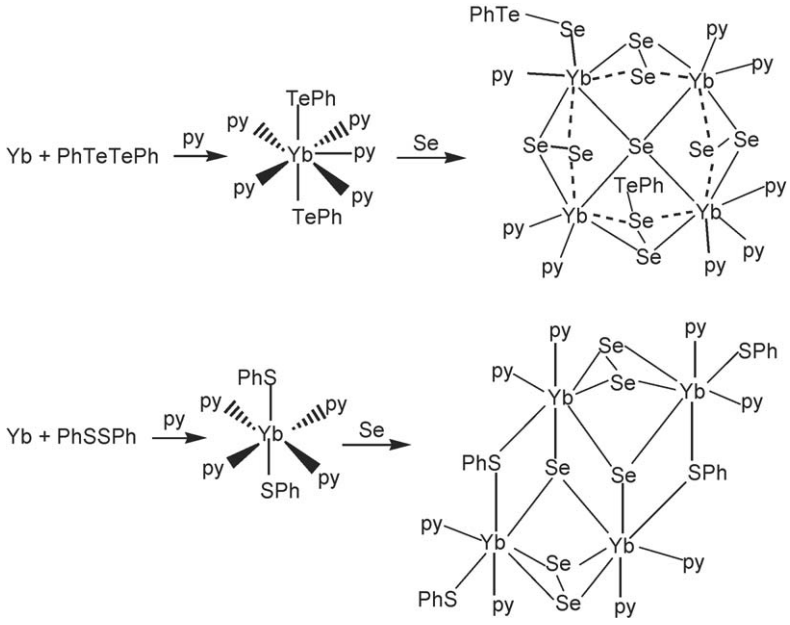

Scheme 17.

prepared in a similar manner:

$$4Ln/Hg + 2PhTeTePh + 9Te \xrightarrow{py} (py)_8Ln_4(Te)(TeTe)_2(Te_5Ph)(Te_{0.1}TePh) \quad (Ln = Tb, Ho) \tag{40}$$

$$4Sm/Hg + 2PhTeTePh + 9Te \xrightarrow{py} (py)_9Sm_4(\mu_4\text{-}Te)(\mu\text{-}TeTe)_2(\mu\text{-}Te_3(Ph)Te_2)(TePh) \tag{41}$$

$$4Tm/Hg + 2PhTeTePh + 9Te \xrightarrow{py} py_7Tm_4(\mu_4\text{-}Te)[(TeTe)_4TePh](Te_{0.6}TePh) \tag{42}$$

Compound $[(THF)_8Sm_4Se(SePh)_8][Zn_8Se(SePh)_{16}]$ was isolated by reaction of a stoichiometric mixture of $Zn(SePh)_2$/$Sm(SePh)_3$ with Se in THF. The neodymium analogue $[(THF)_8Nd_4Se(SePh)_8][Zn_8Se(SePh)_{16}]$ was obtained by stoichiometric combination of Nd/Zn/Se/SePh in THF (Eq. (43)). In a separate but similar vein, attempts to produce heterometallic cubane-like clusters containing Yb and Fe led to the isolation of the ion–pair compound $[Yb(THF)_6][Fe_4Se_4(SePh)_4]$ (Eq. (44)) [81]:

$$8Zn(SePh)_2 + 4Ln(SePh)_2 + 2Se \xrightarrow[-2PhSeSePh]{THF,RT} [(THF)_8Ln_4Se(SePh)_8][Zn_8Se(SePh)_{16}] \quad (Ln = Sm, Nd) \tag{43}$$

$$Yb + FeI_2 + PhSeSePh + Se \xrightarrow{THF} [Yb(THF)_6][Fe_4Se_4(SePh)_4] \tag{44}$$

As described in Eq. (45), octanuclear lanthanide sulfide clusters $(THF)_8Ln_8S_6(SPh)_{12}$ (Ln = Ce, Pr, Nd, Sm, Gd, Tb, Dy, Ho, Er) and $(py)_8Ln_8S_6(SPh)_{12}$ (Ln = Nd, Sm, Er) could be isolated from the reactions of $Ln(SPh)_3$ with elemental S [82,83]. The similar selenide clusters $(py)_8Ln_8Se_6(SePh)_{12}$ (Ln = Sm, Nd) [84] were made by reaction of $Ln(SePh)_3$ with Se (Eqs. (46) and (47)). In addition, all involved ligands (i.e. L, E, EPh) could be varied systematically to further the understanding of structure/property relationships because all possible ligand sites are reactive [84]. For example, chalcogenolate ligands may be selectively varied, as in the reaction of $(THF)_8Sm_8Se_6(SePh)_{12}$ with PhSSPh to form $(THF)_8Sm_8Se_6(SPh)_{12}$ [84] (Eqs. (48) and (49)). Neutral L ligands may be altered without disrupting the structure, as in the replacement of THF ligands in $(THF)_8Sm_8Se_6(SePh)_{12}$ with pyridine to yield $(py)_8Sm_8Se_6(SePh)_{12}$. Even E^{2-} ligands could be chemically replaced: the reaction of $(THF)_8Sm_8Se_6(SPh)_{12}$ with elemental S produced the all-sulfur cluster $(THF)_8Sm_8S_6(SPh)_{12}$ (Scheme 18) [84]. In the case of DME as a reagent, a heptanuclear chalcogenide cluster $[Sm_7S_7(SePh)_6(DME)_7][Hg_3(SePh)_7]$ was obtained by reaction of $Sm(SePh)_3$ with S_8 (Eq. (50)) [85]:

$$8Ln(SPh)_3 + 6S \rightarrow (L)_8Ln_8S_6(SPh)_{12} + PhSSPh \quad (Ln = Ce, Pr, Nd, Sm, Gd, Tb, Dy, Ho, Er, L = THF; \quad Ln = Nd, Sm, Er, \quad L = py) \tag{45}$$

$$Ln(SePh)_3 + Se \xrightarrow{py} (py)_8Ln_8Se_6(SePh)_{12} \quad (Ln = Sm, Nd) \tag{46}$$

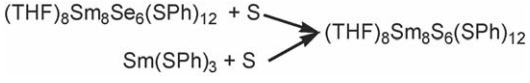

Scheme 18.

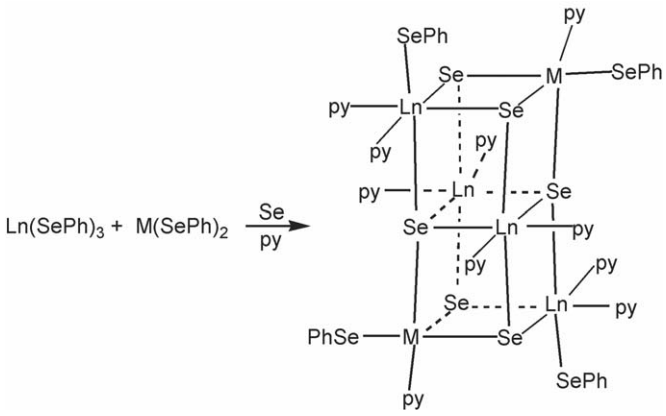

Scheme 19.

$$8Sm(SePh)_3 + 6S \xrightarrow{THF} (THF)_8Sm_8S_6(SePh)_{12} \quad (47)$$

$$8Sm(SePh)_3 + 6PhSSPh \xrightarrow{THF} (THF)_8Sm_8Se_6(SPh)_{12} \quad (48)$$

$$(THF)_8Sm_8Se_6(SPh)_{12} \xrightarrow{PhSSPh} (THF)_8Sm_8Se_6(SPh)_{12} + PhSeSePh \quad (49)$$

$$Sm/Hg + \tfrac{3}{2}PhSeSePh \xrightarrow{S} [Sm_7S_7(SePh)_6(DME)_7][Hg_3(SePh)_7] \quad (50)$$

Compounds $(py)_8Ln_4M_2Se_6(SePh)_4$ (Ln/M = Er/Cd, Er/Hg, Yb/Cd, Yb/Hg, Lu/Hg) [87] could be isolated by reaction of $Ln(SePh)_3$ and $M(SePh)_2$ with elemental Se (Scheme 19).

Although the samarium(II) selenolate compound $Sm(SePh)_2$ was unstable in solution, it reacted with equimolar $Zn(SePh)_2$ to form the relatively stable heterometallic cluster $[(THF)_3Sm(\mu\text{-}SePh)_3Zn(\mu\text{-}SePh)]_n$ (Scheme 20) [63].

Intriguingly, addition of elemental Se to a solution of "$Sm(SePh)_2$" gave rise to the heterovalent cluster $(DME)_4Sm_4Se(SePh)_8$ [86]. The isostructural Yb cluster

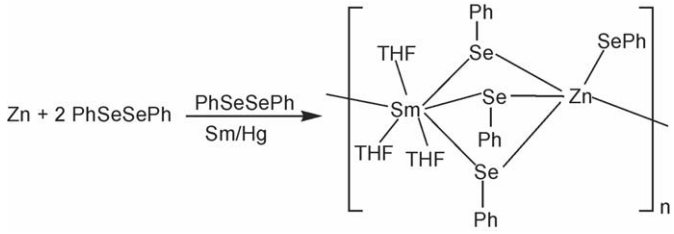

Scheme 20.

$(DME)_4Yb_4Se(SePh)_8$ was also prepared in a stepwise fashion [86]. Reaction of $Sm(SePh)_3$ with Yb metal produced a heterometallic Sm(III)/Yb(II) cluster $(DME)_4Sm_2Yb_2Se(SePh)_8$ [86]. Another heterometallic cluster $(DME)_4Nd_2Yb_2Se(SePh)_8$ was made, either by the reduction of $Yb(SePh)_3$ with Nd in ca. 20% yield or by the reduction of $Nd(SePh)_3$ with Yb in less than 1% yield [86] (Scheme 21).

The cleavage of C–Se bonds by thermally unstable "$Sm(SePh)_2$" in DME produced heterovalent complex $(DME)_4Sm_4Se(SePh)_8$ with 0.2% yield (Scheme 22). However, the similar reaction in THF produced an octanuclear cluster $(THF)_8Sm_8Se_6(SePh)_{12}$ in relatively high yield (5%) [85]. There were some other examples in which minor changes of the reaction conditions or the choice of the reagents may greatly influence the product formation and the yield. For example, the reductive cleavage of C–Se in $[(THF)_3Sm(SePh)_2Zn(SePh)_2]_n$ instead of "$Sm(SePh)_2$" produced two clusters $(THF)_8Sm_8Se_6(SePh)_{12}$ (major product) and $[(THF)_8Sm_4Se(SePh)_8][Zn_8Se(SePh)_{16}]$ (minor product). In the C–Se bond cleavage reaction, the isolation of pure $[(THF)_8Sm_4Se(SePh)_8][Zn_8Se(SePh)_{16}]$ in a higher yield was accomplished by starting with 1:2 (molar ratio) mixture of $Sm(SePh)_2$ and $Zn(SePh)_2$ (Scheme 23) [81,85]. Reactions of $Ln(SePh)_3$ with SeO_2 in THF gave octanuclear oxoselenido clusters with the general formula $(THF)_8Ln_8O_2Se_2(SePh)_{16}$ (Ln = Ce, Pr, Nd, Sm) (Eq. (51)) [15]:

$$Ln(SePh)_3 + SeO_2 \xrightarrow{THF} (THF)_8Ln_8O_2Se_2(SePh)_{16} \quad (Ln = Ce, Pr, Nd, Sm) \quad (51)$$

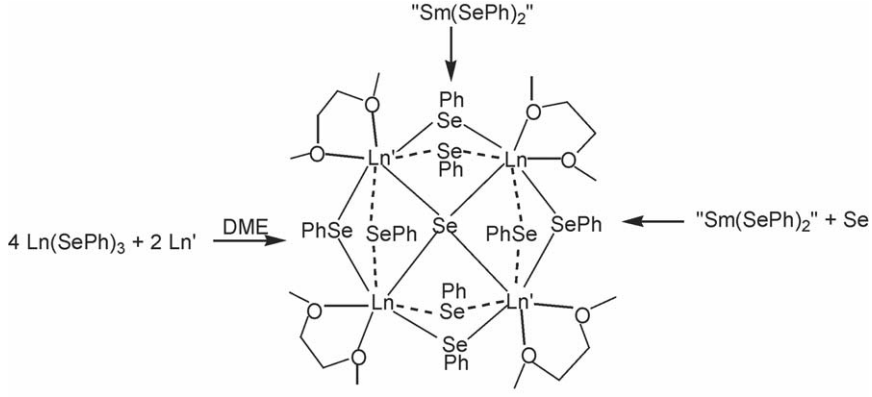

(Ln = Ln' = Sm, Yb; Ln = Sm, Ln' = Yb; Ln = Nd, Ln' = Yb; Ln = Yb, Ln' = Nd)

Scheme 21.

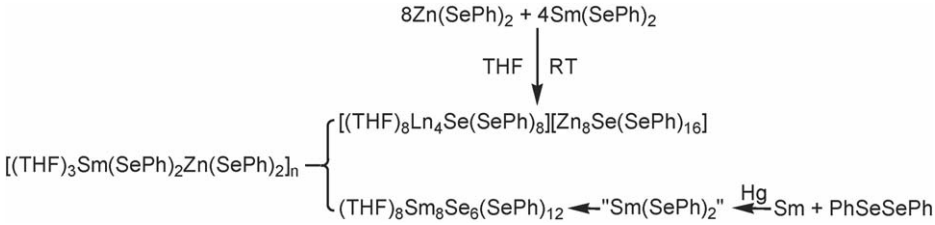

Scheme 22.

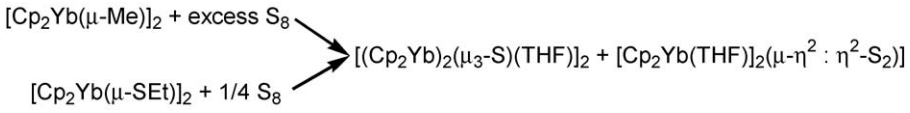

Scheme 23.

2.4. Insertion reaction

Insertion of elemental S into the metal–carbon σ-bond of complexes $[Cp_2Ln(\mu\text{-}Me)]_2$ forms the corresponding thiolates $[Cp_2Ln(\mu\text{-}SMe)]_2$ (Ln = Yb, Y, Er, Dy) [131] in good yield (Eq. (52)). While reaction of $Cp_2Y(Bu^n)$ with elemental sulfur in 1:1 molar ratio under the same conditions yielded $[(Cp_2Y)_2(\mu_3\text{-}S)(THF)]_2$ as the metal-containing product with the extrusion of Bu^nSBu^n and Bu^nSSBu^n, the corresponding insertion intermediate $[Cp_2Y(\mu\text{-}SBu^n)]_2$ could be isolated only by decreasing the amount of S_8 under more mild reaction conditions (Eqs. (53) and (54)). Furthermore, $[Cp_2Yb(\mu\text{-}SEt)]_2$ reacted with 2 equiv. of sulfur to produce a mixture of $[(Cp_2Yb)_2(\mu_3\text{-}S)(THF)]_2$ and $[Cp_2Yb(THF)]_2(\mu\text{-}\eta^2\text{:}\eta^2\text{-}S_2)$, which could also be prepared from the reaction of $[Cp_2Yb(\mu\text{-}Me)]_2$ with excess elemental sulfur in THF (Scheme 23):

$$[Cp_2Ln(\mu\text{-}Me)]_2 \xrightarrow[RT]{1/4S_8} [Cp_2Ln(\mu\text{-}SMe)]_2 \quad (Ln = Yb, Y, Er, Dy) \tag{52}$$

$$Cp_2YBu^n(THF) \xrightarrow[RT]{1/4S_8} [Cp_2Y(\mu\text{-}SBu^n)(THF)]_2 \tag{53}$$

$$Cp_2YBu^n(THF) \xrightarrow[-30\,^\circ C]{1/4S_8} [(Cp_2Y)_2(THF)(\mu\text{-}S)]_2 \tag{54}$$

Monoanionic β-diketiminato ligands, ArNC(R)CHC(R)NAr, are useful to synthesize organolanthanide complexes [156–159] and have recently been employed for the synthesis of novel di-tellurolate scandium complexes [137]. As shown in Scheme 24, reactions of the well-defined, base-free dialkyl

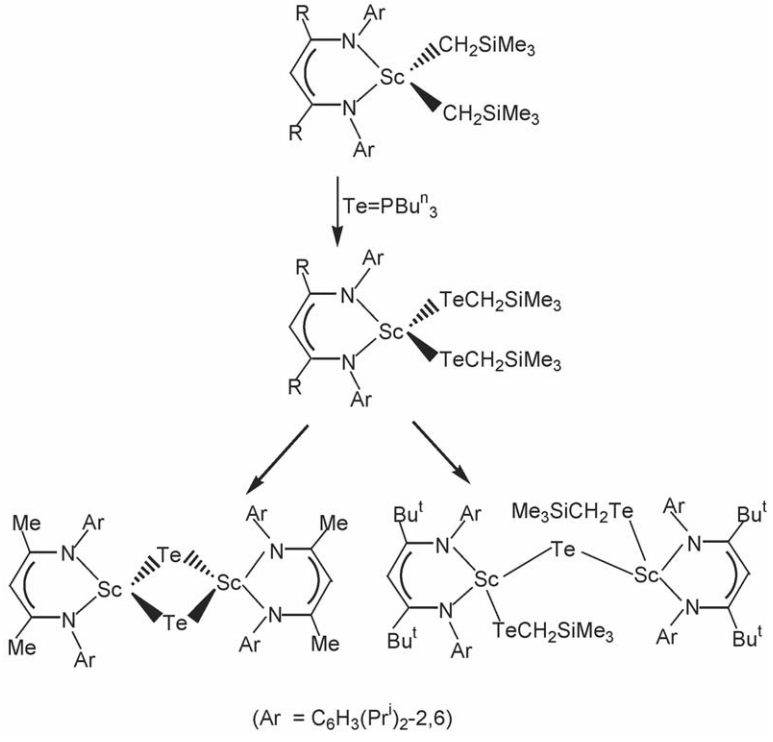

Scheme 24.

scandium compounds [ArNC(R)CHC(R)NAr]Sc(CH_2SiMe_3)$_2$ (Ar = $C_6H_3Pr^i_2$-2,6; R = Me, Bu^t) with two equiv. of Bu^n_3P = Te generated the bis–tellurolate complex [ArNC(R)CHC(R)NAr]Sc($TeCH_2SiMe_3$)$_2$. The tellurolate compound [ArNC(Me)CHC(Me)NAr]Sc($TeCH_2SiMe_3$)$_2$ was only moderately stable and decomposes into a dimeric complex [{ArNC(Me)CHC(Me)NAr}Sc(μ-Te)]$_2$ with elimination of two equiv. of Te(CH_2SiMe_3)$_2$. However, if [ArNC(Bu^t)CHC(Bu^t)NAr]Sc($TeCH_2SiMe_3$)$_2$ lost one equiv. of Te(CH_2SiMe_3)$_2$, the other dinuclear compound [{ArNC(Bu^t)CHC(Bu^t)NAr}Sc($TeCH_2SiMe_3$)(μ-Te)]$_2$ could be isolated (Scheme 24).

3. Specific structures

According to the ancillary ligands coordinated to rare earth ions, the lanthanide chalcogenolate complexes can be divided into two groups: lanthanide chalcogenolates coordinated with cyclopentadienyl or cyclopentadienyl derivatives or cyclooctatetraenyl ligands, and with other N or O donor ligands (e.g. [N($SiMe_3$)$_2$]$^-$, benzamidinate, hydrotri(pyrazolyl)borate, β-diketiminato ligands). Structural parameters for these two groups are given in Tables 1 and 2, respectively. In the following two subsections, we describe their important structural features in the order of Ln nuclearity.

3.1. Lanthanide chalcogenolates with cyclopentadienyl or cyclopentadienyl derivatives or cycloctatetraenyl ligands

3.1.1. Mononuclear complexes

There are a great many mononuclear lanthanide chalcogenolates with cyclopentadienyl or cyclopentadienyl derivatives or cycloctatetraenyl ligands. The coordination number around the central Ln in these compounds varies from 7 to 9. For example, the Sm atom in (C_5Me_5)$_2$Sm(TePh)(THF) [41] is coordinated by two η^5-C_5Me_5 rings, one Te atom from TePh ligand and one O atom from the THF molecule.

The structures of the solvated organosamarium chalcogenolate complexes (Me_5C_5)$_2$Sm($SeC_6H_2(CF_3)_3$-2,4,6)(THF), (C_5Me_5)$_2$Sm($TeC_6H_2Me_3$-2,4,6)(THF) [37], (Me_5C_5)$_2$Yb(EPh)(NH_3) (E = S, Te) [38,39], (C_5Me_5)$_2$Sm(EPh)(THF) (E = S, Se, Te) [41], (Cp)$_2$Yb(SR)(THF) (R = $C_6H_2(CF_3)_3$-2,4,6, $C_6H_4(H_2N)$-4) [95,102] are very similar. Therefore, only the structure of (Me_5C_5)$_2$Sm(SPh)(THF) is shown in Fig. 1. In this complex, the pseudo-tetrahedral coordination sphere of the Sm atom is completed by two η^5-cyclopentadienyl rings and one sulfide atom and one oxygen atom from THF molecule. The coordination number of the Sm atom is eight. In (Cp)$_2$Ln(SC_7H_4NS)(THF) coordinated with a chelating thiolate ligand (Ln = Dy, Tm, Yb; SC_7H_4NS = benzothiazole-2-thiolate) [96,97], each Ln is coordinated by two η^5-C_5H_5 groups, one nitrogen and one sulphur atom from the benzothiazole-2-thiolate ligand and one oxygen atom of THF molecule, leading to a distorted trigonal bipyramidal geometry with two η^5-C_5H_5 ring centroids in axial positions. The coordination number of the Ln atom is nine. The Yb–S bond distance of 2.843(2) Å in (Cp)$_2$Yb(SC_7H_4NS)(THF) is somewhat longer than the corresponding ones found in (Cp)$_2$Yb($SC_6H_4(H_2N)$-4) (2.641(2) Å) [10], (Cp)$_2$Yb($SC_6H_2(CF_3)_3$-2,4,6)(THF) (2.639(3) Å) and (Me_5C_5)$_2$Yb(SPh)(NH_3) (2.675(3) Å) [39]. The difference may be due to the difference of the coordination number of the central ytterbium atom.

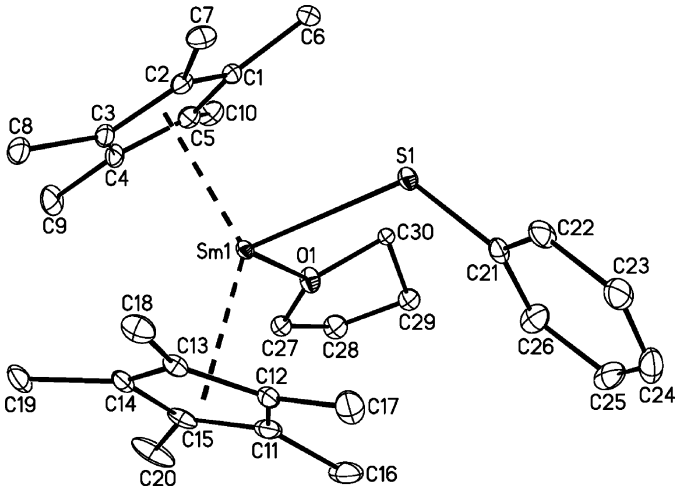

Fig. 1. Molecular structure of (Me_5C_5)$_2$Sm(SPh)(THF) with thermal ellipsoids drawn at the 12% probability level. All H atoms are omitted for clarity [41].

Each Ln atom in [Li(TMEDA)$_2$][(Me_5C_5)$_2$Sm(μ-SCCPh)$_2$] [108] and [K(15-crown-5)$_2$][Ln(C_5Me_5)$_2$(dddt)] (Ln = Nd, Ce; dddt = 5,6-dihydro-1,4-dithiine-2,3-dithiolate) [128] (Fig. 2) adopts a pseudo-tetrahedral coordination geometry, coordinated by two η^5-pentamethylcyclopentadienyl rings and two S atoms. In [Li(TMEDA)$_2$][(Me_5C_5)$_2$Sm(μ-SCCPh)$_2$] [108], the mean Sm–S bond distance of 2.794(4) Å is comparable to that in (py)$_2$(THF)Sm($SC_6H_2Pr^i_3$-2,4,6)$_3$ (average 2.740(3) Å) [56], but is shorter than those in (HMPA)$_3$Sm(SPh)$_3$ (average 2.821(2) Å) [55], [(HMPA)$_3$Sm(SC_4H_5N)$_2$]I (average 2.870(3) Å) [57], and [Sm{(μ-SBu^t)$_2$Li(TMEDA)}$_3$] (average 2.827(3) Å) [109]. The mean Ln–S bond lengths of 2.794(19) Å for Ln = Ce and 2.753(8) Å for Ln = Nd in

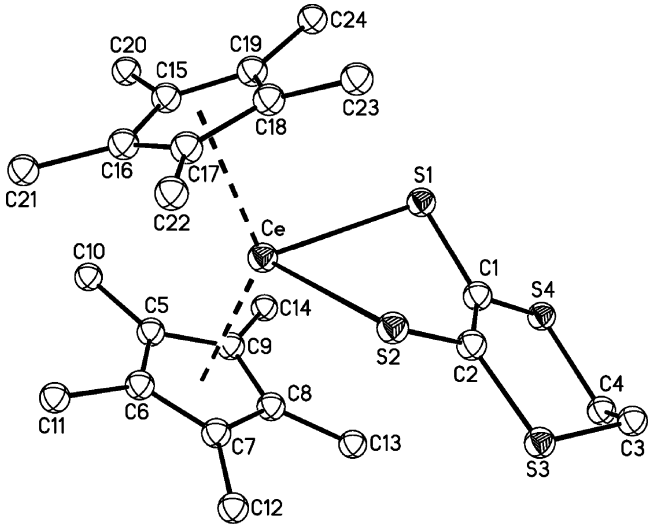

Fig. 2. Structure of anion in [K(15-crown-5)$_2$][Ln(C_5Me_5)$_2$(dddt)]. The thermal ellipsoids drawn at the 30% probability level. All H atoms are omitted for clarity [128].

Table 1
Structural parameters of lanthanide chalcogenolate complexes coordinated with cyclopentadienyl or cyclopentadienyl derivatives or cyclooctatetraenyl ligands

Compound	c.n.[a]	o.s.[b]	Bond type	Bond length (Å)	Ref.
Mononuclear complexes					
$(Me_5C_5)_2Sc(TeCH_2Ph)$	7	3	Sc—Te	2.8337(14)	[132]
$(C_5Me_5)_2Sm(SPh)(THF)$	8	3	Sm—S	2.7605(12)	[41]
$(C_5Me_5)_2Sm(SePh)(THF)$	8	3	Sm—Se	2.8837(6)	[41]
$(C_5Me_5)_2Sm(TePh)(THF)$	8	3	Sm—Te	3.1279(3)	[41]
$(Cp)_2Yb(SC_6H_4(H_2N)\text{-}4)(THF)$	8	3	Yb—S	2.641(2)	[10]
$(Cp)_2Yb[SC_6H_2(CF_3)_3\text{-}2,4,6](THF)$	8	3	Yb—S	2.639(3)	[95]
$(Me_5C_5)_2Yb(SPh)(NH_3)$	8	3	Yb—S	2.675(3) average	[39]
$(C_5Me_5)_2Sm(SeC_6H_2(CF_3)_3\text{-}2,4,6)(THF)$	8	3	Sm—Se	2.919(1)	[37]
$(C_5Me_5)_2Sm(TeC_6H_2Me_3\text{-}2,4,6)(THF)$	8	3	Sm—Te	3.088(2)	[37]
$(Me_5C_5)_2Yb(TePh)(NH_3)$	8	3	Yb—Te	3.039(1)	[38]
$(Cp)_2Dy(SC_7H_4NS)(THF)$	9	3	Dy—S	2.898(3)	[96]
$(Cp)_2Tm(SC_7H_4NS)(THF)$	9	3	Tm—S	2.863(4)	[97]
$(Cp)_2Yb(SC_7H_4NS)(THF)$	9	3	Yb—S	2.843(2)	[96]
$Cp_2YN(SPPh_2)_2$	9	3	Y—S	2.9130(11) average	[98]
$Cp_2YN(SePPh_2)_2$	9	3	Y—Se	2.9112(8) average	[98]
$Cp_2YbN(SPPh_2)_2$	8	3	Yb—S	2.9109(6) average	[99]
$Cp_2LaN(SePPh_2)_2$	9	3	La—Se	3.1273(4) average	[99]
$Cp_2GdN(SePPh_2)_2$	9	3	Gd—Se	3.0541(6) average	[99]
$Cp_2ErN(SePPh_2)_2$	9	3	Er—Se	3.0286(8) average	[99]
$Cp_2YbN(SePPh_2)_2$	8	3	Yb—Se	2.8283(8) average	[99]
$[(Cp)_2Lu(\mu\text{-}SePh)_2Li(THF)_2]$	8	3	Lu—μ-Se	2.799(7) average	[89]
$[(Me_5C_5)_2Lu(\mu\text{-}SBu^t)_2Li(THF)_2]$	8	3	Lu—μ-S	2.716(3) average	[88]
$(C_8H_8)Sm(SC_4H_5N)(HMPA)_2$	8	3	Sm—S	2.932(7)	[60]
$(C_8H_8)Sm(SC_6H_2Pr^i_3\text{-}2,4,6)(HMPA)_2$	7	3	Sm—S	2.817(3)	[60]
$[Li(TMEDA)_2][(Me_5C_5)_2Sm(\mu\text{-}SCCPh)_2]$	8	3	Sm—S	2.794(4) average	[108]
$[K(15\text{-crown-}5)_2][Ce(C_5Me_5)_2(dddt)]$	8	3	Ce—S	2.7822 average	[128]
$[K(15\text{-crown-}5)_2][Nd(C_5Me_5)_2(dddt)]$	8	3	Nd—S	2.753(1) average	[128]
Binuclear complexes					
$[Cp_2Y(\mu\text{-}SBu^n)]_2$	8	3	Y—μ-S	2.7450(18) average	[131]
$[(C_5H_4Bu^t)_2Y(\mu\text{-}SePh)]_2$	8	3	Y—μ-Se	2.915(1)	[113]
$[(C_5Me_5)_2Sm(\mu\text{-}SPh)]_2$	8	3	Sm—μ-S	2.9365(6) average	[41]
$[(C_5Me_5)_2Sm(\mu\text{-}SePh)]_2$	8	3	Sm—μ-Se	3.0518(4) average	[41]
$[(C_5Me_5)_2Sm(\mu\text{-}TePh)]_2$	8	3	Sm—μ-Te	3.2617(4) average	[41]
$[(Bu^tC_5H_4)_2Ce(\mu\text{-}SPr^i)]_2$	8	3	Ce—μ-S	2.882(2) average	[93]
$[Cp_2Yb(\mu\text{-}SMe)]_2$	8	3	Yb—μ-S	2.705 average	[131]
$[(Cp)_2Yb(\mu\text{-}SPr^n)]_2$	8	3	Yb—μ-S	2.705(8) average	[92]
$[(Cp)_2Yb(\mu\text{-}SBu^n)]_2$	8	3	Yb—μ-S	2.707(3) average	[91]
$[(MeC_5H_4)_2La(\mu\text{-}SPh)(THF)]_2$	9	3	La—μ-S	2.9759(13) average	[94]
$[(MeC_5H_4)_2Nd(\mu\text{-}SPh)(THF)]_2$	9	3	Nd—μ-S	2.9290(14) average	[8]
$[(MeC_5H_4)_2Sm(\mu\text{-}SPh)(THF)]_2$	9	3	Sm—μ-S	–	[35]
$[(Cp)_2Yb(SC_6H_4(H_2N)\text{-}2)]_2$	9	3	Yb—μ-S	2.794(1) average	[10]
$[Li(THF)_4][(Bu^tC_5H_4)_2NdS_2C_2B_{10}H_{10}]_2$	9	3	Nd—μ-S	2.9669(14)	[110]
	9	3	Nd—S	2.8237(15)	
$[Li(THF)_4][(Bu^tC_5H_4)_2NdSe_2C_2B_{10}H_{10}]_2$	9	3	Nd—μ-Se	3.1065(14)	[110]
	9	3	Nd—Se	2.9612(15)	
$[Li(THF)_4][(Cp)_2NdS_2C_2B_{10}H_{10}]_2$	9	3	Nd—μ-S	2.640(4)	[111]
	9	3	Nd—S	2.652(3)	
$[Li(THF)_4][(Cp)_2YbS_2C_2B_{10}H_{10}]_2$	9	3	Yb—μ-S	2.682(3)	[111]
	9	3	Yb—S	2.663(4)	
$[Li(THF)_4][(Cp)_2YbSe_2C_2B_{10}H_{10}]_2$	9	3	Yb—μ-Se	2.8716(14)	[111]
	9	3	Yb—Se	2.9077(15)	
$[\{(C_8H_8)Nd\}_2(\mu\text{-}SBu^t)(\mu_3\text{-}SBu^t)_2Na(THF)_2]$	7	3	Nd—μ-S	2.881(2)	[115]
	7	3	Nd—μ_3-S	2.935(2)	
$[(C_8H_8)Sm(\mu\text{-}SPh)(THF)_2]_2$,	8	3	Sm—μ-S	2.924(8) average	[59]
$[(C_8H_8)Sm(\mu\text{-}SC_6H_2Pr^i3\text{-}2,4,6)(THF)]_2$	7	3	Sm—μ-S	2.883(5)	[59]
$[(C_8H_8)Sm(\mu\text{-}SePh)(THF)_2]_2$	8	3	Sm—μ-Se	3.09(3) average	[58]
$[Yb(\mu\text{-}SPh)(\eta^5\text{-}C_4Me_4P)(THF)_2]_2$	7	2	Yb—μ-S	2.830(4) average	[61]
$[Ce(C_5Me_5)_2(dddt)K(THF)_2]_2$	8	3	Ce—μ-S	2.8381(8) average	[128]
$[Nd(C_5Me_5)_2(dddt)K(THF)_2]_2$	8	3	Nd—μ-S	2.8063(9) average	[128]

[a] c.n.: Coordination number.
[b] o.s.: Oxidation state.

Table 2
Structural parameters of lanthanide chalcogenolate complexes with other N or N donor ligands

Compound	c.n.[a]	o.s.[b]	Bond type	Bond length (Å)	Ref.
Mononuclear complexes					
$Eu[SC_6H_3(C_6H_2Pr^i_3\text{-}2,4,6)_2\text{-}2,6]_2$	2	2	Eu—S	2.817(1) average	[106]
$Yb[SC_6H_3(C_6H_2Pr^i_3\text{-}2,4,6)_2\text{-}2,6]_2$	2	2	Yb—S	2.690(2) average	[106]
$Sm(SC_6H_2Bu^t_3\text{-}2,4,6)_3$	3	3	Sm—S	2.644(9) average	[102]
$ArNC(Bu^t)CHC(Bu^t)NArSc(TeCH_2SiMe_3)_2$	4	3	Sc—Te	2.8137	[137]
$(py)_4Yb(SPh)_2$	6	2	Yb—S	2.827(3)	[62]
$(DME)_2Yb(SC_6H_2Bu^t_3\text{-}2,4,6)_2$	6	2	Yb—S	2.756(8)	[102]
$(DME)_2Yb\{SC_6H_3(C_6H_2Pr^i_3\text{-}2,4,6)_2\text{-}2,6\}_2$	6	2	Yb—S	2.739(3) average	[106]
$(py)_4Yb(SePh)_2$	6	2	Yb—Se	2.960(1)	[62]
$(HMPA)_3Sm(SPh)_3$	6	3	Sm—S	2.821(3) average	[55]
$(HMPA)_3Yb(SPh)_3$	6	3	Yb—S	2.728(1) average	[55]
$(py)_2(THF)Sm(SC_6H_2Pr^i_3\text{-}2,4,6)_3$	6	3	Sm—S	2.740(3)	[56]
$(py)_3Yb(SPh)_3$	6	3	Yb—S	2.647(4) average	[64]
$(py)_3Yb(SC_6H_2Pr^i_3\text{-}2,4,6)_3$	6	3	Yb—S	2.648(7) average	[56]
$(THF)_3Er(SePh)_3$	6	3	Er—Se	2.7766(7)	[65]
$(THF)_3Yb(SePh)_3$	6	3	Yb—Se	2.774(3)	[66]
$(THF)_3YbI_2[SC_6H_3(C_6H_2Pr^i_3\text{-}2,4,6)_2\text{-}2,6]$	6	3	Yb—S	2.581(2)	[106]
$[(py)_2Yb(SePh)_2(\mu\text{-}SePh)_2Li(py)_2]$	6	3	Yb—Se	2.772(2) average	[119]
	6	3	Yb—μ-Se	2.823	
$(py)_3Yb(SC_5H_4N)_2$	7	2	Yb—S	2.884(2) average	[71]
$(py)_5Yb(TePh)_2)$	7	2	Yb—Te	3.282(3) average	[62]
$[Sm(Tp^{Me2})_2SC_6H_4Me\text{-}4]$	7	3	Sm—S	2.8620(9)	[45]
$[Sm(Tp^{Me2})_2SePh]$	7	3	Sm—Se	2.9621(3)	[45]
$[Sm(Tp^{Me2})_2SeC_6H_4Bu^t\text{-}4]$	7	3	Sm—Se	2.9457(3)	[45]
$[Sm(Tp^{Me2})_2(TePh)]$	7	3	Sm—Te	3.1874(4)	[45]
$(THF)_3Ho(SC_6F_5)_3$	7	3	Ho—S	2.7174(14) average	[68]
$(py)_4Yb(SC_6F_5)_3$	7	3	Yb—S	2.758(2)average	[68]
$(THF)_4Eu(\mu\text{-}SePh)_3Zn(SePh)$	7	2	Eu—μ-Se	3.207(2) average	[74]
$[Na(18c6)(py)_2]_2[Na(18c6)(py)][Nd(dddt)_3(py)]$	7	3	Nd—S	2.857(2)	[129]
$(py)_4Eu(SC_5H_4N)_2$	8	2	Eu—S	3.046(4) average	[70]
$(THF)_2(Bipy)Eu(SC_5H_4N)_2$	8	2	Eu—S	3.007(3) average	[70]
$(THF)_2Eu(\mu\text{-}SePh)_6Ph_2$	8	2	Eu—μ-Se	3.287(5) average	[76]
$(py)_4Sm(SC_6F_5)_3$	8	3	Sm—S	2.836(3) average	[68]
$(DME)_2Er(SC_6F_5)_3$	8	3	Er—S	2.7040(16) average	[68]
$[(DME)_3La(SC_6F_5)_2]_2[Hg_2(SC_6F_5)_6]$	8	3	La—S	2.9106(10) average	[69]
$[(DME)_3Ce(SC_6F_5)_2]_2[Hg_2(SC_6F_5)_6]$	8	3	Ce—S	2.8863(12) average	[69]
$[(DME)_3Pr(SC_6F_5)_2]_2[Hg_2(SC_6F_5)_6]$	8	3	Pr—S	2.8619(8) average	[69]
$[(DME)_3Nd(SC_6F_5)_2]_2[Hg_2(SC_6F_5)_6]$	8	3	Nd—S	2.8486(18) average	[69]
$[(DME)_3Sm(SC_6F_5)_2]_2[Hg_2(SC_6F_5)_6]$	8	3	Sm—S	2.8159(15) average	[69]
$[(DME)_3Gd(SC_6F_5)_2]_2[Hg_2(SC_6F_5)_6]$	8	3	Gd—S	2.8040(10) average	[69]
$(DMSO)_2Sm(C_5H_4NOS)_3$	8	3	Sm—S	2.894(3) average	[123]
$[NHEt_3][(py)_2Sm\{C_6H_5P(C_6H_3S\text{-}2)_2\}_2]$	8	3	Sm—S	2.856(2) average	[116]
$[Sm(Tp^{Me2})_2(SC_5H_4N)]$	8	3	Sm—S	2.862(4)	[46]
$[Sm(Tp^{Me2})_2(SeC_5H_4N)]$	8	3	Sm—Se	3.00 average	[46]
Binuclear complexes					
$[\{(ArNC(Bu^t))_2CH\}Sc(TeCH_2SiMe_3)(\mu\text{-}Te)]_2$	4	3	Sc—Te	2.8326(4) average	[137]
			Sc—μ-Te	2.7088(4) average	
$[\{(THF)((Me_3Si)_2N)_2La\}_2(\mu\text{-}SPh)(\mu\text{-}Cl)]$	5	3	La—μ-S	2.9333(7) average	[165]
$[\{(THF)((Me_3Si)_2N)_2La\}(\mu\text{-}SePh)]_2$	5	3	La—μ-Se	3.110 average	[165]
$[(THF)_3Sm(SC_6H_2Pr^i_3\text{-}2,4,6)(\mu\text{-}SC_6H_2Pr^i_3\text{-}2,4,6)]_2$	6	2	Sm—S	2.908(6)	[56]
			Sm—μ-S	3.017(3) average	
$[(THF)_3Eu(SC_6H_2Pr^i_3\text{-}2,4,6)(\mu\text{-}SC_6H_2Pr^i_3\text{-}2,4,6)]_2$	6	2	Eu—S	2.898(4)	[56]
			Eu—μ-S	3.016(3) average	
$[(bipy)Yb(SBu^t)_2(\mu\text{-}SBu^t)]_2$	6	3	Yb—S	2.623(3) average	[101]
			Yb—μ-S	2.747(3) average	
$[(THF)_3I_2Sm(\mu\text{-}SC_6H_4(Me_2N)\text{-}4)]_2$	7	3	Sm—μ-S	2.8496(11) average	[49]
$[(py)_3Tm(SPh)_2(\mu\text{-}SPh)]_2$	7	3	Tm—S	2.8086(11) average	[65]
			Tm—μ-S	2.8143(10) average	

Table 2 (*Continued*)

Compound	c.n.[a]	o.s.[b]	Bond type	Bond length (Å)	Ref.
$[(py)_3Eu(\mu\text{-}SPh)_2(\mu_3\text{-}SPh)Hg(SPh)]_2$	7	2	Eu—μ-S	3.027(3) average	[75]
			Eu—μ_3-S	3.019(3) average	
$[(py)_3Eu(\mu\text{-}SPh)_2(\mu_3\text{-}SPh)Cd(SPh)]_2$	7	2	Eu—μ-S	3.023(3) average	[75]
			Eu—μ_3-S	3.046(3) average	
$[(THF)_3Eu(\mu\text{-}SPh)_2(\mu_3\text{-}SPh)Zn(SPh)]_2$	7	2	Eu—μ-S	2.988(2) average	[75]
			Eu—μ_3-S	3.052(2) average	
$[(py)_3Sm(SePh)_2(\mu\text{-}SePh)]_2$	7	3	Sm—Se	2.9048(11) average	[65]
			Sm—μ-Se	3.0181(14) average	
$[(py)_3Tm(SePh)_2(\mu\text{-}SePh)]_2$	7	3	Tm—Se	2.8314(8) average	[64]
			Tm—μ-Se	2.9529(8) average	
$[(py)_2Sm(SePh)(\mu\text{-}SePh)_3Na(py)_2]_2$	7	3	Sm—μ-Se	2.980(2)	[74]
$[(py)_2Er(SePh)(PhNNPh)]_2$	7	3	Er—Se	2.7935(7) average	[72]
$[(py)_2Ho(TePh)(PhNNPh)]_2$	7	3	Ho—Te	3.0630(15) average	[72]
$[(THF)_2Sm(SC_6F_5)_2(\mu\text{-}SC_6F_5)]_2$	8	3	Sm—S	2.756(4) average	[67]
			Sm—μ-S	2.891(4) average	
$[(THF)_3Ce(SC_6F_5)_2(\mu\text{-}SC_6F_5)]_2$	8	3	Ce—S	2.8632(17) average	[68]
			Ce—μ-S	3.0235(19) average	
Trinuclear complexes					
$[\{(DME)_2Yb(\mu\text{-}SePh)_3\}_2Yb][Yb(SePh)_4(DME)]$	6	3	Yb—μ-Se	2.819 average	[66]
	7	2	Yb—μ-Se	3.035 average	
	6	3	Yb—Se	2.786 average	
Tetranuclear complex					
$Li[\{(Me_3Si)_2N\}_4(\mu_4\text{-}Cl)Nd_4(\mu\text{-}SPh)_8]$	6	3	Nd—μ-S	2.921 average	[36]
$[(py)_2Sm(SPh)_3]_4$	7	3	Sm—S	2.754(3) average	[65]
			Sm—μ-S	2.855(3) average	
$[(Me_3Si)_2N]_4(\mu_4\text{-}Cl)Sm_4(\mu\text{-}SPh)_4(\mu_3\text{-}Cl)_4Li(THF)$	6	3	Sm—μ-S	2.824 average	[36]
$(THF)_6Yb_4S(SS)_4(SC_6F_5)_2$	7	3	Yb—S	2.675(3) average	[78]
$(THF)_6Yb_4Se(SeSe)_4(SC_6F_5)_2$	7	3	Yb—S	2.667(3) average	[78]
$(py)_8Yb_4(SeSe)_2Se_2(\mu\text{-}SPh)_2(SPh)_2$	7	3	Yb—S	2.675(3)	[79]
			Yb—μ-S	2.770(3) average	
			Yb—μ_3-Se	2.790(2) average	
			Yb—μ-Se	2.854(2) average	
$[(THF)_8Nd_4Se(SePh)_8][Zn_8Se(SePh)_{16}]$	7	3	Nd—μ-Se	2.969 average	[81]
			Nd—μ_4-Se	2.960 average	
$[(THF)_8Sm_4Se(SePh)_8][Zn_8Se(SePh)_{16}]$	7	3	Sm—μ-Se	2.97 average	[81]
			Sm—μ_4-Se	2.93 average	
$(py)_8Yb_4Se_4(SePh)_4$	6	3	Yb—Se	2.842(2) average	[77]
			Yb—μ_3-Se	2.781(2) average	
$(py)_8Yb_4(SeSe)_3Se(SeSeSePh)_2(Se_{0.38}SePh)$	7	3	Yb—Se	2.749(2)	[79]
$(py)_8Yb_4(SeSe)_2Se_2(SeSeTePh)_2(SeTePh)$	7/8	3	Yb—Se	2.760(3)	[79]
$(DME)_4Yb_4Se(SePh)_8$	7	2/3	Yb—μ-Se	2.958 average	[86]
			Yb—μ_4-Se	2.833 average	
$(DME)_4Sm_2Yb_2Se(SePh)_8$	7	2/3	Ln—μ-Se	3.020 average	[86]
			Ln—μ_4-Se	2.887 average	
$(DME)_4Nd_2Yb_2Se(SePh)_8$	7	2/3	Ln—μ-Se	3.025 average	[86]
			Ln—μ_4-Se	2.894 average	
$(DME)_4Sm_4Se(SePh)_8$	7	2/3	Sm—μ-Se	3.037 average	[86]
			Sm—μ_4-Se	2.930 average	
$(py)_9Sm_4(\mu_4\text{-}Te)(\mu\text{-}Te_2)_2(\mu\text{-}\eta^2,\eta^2\text{-}Te_5Ph)(TePh)$	7	3	Sm—Te	3.067(2)	[80]
	7		Sm—μ-Te	3.1184(18) average	
	8		Sm—μ-Te	3.1588(19) average	
	7		Sm—μ_4-Te	3.0981(18) average	
	8		Sm—μ_4-Te	3.2528(18) average	

Table 2 (*Continued*)

Compound	c.n.[a]	o.s.[b]	Bond type	Bond length (Å)	Ref.
$(py)_8Tb_4(\mu_4\text{-Te})(\mu\text{-Te}_2)_2(\mu\text{-}\eta^2,\eta^2\text{-Te}_5Ph)(Te_{0.1}TePh)$	7	3	Tb—Te	2.964(3)	[80]
	7		Tb—μ-Te	3.079(3) average	
	8		Tb—μ-Te	3.132(3) average	
	7		Tb—μ_4-Te	3.076(3) average	
	8		Tb—μ_4-Te	3.317(3)	
$(py)_7Tm_4(\mu_4\text{-Te})[(TeTe)_4TePh](Te_{0.6}TePh)$	7	3	Tm—Te	3.033(4)	[80]
			Tb—μ-Te	3.037(8) average	
			Tb—μ_4-Te	3.083(8) average	
$(py)_8Er_4Hg_2Se_6(SePh)_4$	6	3	Er—Se	2.833(1)	[87]
$(py)_8Yb_4Cd_2Se_6(SePh)_4$	6	3	Yb—Se	2.8168(9)	[87]
$(py)_8Yb_4Hg_2Se_6(SePh)_4$	6	3	Yb—Se	2.813(1)	[87]
Pentanuclear complexes					
$[(Me_3Si)_2N]La_5O(SPh)_{10}LiCl_2(THF)_2$	6	3	La—μ-S	3.024(5) average	
	7	3	La—μ-S	2.856(5) average	
	7	3	La—μ_3-S	2.965(5) average	
	8	3	La—μ-S	2.977(5) average	
	8	3	La—μ_3-S	3.077(5) average	
Hexanuclear complexes					
$(py)_{10}Yb_6(SPh)_6$	6	3	Yb—S	2.674(3) average	[77]
			Yb—μ_3-S	2.649(3) average	
			Yb—μ_4-S	2.707(3) average	
Heptanuclear complexes					
$[Sm_7S_7(SePh)_6(DME)_7][Hg_3(SePh)_7]$	7/8	3	Sm—μ-Se	3.03 average	[85]
			Sm—μ_3-S	2.74 average	
			Sm—μ_4-S	2.83 average	
Octanuclear complexes					
$(THF)_8Sm_8S_6(SPh)_{12}$	7	3	Sm—μ-S	2.850(5) average	[83]
			Sm—μ_4-S	2.821(3) average	
$(THF)_8Tb_8S_6(SPh)_{12}$	7	3	Tb—μ-S	2.817(6) average	[83]
			Tb—μ_4-S	2.779(6) average	
$(py)_8Sm_8S_6(SPh)_{12}$	7	3	Sm—μ-S	2.843(5) average	[83]
			Sm—μ_4-S	2.814(4) average	
$(py)_8Er_8S_6(SPh)_{12}$	7	3	Er—μ-S	2.754(7) average	[83]
			Er—μ_4-S	2.744(2) average	
$(THF)_8Sm_8Se_6(SPh)_{12}$	7	3	Sm—μ-S	2.92 average	[84]
			Sm—μ_4-Se	2.88 average	
$(py)_8Sm_8Se_6(SePh)_{12}$	7	3	Sm—μ-Se	2.96 average	[84]
			Sm—μ_4-Se	2.94 average	
			Sm—μ_4-Se	2.93 average	
$(THF)_8Sm_8S_6(SePh)_{12}$	7	3	Sm—μ-Se	2.96 average	[84]
			Sm—μ_4-S	2.83 average	
$(THF)_8Sm_8Se_6(SePh)_{12}$	7	3	Sm—μ-Se	2.98 average	[85]
Polymer complexes					
$[(C_5Me_5)Sm(SC_6H_2Pr^i_3\text{-}2,4,6)(\mu\text{-}C_5Me_5)K(THF)]_\infty$	8	2	Sm—S	2.936(3)	[31]
$[(THF)_3Sm(\mu\text{-SePh})_3Zn(\mu\text{-SePh})]_n$	7	3	Sm—μ-Se	3.2575(13) average	[63]
$[(THF)Sm(SPh)_3]_{4n}$	7	3	Sm—μ-S	2.854(2) average	[65]
$[(THF)_4Nd(SePh)_9]_n$	7	3	Nd—μ-Se	3.006(5) average	[65]
	8		Nd—μ-Se	3.074(5) average	
$[(THF)_2Eu(\mu\text{-}SC_6F_5)_2]_n$	8	2	Eu—μ-S	3.025(3) average	[67]
$[(THF)_3Eu(\mu\text{-SePh})_2]_n$	7	2	Eu—μ-Se	3.14(1)	[120]
$[(py)_2Eu(\mu\text{-SePh})_2]_n$	6	2	Eu—μ-Se	3.10(3)	[120]
$[\{Na(18c6)(py)_2\}_{0.5}\{Na(18c6)(py)_{1.5}\}\{Na_{1.5}Nd(dddt)_3\}]_\infty$	6	3	Nd—μ-S	2.8564(19)	[129]
$[\{Na_3(18c6)_{1.5}Nd(dddt)_3(THF)\}]_\infty$	6	3	Nd—μ-S	2.886(2)	[129]
$[K_3(18c6)_{1.5}Nd(dddt)_3(py)]_\infty$	6	3	Nd—μ-S	2.8964(12)	[129]
$[Na_2(18c6)Na(py)_2Ce(dddt)_3(py)]_\infty$	6	3	Ce—μ-S	2.922(2)	[129]

[a] c.n.: Coordination number.
[b] o.s.: Oxidation state.

$[Ln(C_5Me_5)_2(dddt)]^-$ (Ln = Ce, Nd) are shorter than the corresponding ones in $[PEt_4][Ce(SC_5H_4N)_4]$ (2.928(3) Å), $[(DME)_3Nd(SC_6F_5)_2]_2[Hg_2(SC_6F_5)_6]$ (2.8486 Å).

The Sm atom in $(C_8H_8)Sm(SC_4H_5N)(HMPA)_2$ has a four-legged piano-stool geometry, coordinated by a planar η^8-C_8H_8 ring, a chelating pyridine-2-thiolate ligand, and two HMPA ligands while that in $(C_8H_8)Sm(SC_6H_2Pr^i_3$-2,4,6)$(HMPA)_2$ [60] takes a three-legged piano-stool geometry, coordinated by a planar η^8-C_8H_8 ring, a thiolate ligand, and two HMPA ligands.

The structures of $Cp_2YN(EPPh_2)_2$ (E = S, Se) and $Cp_2LnN(SePPh_2)_2$ (Ln = La, Gd, Er) [98,99] are similar, with each comprising a η^3-$[N(EPPh_2)_2]^-$ ligand coordinated through two E atoms and N atom to a Cp_2Y fragment. However, the structures of $Cp_2Yb(N(EPPh_2)_2$ (E = S, Se) [99] look somewhat different. The Yb atom is eight-coordinated by two E atoms of η^2-$[N(EPPh_2)_2]^-$ and two Cp groups.

3.1.2. Dinuclear complexes

There are a number of binuclear organolanthanide chalcogenolate complexes $[(C_5Me_5)_2Sm(\mu\text{-}EPh)]_2$ (E = S, Se, Te) [41], $[Cp_2Yb(\mu\text{-}SMe)]_2$, $[(Cp)_2Yb(\mu\text{-}SR)]_2$ (R = Bu^n, Pr^n) [91,92], $[(C_5H_4Bu^t)_2Ce(\mu\text{-}SPr^i)]_2$ [93], $[(C_5H_4Bu^t)_2Yb(\mu\text{-}SePh)]_2$ [113], and $[Cp_2Y(\mu\text{-}SBu^n)]_2$ [131]. They possess a dimeric structure in which each Ln atom is bound by two η^5-cyclopentadienyl rings and two bridging E (E = S, Se, Te) atoms. The molecular structure of $[(C_5Me_5)_2Sm(\mu\text{-}SPh)]_2$ is shown in Fig. 3. While in the solvated complexes $[(CpMe)_2Ln(SPh)(THF)]_2$ (Ln = La, Nd, Sm) [8,35,94] and $[(Cp)_2Yb(SC_6H_4(H_2N)$-2)$]_2$ [10], the pseudo-trigonal bipyramidal coordination geometry of each Ln atom is completed by two η^5-cyclopentadienyl rings, two bridging S atoms and a donor atom (N or O atom). The mean Yb–S bond distance of 2.794(2) Å in $[(Cp)_2Yb(SC_6H_4(H_2N)$-2)$]_2$ is slightly longer than those found in $[(Cp)_2Yb(\mu\text{-}SMe)]_2$ (average 2.705(3) Å), $[(Cp)_2Yb(\mu\text{-}SPr^n)]_2$ (average 2.705(1) Å), and $[(Cp)_2Yb(\mu\text{-}SBu^n)]_2$ (average 2.708(2) Å).

The structure of $[\{(C_8H_8)Nd\}_2(\mu\text{-}SBu^t)(\mu_3\text{-}SBu^t)_2Na(THF)_2]$ [115] is shown in Fig. 4. In this bimetallic complex, the two "$(C_8H_8)Nd$" units are connected by three SBu^t groups, two of which are coordinated to the $Na(THF)_2$ moiety. Each

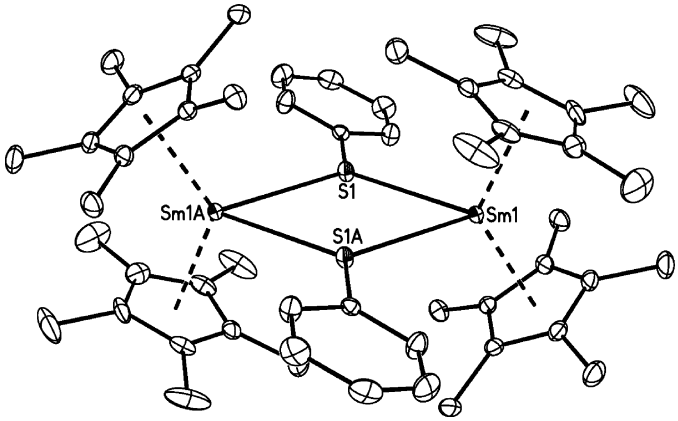

Fig. 3. Molecular structure of $[(Me_5C_5)_2Sm(SPh)]_2$ with thermal ellipsoids drawn at the 30% probability level. All H atoms are omitted for clarity [41].

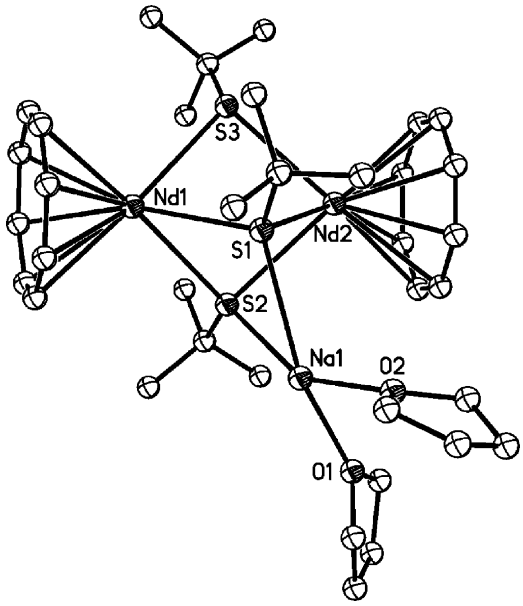

Fig. 4. Molecular structure of $[\{(C_8H_8)Nd\}_2(\mu\text{-}SBu^t)(\mu_3\text{-}SBu^t)_2Na(THF)_2]$ with thermal ellipsoids drawn at the 20% level. All H atoms are omitted for clarity [115].

Nd atom has a pseudo-tetrahedral coordination geometry. The two Nd tetrahedra share the common trigonal basis defined by the three S atoms. As expected, the mean Nd–μ_3-S bond length of 2.935(2) Å is longer than the Nd–μ_2-S bond distance (2.881(2) Å).

In the structure of the anion of $[Li(THF)_4]_2[(C_5H_4Bu^t)_2NdE_2C_2B_{10}H_{10}]_2$ (E = S, Se) [110] and $[Li(THF)_4]_2[(Cp)_2LnE_2C_2B_{10}H_{10}]_2$ (E = S, Ln = Nd, Yb; E = Se, Ln = Yb) [111], the Ln^{3+} ion is η^5-bound to two cyclopentadienyl rings and σ-bound to two bridging S/Se atoms of two dithiocarboranes and to one terminal S/Se atom of dithiocarborane in a distorted-pentahedral fashion.

Complexes $[\{Ln(C_5Me_5)_2(dddt)K(THF)_2\}_2]$ (Ln = Ce, Nd) [128] are isomorphous, and the structure of the cerium derivative is shown in Fig. 5. The centrosymmetric dimer is built up from two "$Ln(C_5Me_5)_2(dddt)$" units that are bridged by two $K(THF)_2$ fragments. Each lanthanide atom is in the pseudo-tetrahedral environment, which is quite invariably found in the complexes $[(Me_5C_5)_2Lu(\mu\text{-}SBu^t)_2Li(THF)_2]$ [88] and $(Cp)_2Lu(\mu\text{-}SePh)_2Li(THF)_2]$ [89]. The Ce–μ-S and Nd–μ-S bond lengths, with average values of 2.838(13) and 2.806(10) Å, respectively, are shorter than the corresponding ones in $[(C_5H_4Bu^t)_2Ce(\mu\text{-}SPr^i)]_2$ (2.882 Å) [93] and $[(C_5H_4Me)_2Nd(\mu\text{-}SPh)(THF)]_2$ (2.9290 Å) [8].

3.2. Lanthanide chalcogenolates with other N or O donor ligands

According to the number of lanthanide atom in these compounds, they are also sub-classified into nine categories: mono-, di-, tri-, tetra-, penta-, hexa-, hepta-, octa-nuclear and polymeric compounds, and we briefly discuss their important structural features in the following subsections.

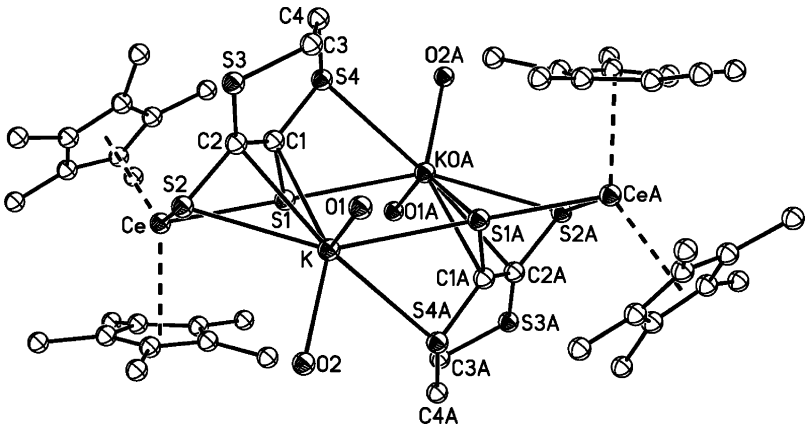

Fig. 5. Structure of $[\{Ce(C_5Me_5)_2(dddt)K(THF)_2\}_2]$ with thermal ellipsoids drawn at the 200% level. The carbon atoms of the THF and all H atoms are omitted for clarity [129].

3.2.1. Mononuclear complexes

3.2.1.1. Two-coordination. As the complexes Ln(II)[$SC_6H_3(C_6H_2Pr^i_3$-2,4,6)$_2$-2,6]$_2$ (Ln = Eu, Yb) [106] have similar structural features, only the molecular structure of the europium derivative is depicted in Fig. 6. Each Ln(II) atom is coordinated by two sulfur atoms from two *trans*-thiolate ligands. The mean Eu–S and Yb–S bond distances are 2.817(2) and 2.691(2) Å, respectively, and relatively shorter than the corresponding ones in $(py)_4Eu(SC_5H_4N)_2$ (3.045(3) Å) [70] and $(py)_4Yb(SPh)_2$ (2.827(1) Å) [62]. The *trans* influence usually result in the lengthening of Ln–E bonds in lanthanide chalcogenolates [62]. Therefore, the shortening of Eu–S and Yb–S bonds in these two compounds may be ascribed to additional η^6–π-interactions of Eu(II) or Yb(II) to two *o*-2,4,6-triisopropylphenyl rings of the terphenyl group. The resulting metal–π-arene interactions could be found in some other lanthanide complexes such as $[Yb_2(OC_6H_3Ph_2$-2,6)$_2(\mu$-$OC_6H_3Ph_2$-2,6)$_2]$, Yb(II)/Yb(III) trimetallic $[Yb_2(\mu$-$OC_6H_3Ph_2$-2,6)$_3]$ $[Yb(OC_6H_3Ph_2$-2,6)$_4]$ [160], Ln(η^6-$C_6H_3Bu^t_3$-1,3,5)$_2$ (M = Y, Gd, Ho) [161] and some bis(arene)lanthanide(0) derivatives [162,163]. The S–Ln–S bond angles are in the range of 141.89(4) and 142.73(8)°.

3.2.1.2. Three-coordination. In $Sm(SC_6H_2Bu^t_3$-2,4,6)$_3$ [102], the Sm atom is only coordinated by three terminal $SC_6H_2Bu^t_3$-2,4,6 ligand. Therefore, the average Sm–S bond distance of 2.645(9) Å is much shorter than those found in solvated compounds $[(HMPA)_3Sm(SPh)_3]$ (2.824(4) Å) [55], $[(py)_2(THF)Sm(SC_6H_2Pr^i_3$-2,4,6)$_3]$ (2.751(3) Å) [56], and $[(HMPA)_3Sm(SC_4H_5N)_2]I$ (2.870(8) Å) [57]. The "SmS_3" core is in an approximate plane with the average S–Sm–S bond angel of 119.4(2)°.

3.2.1.3. Four-coordination. In $[ArNC(Bu^t)CHC(Bu^t)NAr]Sc(TeCH_2SiMe_3)_2$ (Ar = $C_6H_3(Pr^i)_2$) [137], the Sc atom is coordinated by two N atoms from the β-diketiminato ligand and two Te atoms from $TeCH_2SiMe_3$ ligands, forming a distorted tetrahedral coordination geometry. The mean Sc–Te bond distance of 2.8137 Å is comparable to that in dimeric complex $[ArNC(Bu^t)CHC(Bu^t)NArSc(TeCH_2SiMe_3)]_2Te$ (2.8326 Å) [137].

3.2.1.4. Six-coordination. The structures of a set of $(HMPA)_3Ln(SPh)_3$ (Ln = Sm, Yb) [55], $(py)_2(THF)Sm(SC_6H_2Pr^i_3$-2,4,6)$_3$, $(py)_3Yb(SC_6H_2Pr^i_3$-2,4,6)$_3$ [56], $(py)_3Yb(SPh)_3$ [64], and $(THF)_3Ln(SePh)_3$ (Ln = Er, Yb) [65,66] are quite similar. Each Ln atom is bound to three chalcogenide atoms and three solvent molecules, forming a distorted octahedral geometry. In $(THF)_3YbI_2[SC_6H_3(C_6H_2Pr^i_3$-2,4,6)$_2$-2,6] [106],

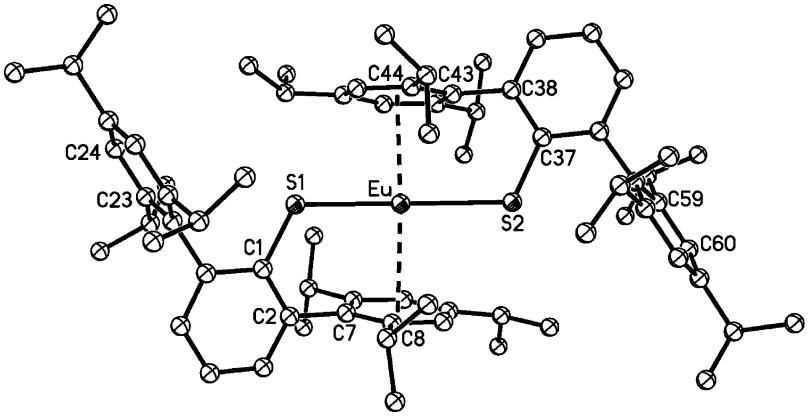

Fig. 6. Molecular structure of $Eu(SC_6H_3(C_6H_2{}^iPr_3$-2,4,6)$_2$-2,6)$_2$ with all H atoms and the minor parts of the disordered isopropyl groups omitted for clarity [106].

the central Yb atom shows a distorted octahedral coordination geometry with two iodine atoms, and one S atom from $SC_6H_3(C_6H_2Pr^i_3$-2,4,6)$_2$-2,6 ligands and three THF molecules. Despite the presence of the sterically crowded $SC_6H_3(C_6H_2Pr^i_3$-2,4,6)$_2$-2,6 ligand, the Yb–S bond length is 2.581(2) Å, which is even shorter than that in the two-coordinated compound $Yb(SC_6H_3(C_6H_2Pr^i_3$-2,4,6)$_2$-2,6)$_2$ (average 2.690 Å) [106].

3.2.1.5. Seven-coordination. The two complexes $(THF)_3Ln(SC_6F_5)_3$ (Ln = Ho, Er) [68] are isostructural, and the structural analysis reveals that the pentagonal bipyramidal geometry of each Ln atom is coordinated with three S atoms, one F atom and three O atoms. While, in the pyridine derivative $(py)_4Yb(SC_6F_5)_3$ [68], each Yb is bound to four pyridine molecules and three S atoms from SC_6F_5 ligands, forming a distorted-pentagonal bipyramidal geometry without any Yb–F bonding interaction.

The molecular structures of $[Sm(Tp^{Me,Me})_2(TePh)]$, $[Sm(Tp^{Me,Me})_2SC_6H_4Me$-4], $[Sm(Tp^{Me,Me})_2SePh]$, and $[Sm(Tp^{Me,Me})_2SeC_6H_4Bu^t$-4] [45] are similar. Each Sm atom is coordinated by a terminal chalcogenolate and two pyrazolylborates in η^3-fashion, forming a pentagonal bipyramidal fashion.

In the structure of the $[Nd(dddt)_3(py)]^{3-}$ trianoin of [Na(18-crown-6)(py)$_2$]$_2$[Na(18-crown-6)(py)][Nd(dddt)$_3$(py)] [129], each Nd atom is in a very distorted square capped trigonal prismatic configuration, and the trigonal faces of the prism is defined either by S(1A), S(2A), S(1B) and S(1C), S(2B), S(2C) atoms or S(1A), S(1C), S(2C) and S(1B), S(2B), N(1) atoms with N(1) or S(2A) in capping positions (Fig. 7). The average Nd–S bond distance of 2.86(2) Å is close to the corresponding one found in $[(DME)_3Nd(SC_6F_5)_2]_2[Hg_2(SC_6F_5)_6]$ (2.8486(18) Å) [69].

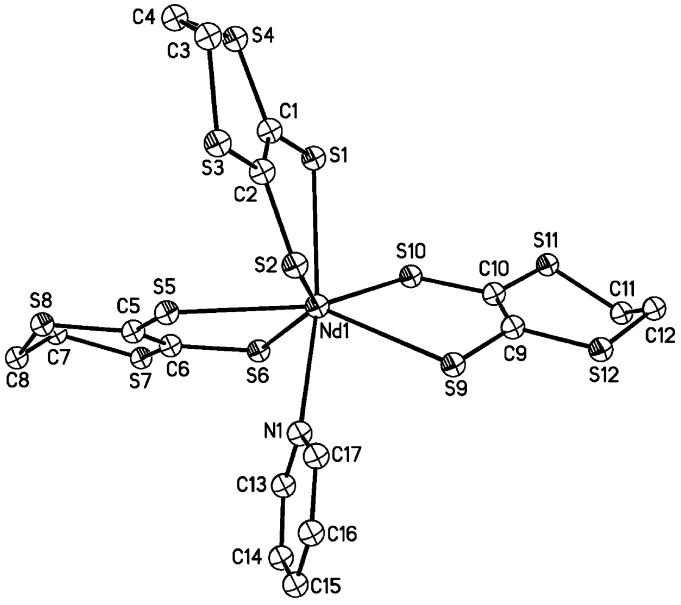

Fig. 7. Structure of the $[Nd(dddt)_3(py)]^{3-}$ anion in compound [Na(18-crown-6)(py)$_2$]$_2$[Na(18-crown-6)(py)][Nd(dddt)$_3$(py)] with displacement ellipsoids drawn at 50% probability level. All H atoms are omitted for clarity [129].

3.2.1.6. Eight-coordination. In $(DME)_2Er(SC_6F_5)_3$ and $(py)_4Sm(SC_6F_5)_3$ [68], each Ln atom is bound to four O or N atoms from DME or pyridine molecules, three S atoms and one F atom from SC_6F_5 ligands. The mean Ln–S distances are 2.836(3) Å for Ln = Er, and 2.7040(16) Å for Ln = Sm.

Each Sm atom in $[Sm(Tp^{Me2})_2(EC_5H_4N)]$ (E = S, Se) [46] is eight-coordinated by two pyrazolylborate ligands in a tridentate fashion and by the chalcogenolate ligand in a bidentate fashion. The Sm–S bond distance of 2.862(4) Å is consistent with those in $(py)_3Yb(SC_5H_4N)_2$ (2.889(2) Å) [71], but is slightly shorter than those found in $[(HMPA)_3Sm(SC_5H_4N)_2]I$ (average 2.870(3) Å) [57] and in $(C_8H_8)Sm(SC_5H_4N)(HMPA)_2$ (2.932(7) Å) [60].

Compound $(DMSO)_2Sm(C_5H_4NOS)_3$ [123] crystallizes as a bisolvated complex, in which the Sm atom is eight-coordinated by three S and three O atoms from C_5H_4NOS ligands and two O atoms from two monodentate DMSO molecules.

3.2.1.7. Night-coordination. Compounds $[(DME)_3Ln(SC_6F_5)_2]_2[Hg_2(SC_6F_5)_6]$ (Ln = La, Ce, Pr, Nd, Sm, Gd) [69] are isostructural. The structure of the cation in the samarium derivative is shown in Fig. 8. In the cations of these complexes, each Ln is chelated by three bidentate DME ligands distributed on one side of the metal. There are two terminal thiolates on the other side, one of which also coordinates to the Ln through a dative bond to the *ortho* fluoride F atom. The Ln–S bond distances decrease along with the ionic radii in the order of La > Ce > Pr > Nd > Sm > Gd.

3.2.2. Dinuclear complexes

3.2.2.1. Four-coordination. The compound $[\{((Me_3Si)_2N)_2Eu\}(\mu\text{-}SBu^t)]_2$ [164], which is isostructural to the Gd analogue [107], is a dimer in which two $\{((Me_3Si)_2N)_2Eu\}$ moieties are bridged by two μ-SBu^t ligands with a crystallographic inversion center lying at the midpoint of the Eu···Eu line. Each Eu atom is coordinated by two μ-S and two N atoms to form a distorted tetrahedral geometry.

$[ArNC(Bu^t)CHC(Bu^t)NArSc(TeCH_2SiMe_3)]_2Te$ [137] is a dinuclear complex with one bridging telluride linking two $[ArNC(Bu^t)CHC(Bu^t)NArSc(TeCH_2SiMe_3)]$ fragments. The tetrahedral coordination sphere of the Sc atom is completed by two N atoms, one μ-Te atom and one terminal Te atom from the $TeCH_2SiMe_3$ ligand.

3.2.2.2. Five-coordination. X-ray analysis revealed that compound $[\{((Me_3Si)_2N)_2La(THF)\}_2(\mu\text{-}SPh)(\mu\text{-}Cl)]$ [165] contains two $\{((TMS)_2N)_2La(THF)\}^+$ fragments that are interconnected by one μ-Cl^- and one μ-SPh^-, forming a dimeric structure with a crystallographic C_2-axis running along the Cl(1)···S(1)···C(13)···C(16) line (Fig. 9). La(1) and La(1A) adopt a distorted square pyramidal geometry, coordinated by one μ-Cl, one μ-S (SPh), one O (THF), and two N $\{(TMS)_2N\}$ atoms.

3.2.2.3. Six-coordination. As shown in Fig. 10, compound $[(2,2'\text{-bipy})Yb(SBu^t)_2(\mu\text{-}SBu^t)]_2$ [101] is a centrosymmetric dimer, in which each Yb atom is coordinated by one μ-SBu^t,

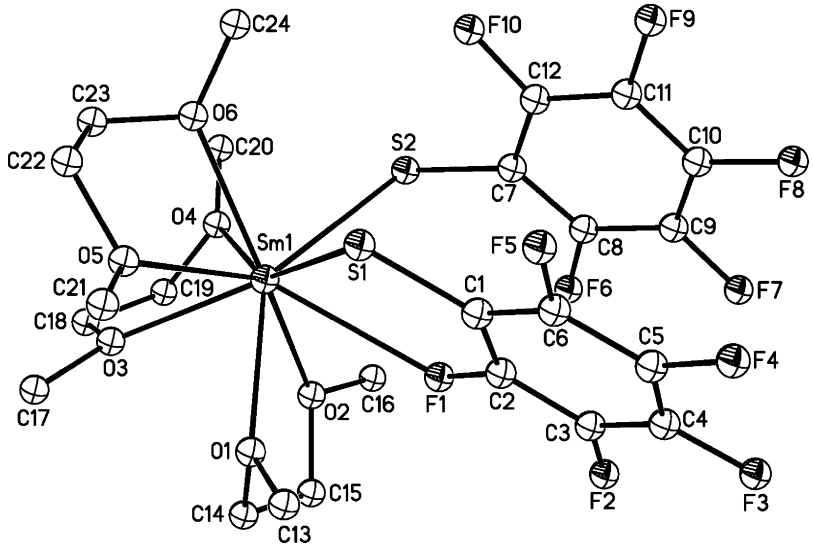

Fig. 8. Structure of the cation in $[(DME)_3Ln(SC_6F_5)_2]_2[Hg_2(SC_6F_5)_6]$. Thermal ellipsoids are drawn at the 50% probability level. All H atoms are omitted for clarity [69].

two terminal SBu^t ligands, and two N atoms from 2,2′-bipy, forming an approximately octahedral coordination geometry.

3.2.2.4. Seven-coordination. Compound $[(THF)_3I_2Sm(\mu\text{-}SC_6H_4(Me_2N)\text{-}4)]_2$ [49] (Fig. 11) consists of two "$Sm(THF)_3I_2$" units interconnected by two μ-$SC_6H_4Me_2N$-4 ligands, forming a dimeric structure with a crystallographic center of symmetry at the midpoint of the separation of the two Sm atoms.

In the complexes $[(py)_2Er(SePh)(PhNNPh)]_2$ and $[(py)_2Ho(TePh)(PhNNPh)]_2$ [72], two Ln(III) ions are bridged by a terminal EPh, a pair of η^2-coordinated (PhNNPh) dianions, and two neutral pyridines saturating the Ln coordination sphere. The Er–Se and Ho–Te bond distances are 2.7935(7) and 3.0630(15) Å, respectively.

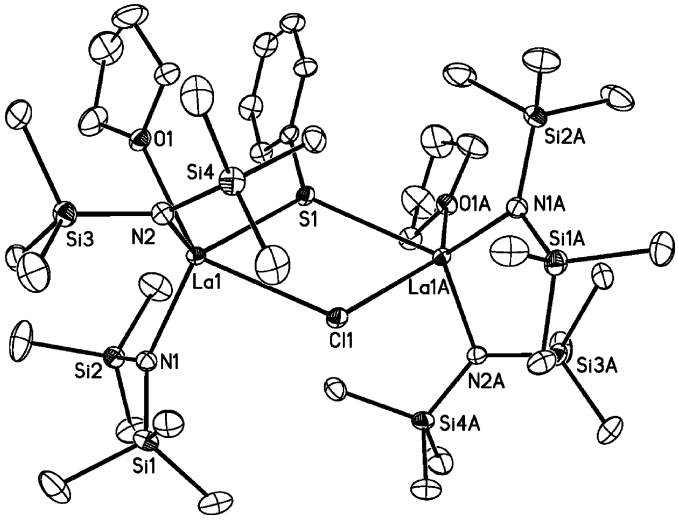

Fig. 9. Molecular structure of $[\{((Me_3Si)_2N)_2La(THF)\}_2(\mu\text{-}SPh)(\mu\text{-}Cl)]$ with 30% probability. All hydrogen atoms are omitted for clarity.

The dimeric structures of $[(py)_3Tm(SPh)_2(\mu\text{-}SPh)]_2$ and $[(py)_3Ln(SePh)_2(\mu\text{-}SePh)]_2$ (Ln = Sm, Tm) [64,65] are similar. Each Ln atom is coordinated by two bridging μ-EPh ligands, two terminal EPh ligands and three pyridine molecules, forming a severely distorted-pentagonal bipyramidal geometry.

3.2.2.5. Eight-coordination. Compound $[(THF)_2Sm(SC_6F_5)_2(\mu\text{-}SC_6F_5)]_2$ [67] is a dimer with a pair of thiolates bridging the two eight-coordinate Sm(III) ions. The two terminal thiolates chelate to each Sm via Sm–S and Sm–F bonds, while the bridging thiolates do not interact through the fluoride. Two THF molecules further complete its inner coordination sphere. The mean Sm–S bond length of 2.755(4) Å is longer than that observed in $Sm(SC_6H_2Bu^t_3\text{-}2,4,6)_3$ (2.645(9) Å) [102]. The mean Sm–μ–S bond length (2.891(4) Å) is much shorter than that in $[(THF)_3Sm(SC_6H_2Pr^i_3\text{-}2,4,6)_3]_2$, (3.017(6) Å) [58]. Compound $[(THF)_3Ce(SC_6F_5)_3]_2$ [68] is also a dimer, with a pair of bridging thiolates connecting the two eight-coordinate Ce(III) ions. One F atom and two S atoms from another two SC_6F_5 ligands and three O atoms from THF molecules are further bound to Ce to complete its primary coordination sphere. The terminal and bridging Ce–S bond distances are 2.8632(17) and 3.0235(19) Å, respectively.

3.2.3. Trinuclear complexes

Only one compound is known: $[\{(DME)_2Yb(\mu\text{-}SePh)_3\}_2Yb][Yb(SePh)_4(DME)]$ [66]. The structure of the anion in the complex is shown in Fig. 12. The internal Yb atom in this anion is connected with two Yb atoms by three μ-SePh ligands. The oxidation states of terminal and internal Yb atoms are +2 and +3, respectively. The octahedral coordination sphere of Yb(4) atom is octahedrally completed by six μ-Se atoms while the Yb(5) and Yb(5A) are coordinated by three Se atoms and four O atoms from two DME ligands, forming a severely distorted-pentagonal bipyramidal geometry.

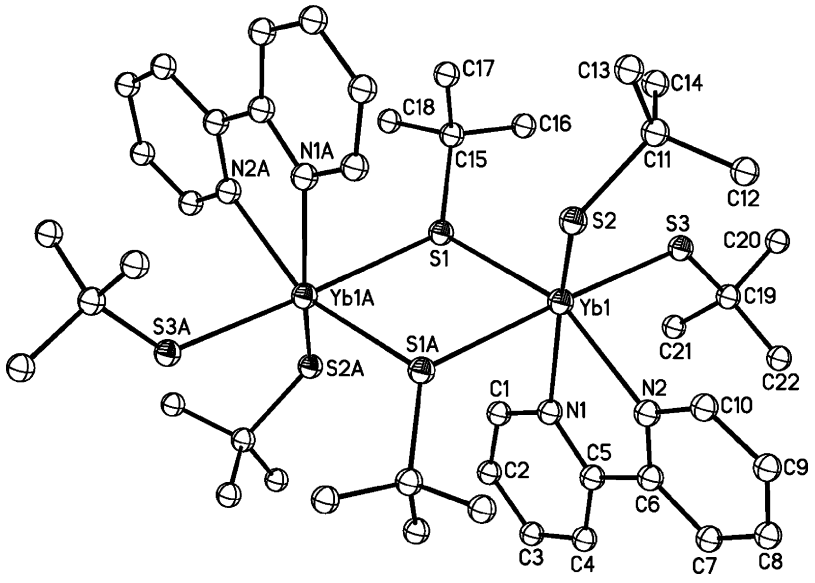

Fig. 10. Molecular structure of $[(2,2'\text{-bipy})Yb(SBu^t)_2(\mu\text{-}SBu^t)]_2$ with 20% probability. All hydrogen atoms are omitted for clarity [101].

The average Yb(4)–Se bond distance (2.819(2) Å) is much shorter than the mean Yb(5)–Se bond length (3.035(3) Å), which may be due to their different oxidation states.

3.2.4. Tetranuclear complexes

Tetranuclear lanthanide chalcogenolate and/or chalcogenide clusters include: $(py)_8Yb_4Se_4(SePh)_4$ [77], $[(py)_2Sm(SPh)_3]_4$ [65], $(py)_8Yb_4(SeSe)_2(Se)_2(\mu\text{-}SPh)_2(SPh)_2$ [79], $[(THF)_6Yb_4(SePh)_2(\mu\text{-}SePh)_6(\mu_3\text{-}O)_2]$ [66], $[(Me_3Si)_2N]_4(\mu_4\text{-}Cl)Sm_4(\mu\text{-}SPh)_4(\mu_3\text{-}Cl)_4Li(THF)$ [36], $Li[\{(Me_3Si)_2N\}_4(\mu_4\text{-}Cl)Nd_4(\mu\text{-}SPh)_8]$ [36], $(THF)_6Yb_4E(EE)_4(SC_6F_5)_2$ (E = S, Se) [78], $(py)_8Yb_4(SeSe)_3Se(SeSeSePh)(Se_{0.38}SePh)$, $(py)_8Yb_4(SeSe)_2Se_2(SeSeTePh)(SeTePh)$ [79], $(py)_8Ln_4(\mu_4\text{-}Te)(\mu\text{-}TeTe)_2(\mu\text{-}\eta^2,\eta^2\text{-}Te_5Ph)(Te_{0.1}TePh)$ (Ln = Tb, Ho), $(py)_9Sm_4(\mu_4\text{-}Te)(\mu\text{-}TeTe)_2(Te_5Ph)(TePh)$, $(py)_7Tm_4(\mu_4\text{-}Te)[(TeTe)_4TePh](Te_{0.6}TePh)$ [80], $[(THF)_8Ln_4Se(SePh)_8][Zn_8Se(SePh)_{16}]$ (Ln = Sm, Nd) [81], $(DME)_4Ln_4Se(SePh)_8]$ (Ln_4 = Sm_4, Yb_4, Sm_2Yb_2, Nd_2Yb_2) [86], and hetero six metal clusters $(py)_8Ln_4M_2Se_6(SePh)_4$ (Ln/M = Er/Cd, Er/Hg, Yb/Cd, Yb/Hg, Lu/Hg) [87].

As shown in Fig. 13, compound $(py)_8Yb_4Se_4(SePh)_4$ [77] consists of a cubane-like Yb_4Se_4 core in which four Yb(III) and four Se^{2-} ions alternatively occupy the eight vertices of a cube, with terminal SePh and two pyridine ligands completing each octahedral Yb(III) coordination sphere.

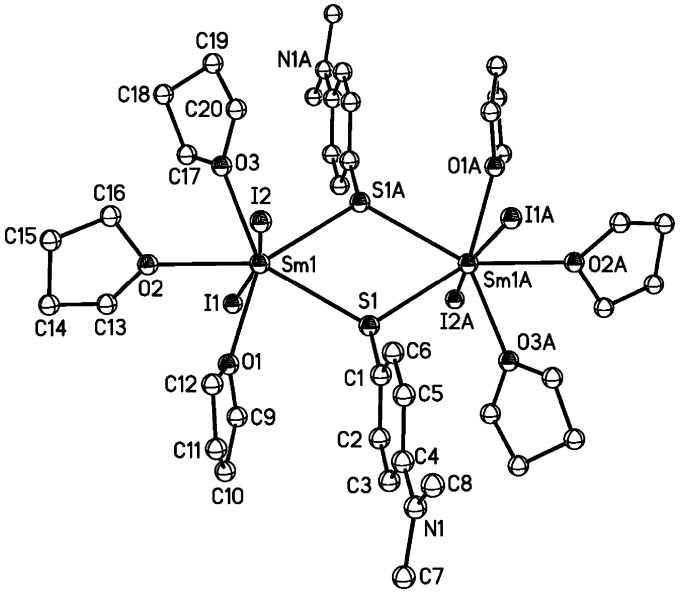

Fig. 11. Molecular structure of $[(THF)_3I_2Sm(\mu\text{-}SC_6H_4(Me_2N)\text{-}4)]_2$ with 30% probability. All hydrogen atoms are omitted for clarity [49].

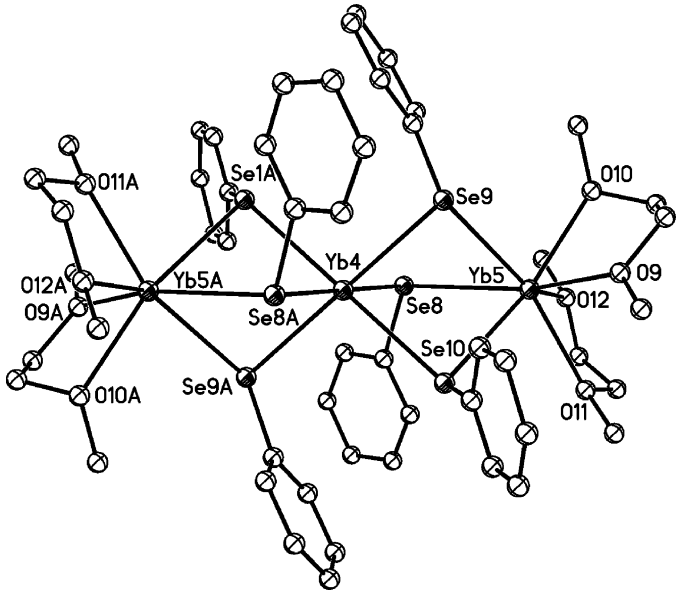

Fig. 12. Structure of the $[\{(DME)_2Yb(\mu\text{-}SePh)_3\}_2Yb]^+$ anion of $[\{(DME)_2Yb(\mu\text{-}SePh)_3\}_2Yb][Yb(SePh)_4(DME)]$. The H atoms are omitted for clarity [66].

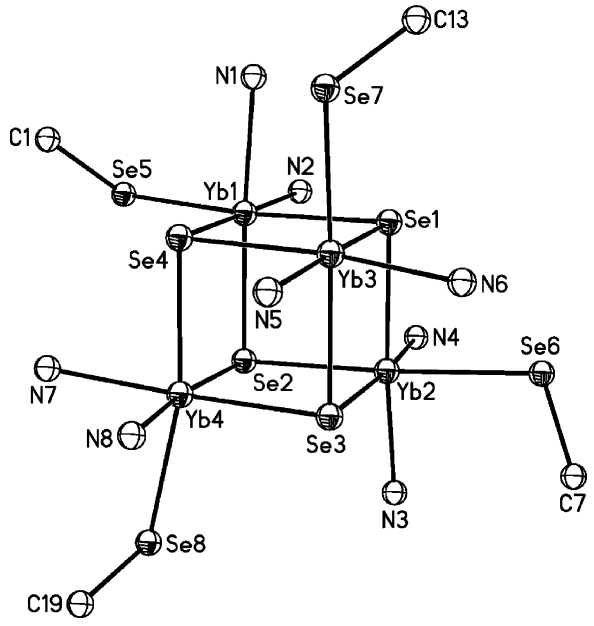

Fig. 13. Molecular structure of $(py)_8Yb_4Se_4(SePh)_4$. All hydrogen atoms and carbon atoms except for those bound to selenium atoms are omitted for clarity [77].

The mean Yb–Se bond distance of 2.842(1) Å is longer than those found in $(THF)_3Yb(SePh)_3$ (2.774(3) Å) [66] and $(THF)[PhC(NSiMe_3)_2]_2Yb(SePh)$ (2.805(1) Å) [43].

Compound $[(py)_2Sm(SPh)_3]_4$ [65] (Fig. 14) contains a non-linear array of four Sm(III) ions having a distorted-pentagonal bipyramidal geometry. The two external Sm(III) ions have terminal benzenethiolates in both axial and equatorial positions, and each of them is bridged to an internal Sm ion by a set of three μ-SPh ligands. The two internal Sm ions are connected by a pair of μ-SPh ligands. The coordination sphere of each inner Sm(III) ions is composed of two pyridine and five bridging μ-SPh ligands, while that of each outer Sm ion contains two pyridine, three bridging, and two terminal thiolate ligands. As expected, the mean Sm–μ-S bond distance (2.854(3) Å) is longer than that of the Sm–S bond length (2.754(3) Å).

The structure of $(py)_8Yb_4(SeSe)_2(Se)_2(\mu\text{-}SPh)_2(SPh)_2$ [79] (Fig. 15) contains a rhomboid array of Yb(III) ions with the Yb–Yb edges spanned by alternating pairs of μ-SPh and μ-SeSe ligands. The top and bottom of the rhombus are capped by μ_3-Se^{2-} ligands, and there are two terminal thiolate ligands coordinated to opposite Yb(III) ions. Yb(1) and Yb(2) are both seven-coordinated, but Yb(1) has bonds to two Se^{2-} ligands while Yb(2) coordinates a terminal thiolate and only one

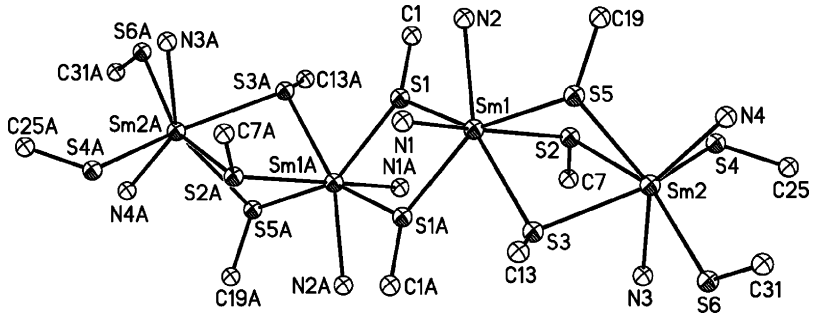

Fig. 14. Molecular structure of $[(py)_2Sm(SPh)_3]_4$. All hydrogen atoms and carbon atoms except for those bound to sulfur atoms are omitted for clarity [65].

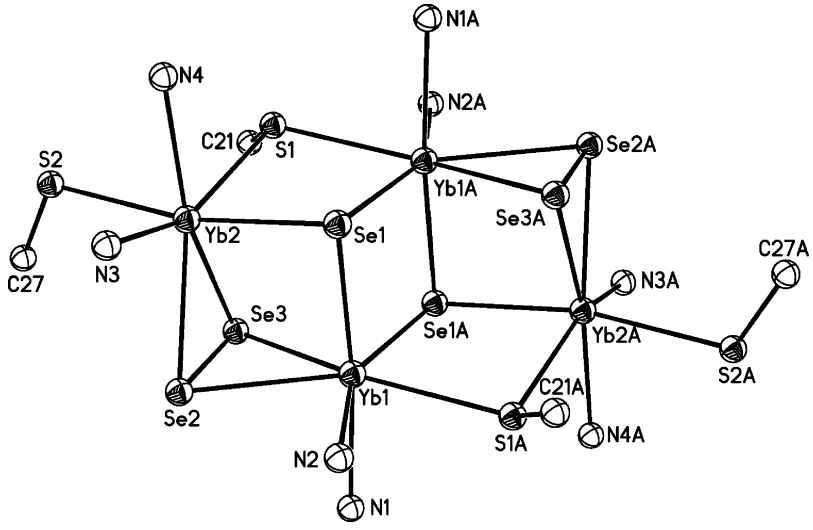

Fig. 15. Molecular structure of $(py)_8Yb_4(SeSe)_2(Se)_2(\mu_2\text{-}SPh)_2(SPh)_2$. All hydrogen atoms and carbon atoms except for those bound to sulfur atoms are omitted for clarity [79].

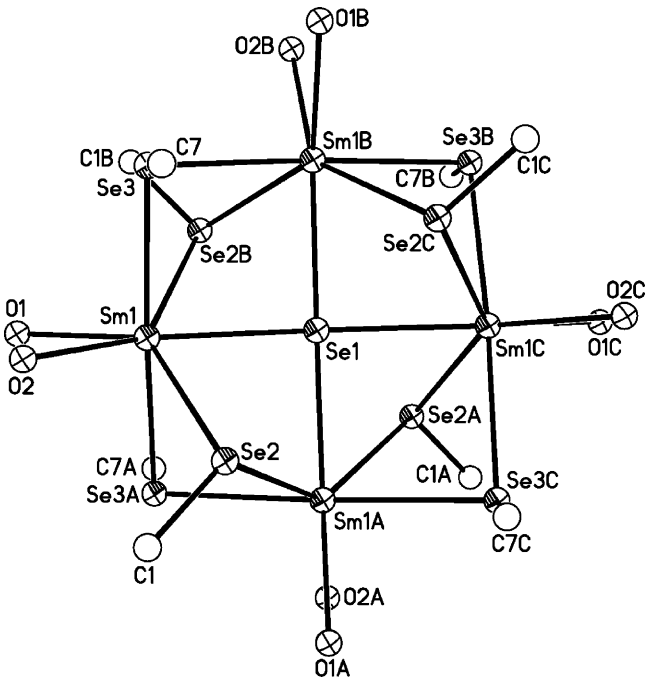

Fig. 16. Molecular structure of $(DME)_4Sm_4Se(SePh)_8$ with the C and H atoms removed for clarity [86].

Se^{2-}. The Yb–S and Yb–μ-S bond distances are 2.678(3) and 2.770(3) Å, respectively.

In the structure of $(DME)_4Sm_4Se(SePh)_8$ [86] (Fig. 16), a selenido ligand caps the square array of Ln ions, and each of the four edges is bridged by a pair of SePh ligands. A chelating DME ligand further saturates the primary coordination sphere of each seven-coordinate Sm. Similar structures are observed in other tetranuclear lanthanide compounds $(DME)_4Yb_4Se(SePh)_8$, $(DME)_4Nd_2Yb_2Se(SePh)_8$, $(DME)_4Sm_2Yb_2Se(SePh)_8$ [78], the anionic part in $Li[\{(Me_3Si)_2N\}_4(\mu_4\text{-}Cl)Nd_4(\mu\text{-}SPh)_8]$ [36], and the cationic part in $[(THF)_8Ln_4Se(SePh)_8][Zn_8Se(SePh)_{16}]$ (Ln = Sm, Nd) [81].

Compound $(THF)_6Yb_4S(SS)_4(SC_6F_5)_2$ [78] contains a Yb_4 square plane that is capped by a $\mu_4\text{-}S^{2-}$ ligand. The whole structure has an approximate C_{2v} symmetry. Each edge of the Yb_4 square is bridged by one disulfide SS^{2-} ligand. The structure is closely related to those of the other tetranuclear Ln/Se (or Te) clusters such as $(THF)_6Yb_4Se(SeSe)_4(SC_6F_5)_2$ [78], $(py)_8Yb_4(SeSe)_3Se(SeSeSePh)(Se_{0.38}SePh)$, $(py)_8Yb_4Se(SeSe)_3(SeSeTePh)(SeTePh)$ [79], $(py)_8Ln_4(\mu_4\text{-}Te)(\mu\text{-}TeTe)_2(\mu\text{-}\eta_2,\eta_2\text{-}Te_5Ph)(Te_{0.1}TePh)$, $(py)_9Sm_4(\mu_4\text{-}Te)(\mu\text{-}TeTe)_2(\mu\text{-}TeTeTe(Ph)TeTe)(TePh)$ and $(py)_7Tm_4(\mu_4\text{-}Te)[(TeTe)_4TePh](Te_{0.6}TePh)$ [80]. Formula representations such as $(Se_{0.38}SePh)$, $(Te_{0.1}TePh)$ or $(Te_{0.6}TePh)$ mean that the product is disordered, with a SeSePh/SePh occupancy of 0.38:0.62, or a TeTePh/TePh occupancy of 0.1:0.9, or a TeTePh/TePh occupancy of 0.60:0.40. All other related compounds in this paper may be explained in a similar way.

Compound $[(Me_3Si)_2N]_4(\mu_4\text{-}Cl)Sm_4(\mu\text{-}SPh)_4(\mu_3\text{-}Cl)_4Li(THF)$ [36] may be viewed as having a wine cup-shaped structure in which a $\{(Me_3Si)_2N\}_2Sm\}_4(\mu_4\text{-}Cl)(\mu\text{-}SPh)_4$ unit and Li atom are bridged by four μ_3-Cl bridges (Fig. 17). The

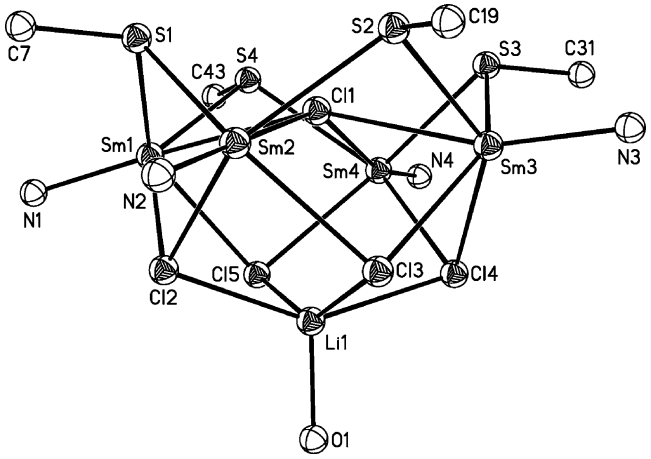

Fig. 17. Molecular structure of $[(Me_3Si)_2N]_4(\mu_4\text{-}Cl)Sm_4(\mu\text{-}SPh)_4(\mu_3\text{-}Cl)_4Li(THF)$ with labeling scheme and 50% probability. The Me_3Si, Ph groups and all hydrogen atoms are omitted for clarity [36].

five metals form a Sm_4Li square pyramidal framework in which the four Sm atoms occupy the four basal sites and one Li atom locates at the apical position. A four-fold crystallographic axis passes through the apical lithium atom and the center of the square pyramid base.

A set of heteronuclear clusters with common formula $(py)_8Ln_4M_2Se_6(SePh)_4$ (Ln/M = Er/Cd, Er/Hg, Yb/Cd, Yb/Hg, Lu/Hg) [87] is isostructural. Only the molecular structure of $(py)_8Er_4Hg_2Se_6(SePh)_4$ is shown in Fig. 18. The structure consists of a double-cubane framework in which two Er_3HgSe_4 single cubanes share the same Er(1)Se(2)Er(1A)Se(2A) plane. In each Er_3HgSe_4 single cubane, the Hg atom is coordinated by one $\mu_4\text{-}Se^{2-}$, two $\mu_3\text{-}Se^{2-}$ atoms and one selenolate, forming a distorted tetrahedral geometry. The three Ln atoms display an octahedral coordination geometry. Er(2) (or Er(2A)) coordinates to two $\mu_3\text{-}Se^{2-}$, and one $\mu_4\text{-}Se^{2-}$, two pyridine molecules, and

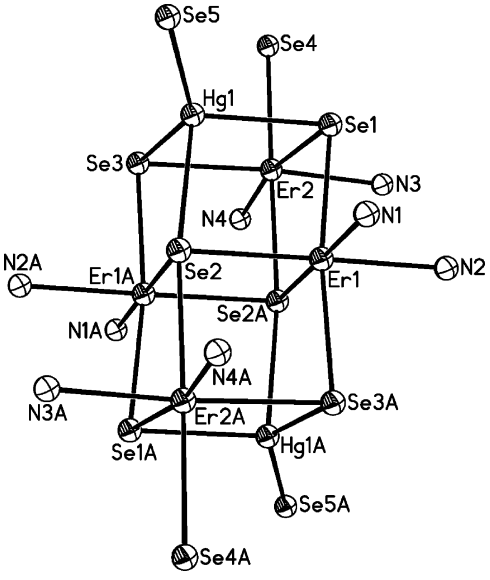

Fig. 18. Molecular structure of cluster $(py)_8Er_4Hg_2Se_6(SePh)_4$ with the C and H atoms omitted for clarity [87].

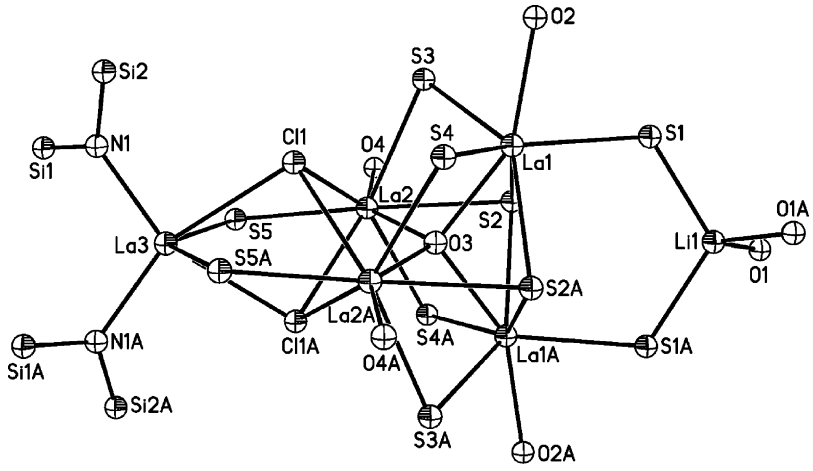

Fig. 19. Molecular structure of $[(Me_3Si)_2N]_2La_5O(SPh)_{10}LiCl_2(THF)_2$. The C atoms of THF, Me_3Si, Ph groups and all hydrogen atoms are omitted for clarity [165].

a terminal selenolate ligand, whereas Er(1) or (or Er(1A)) binds to two pyridine molecules, two μ_3-Se^{2-}, and two μ_4-Se^{2-}.

3.2.5. Pentanuclear complexes

In $[(Me_3Si)_2N]La_5O(SPh)_{10}LiCl_2(THF)_2$ [165] (Fig. 19), the central La_4O tetrahedral core is capped at two opposite sides by a $LaCl_2S_2$ unit and a S_2Li unit. The μ_4-O atom occupies a position in which it interacts with four La atoms in the center of the La_4 tetrahedron. It is noteworthy that the coordination geometry of the five La atoms in this compound may be classified into three sorts: a distorted squarecapped trigonal prismatic coordination geometry (La(1)/La(1A)), a distorted bisquarecapped trigonal prismatic coordination geometry (La(2)/La(2A)), and a distorted octahedral coordination geometry (La(3)).

3.2.6. Hexanuclear complexes

The structure of $(py)_{10}Yb_6S_6(SPh)_6$ [77] consists of two Yb_4S_4 cubane-like units sharing a Yb_2S_2 plane. The structure resembles those of the heteronuclear clusters $(py)_8Ln_4M_2Se_6(SePh)_4$ (Ln/M = Er/Cd, Er/Hg, Yb/Cd, Yb/Hg, Lu/Hg) [87], $(THF)_{10}Er_6S_6I_6$ [140] and $(THF)_{10}Yb_6Se_6I_6$ [143]. The average Yb–S bond distance of 2.674(3) Å, is comparable to that observed in $Yb[SC_6H_3(C_6H_2Pr^i_3\text{-}2,4,6)_2\text{-}2,6]_2$ (2.690(2) Å), but shorter than those found in $[(HMPA)_3Yb(SC_5H_4N)_2]I$ [57] (2.800 Å) and $(py)_4Yb(SC_6F_5)_3$ (2.758(2) Å).

3.2.7. Heptanuclear complexes

Only one compound $[Sm_7S_7(SePh)_6(DME)_7][Hg_3(SePh)_7]$ is known [85]. In the structure of the heptacationic cluster (Fig. 20), the six seven-coordinated (Sm(1), Sm(2), Sm(4)–Sm(7)) and one eight-coordinated Sm(III) (Sm(3)) ions form two square pyramids that share one Sm_3 face with four μ_3-S^{2-} (S(1), S(4), S(6), S(7)) and two μ_4-S^{2-} (S(2), S(5)) capping the external faces of the cluster, and one μ_4-S^{2-} (S(3)) bridging two reentrant Sm_3 faces. Each Sm coordination sphere is saturated with a chelating DME ligand.

3.2.8. Octanuclear complexes

Clusters belonging to this group include: $Ln_8S_6(SPh)_{12}(THF)_8$ (Ln = Ce, Pr, Nd, Sm, Gd, Tb, Dy, Ho, Er), $Ln_8S_6(SPh)_{12}(py)_8$ (Ln = Nd, Sm, Er), $(THF)_8Sm_8E_6(E'Ph)_{12}$ (E = Se, E′ = S, Se; E = S, E′ = Se), and $(py)_8Ln_8Se_6(SePh)_{12}$ (Ln = Sm, Nd) [83–85], and $(THF)_8Ln_8O_2Se_2(SePh)_{16}$ (Ln = Ce, Pr, Nd, Sm) [15]. These clusters have a similar cluster framework. As shown in Fig. 21, the structure of the representative compound $(THF)_8Sm_8S_6(SPh)_{12}$ [83] contains a cube of eight Sm(III) ions, in which each of the six faces is capped by one S^{2-} atom. Each of the 12 S atoms from the SPh ligands bridges one of the 12 edges. Each Sm atom is coordinated by three μ_4-S atoms, three μ_2-S atoms and one O atom (THF), forming a distorted-pentagonal bipyramidal geometry.

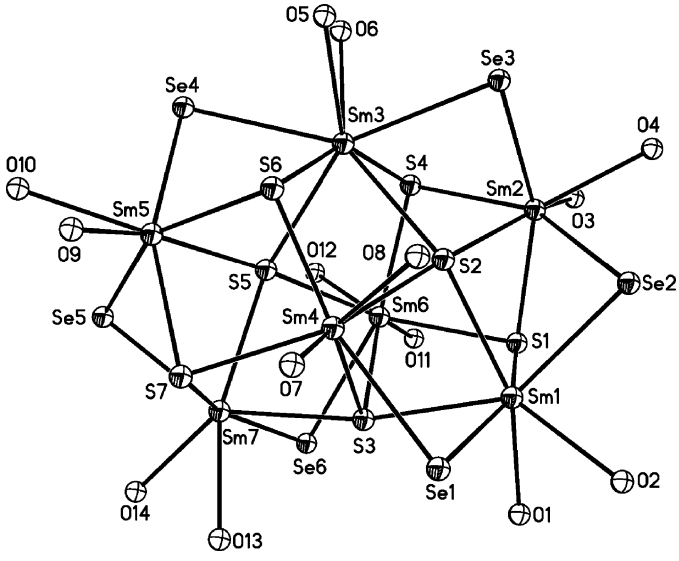

Fig. 20. The structure of the $[Sm_7S_7(SePh)_6(DME)_7]^+$ cation of $[Sm_7S_7(SePh)_6(DME)_7][Hg_3(SePh)_7]$. All C and H are omitted for clarity [85].

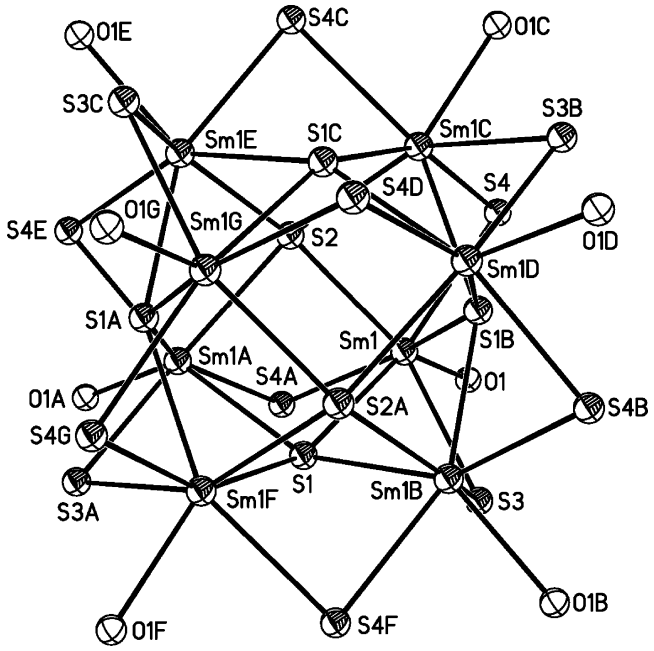

Fig. 21. Molecular structure of $(THF)_8Sm_8S_6(SPh)_{12}$ with all C and H atoms omitted for clarity [83].

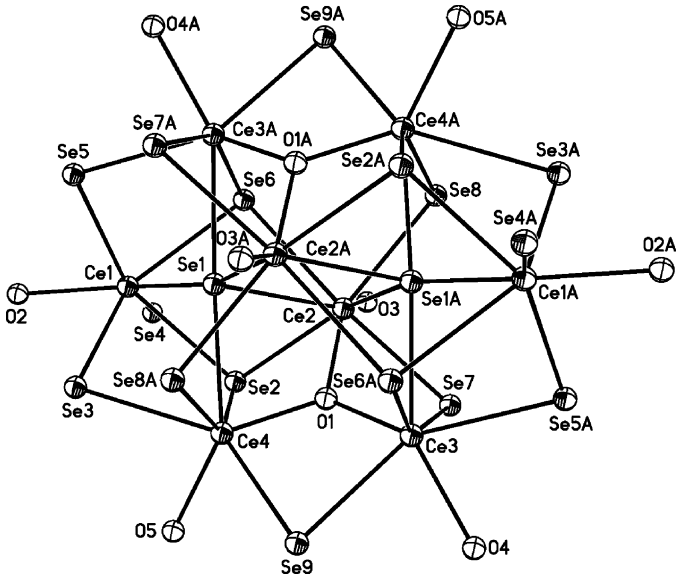

Fig. 22. Perspective view of the $(THF)_8Ce_8O_2Se_2(SePh)_{16}$ core, with the C and H atoms removed for clarity [15].

Complexes $(THF)_8Ce_8O_2Se_2(SePh)_{16}$ (Ln = Ce, Pr, Nd, Sm) [15] have similar structural features, and only the structure of cerium derivative is depicted in Fig. 22. In this isomorphous series, the eight Ln(III) ions are connected in the center by a pair of μ_3-O^{2-} ligands and μ_5-Se^{2-} ligands, with 14 bridging and two terminal selenolate ligands capping the cluster surface. There is a distinctly non-linear change in the bond length between Ln(2) and Se(6), an interaction that arguably can be described as a bond. As the lanthanide contraction progresses, average bond lengths between Ln and O^{2-}, Se^{2-}, O (THF), and SePh all decrease accordingly, with the exception of the Ln(2)–Se(6) separation, which varies from 3.39 Å (Ce) to 3.34 Å (Nd) to 3.63 Å (Sm), presumably in response to an increase in ligand–ligand repulsions as the Ln coordination spheres contract.

3.2.9. Polymeric complexes

The structure of $\{[(THF)Sm(SPh)_3]_4\}_\infty$ [65] (Fig. 23) resembles that of $[(THF)_4Nd_3(SePh)_9]_\infty$ [65]. The former one contains a 1D array of Ln(III) ions connected through sets of three doubly bridging SPh ligands, while a THF ligand further coordinated to each Sm(III), forming a distorted-pentagonal bipyramidal coordination geometry. The latter one also has a 1D chain structure in which Nd(III) ions are bridged by a set of three μ-SePh ligands, and an alternating number (1–1–2) of THF ligands are coordinated to the array of metal ions.

In $[(THF)_2Eu(\mu\text{-}SC_6F_5)_2]_\infty$ [67], each Eu ion is connected to adjacent Eu atoms by a pair of thiolates, forming a linear chain extended along the *b*-axis (Fig. 24). The Eu atom is eight-coordinated with four μ-S atoms and two F atoms from SC_6F_5 ligands and two O atoms from THF molecules. The Eu–μ-S bond distance of 3.025(3) Å is comparable to those observed in $[(THF)_3Eu(SC_6H_2Pr^i_3\text{-}2,4,6)(\mu\text{-}SC_6H_2Pr^i_3\text{-}2,4,6)]_2$ (3.016(3) Å) [56].

In $[(THF)_3Sm(\mu\text{-}SePh)_3Zn(\mu\text{-}SePh)]_\infty$ [63], the $[Sm(THF)_3]^{2+}$ fragment is interconnected by Zn^{2+} alternatively via an alternating number (1 and 3) of doubly bridging SePh ligands, generating an one-dimensional chain structure extended along *b*-axis (Fig. 25). The tetrahedral Zn coordination sphere is comprised entirely of Se atoms, while the larger seven-coordinate Sm(II) ion is coordinated by four Se(Ph) and three additional THF ligands. The structure of the polymer differs from that of the analogous Eu derivative $(THF)_4Eu(\mu\text{-}SePh)_3Zn(SePh)$ [74], which crystallized as a discrete molecule. The difference between them may be due to the fact that the larger Sm(II) ion may increase the tendency of chalcogenolate ligands to bridge Ln ions. The polymer has three nearly equal Sm–Se bonds (Sm–Se(1), 3.192(1) Å; Sm–Se(3),

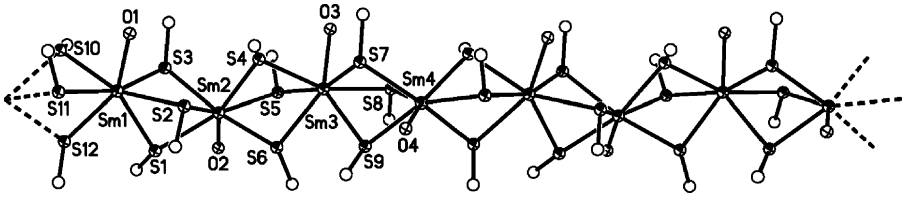

Fig. 23. Extended structure of $\{[(THF)Sm(SPh)_3]_4\}_\infty$. All H and C atoms except for those bound to S atoms are removed for clarity [65].

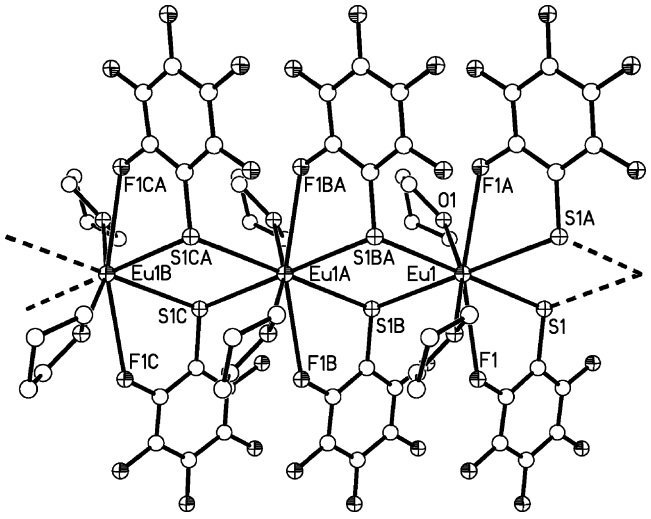

Fig. 24. Extended structure of $[(THF)_2Eu(\mu\text{-}SC_6F_5)_2]_\infty$ looking along the *b*-axis. All H atoms are omitted for clarity [67].

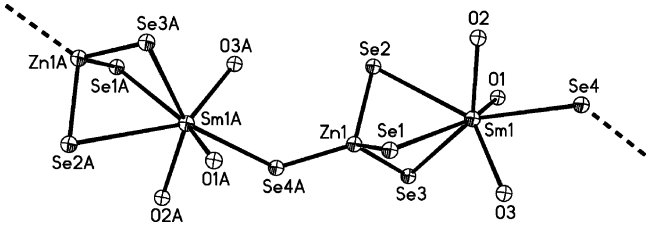

Fig. 25. Perspective view of the repeating unit of $[(THF)_3Sm(\mu_2\text{-}SePh)_3Zn(SePh)]_\infty$, with the thermal ellipsoids drawn at the 50% probability level. All C and H atoms omitted for clarity [63].

3.190(1) Å; Sm–Se(4), 3.201(1) Å) and a fourth longer bond (Sm–Se(2), 3.447(1) Å), which may be due to significant steric interactions. A similar inequivalence in bond length was found in $(THF)_4Eu(\mu\text{-}SePh)_3Zn(SePh)$, although differences in the Eu–Se bond lengths (3.162(1) Å, 3.176(1) Å, 3.282(1) Å) are less pronounced.

In $[(C_5Me_5)Sm(SC_6H_2Pr^i{}_3\text{-}2,4,6)(\mu\text{-}C_5Me_5)K(THF)]_\infty$ [31], a polymeric chain structure results from the intermolecular interactions between the K atom and a C_5Me_5 ligand extended along *a*-axis (Fig. 26). Each Sm atom is coordinated by two $\eta^5\text{-}C_5Me_5$, one S atom and one O atom, and the coordination number of Sm atom is eight. The Sm–S bond distance is 2.936(3) Å.

Complex $[\{(Me_3Si)_2N\}_2Pr(\mu\text{-}SPh)_2Li(THF)_2]_\infty$ [36] has an interesting 1D wave-like chain structure in which the two $\{(Me_3Si)_2N\}_2Pr^+$ and $Li(THF)_2{}^+$ units are alternatively bridged by SPh groups along the crystallographic *a*-axis (Fig. 27). In the structure, each Pr atom is tetrahedrally coordinated by two S and two N atoms while Li ions also show a normal tetrahedral coordination geometry with two μ-SPh and two THF molecules. The La analogue was found to be isostructural [165].

Compound $[Na_2(18\text{-crown-}6)Na(py)_2Ce(dddt)_3(py)]_\infty$ (dddt = 5,6-dihydro-1,4-dithiine-2,3-dithiolate) [129] possesses an interesting zigzag one-dimensional chain, in which "NaCe(dddt)$_3$(py)" units are alternatively connected by 18-crown-6 ligand. The cerium atom is bound to six sulfur atoms of the three dddt ligands and one N atom from pyridine molecule, exhibiting capped octahedral coordination geometry. The average Ce–μ-S bond length of 2.92(2) Å is slightly longer than that observed in $[(C_5H_4Bu^t)_2Ce(\mu\text{-}SPr^i)]_2$ (2.882 Å). The mean value of the chelate bite angle S–Ce–S of 68.9(3)°, is comparable to those in $[Ln\{(\mu\text{-}SBu^t)_2Li(TMEDA)\}_3]$ (Ln = Sm (70.1°), Yb (70.90°) [109].

Compound $[\{Na(18\text{-crown-}6)(py)_2\}_{0.5}\{Na(18\text{-crown-}6)(py)_{1.5}\}\{Na_{1.5}Nd(dddt)_3\}]_\infty$ (dddt = 5,6-dihydro-1,4-dithiine-2,3-dithiolate) contains infinite anionic 2D layers in which the "Nd(dddt)$_3$" units are linked to three neighbours by Na atoms in a hexagonal network (Fig. 29). The Nd atom is six-coordinated by six sulfur atoms of the three dddt ligands. The resulting NdS_6 octahedron is severely distorted. The bidentate attachment of the dddt ligands Nd is asymmetric with three short and three long Nd–μ-S bonds, and therefore the coordination geometry of Nd is different from that of the homoleptic thiolate complexes $[Ln\{(\mu\text{-}SBu^t)_2Li(TMEDA)\}_3]$

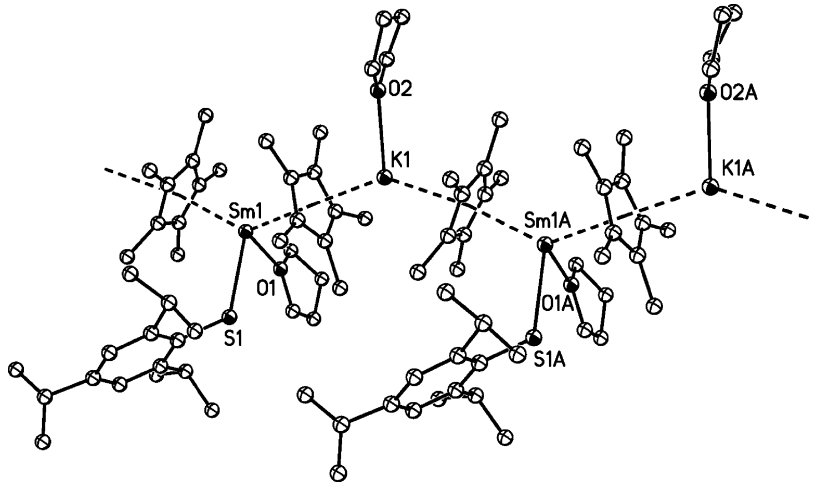

Fig. 26. Perspective view of a section of the polymeric chain of $[(C_5Me_5)Sm(SC_6H_2Pr^i{}_3\text{-}2,4,6)(\mu\text{-}C_5Me_5)K(THF)]_\infty$ with labeling scheme and 30% probability. All hydrogen atoms are omitted for clarity [36].

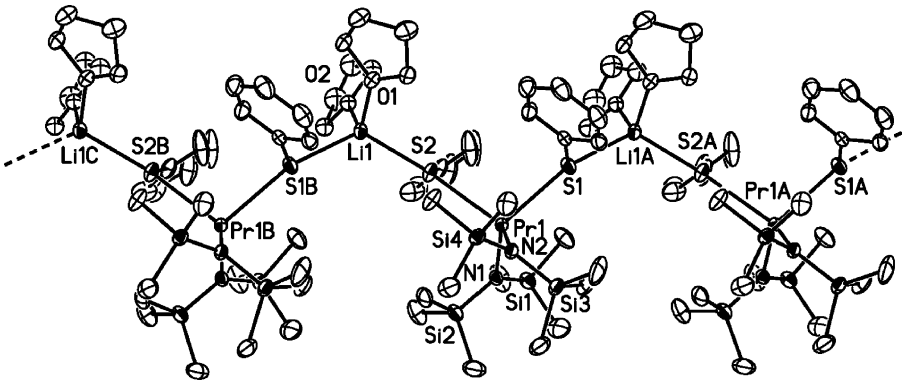

Fig. 27. Perspective view of a section of the polymeric chain of $[\{(Me_3Si)_2N\}_2Pr(\mu\text{-}SPh)_2Li(THF)_2]_\infty$ with labeling scheme and 50% probability. All hydrogen atoms are omitted for clarity [36].

(Ln = Sm, Yb) [109], which adopt an octahedral configuration. The structure of the anionic fragment in this compound is shown in Fig. 28. The Nd–μ-S of 2.856(2) Å is slightly shorter than that observed in $Li[\{(Me_3Si)_2N\}_4(\mu_4\text{-}Cl)Nd_4(\mu\text{-}SPh)_8]$ (2.921(2) Å) [36].

Compound $[\{Na_3(18\text{-crown-}6)_{1.5}Nd(dddt)_3(THF)\}]_\infty$ contains an anionic 2D polymer formed by linking $\{Na_3Nd(dddt)_3(THF)\}$ units with 18-crown-6 bridges. The structure of the polymer $[K_3(18\text{-crown-}6)_{1.5}Nd(dddt)_3(py)]_\infty$ is identical to that of $[\{Na_3(18\text{-crown-}6)_{1.5}Nd(dddt)_3(THF)\}]_\infty$, the THF molecules having been replaced with pyridine molecules and the Na atoms with K atoms. The central Nd is seven-coordinate in the two compounds with six sulfur atoms of the three dddt ligands and one donor O atom. The average Nd–S bond distances are 2.886(13) and 2.90(1) Å, respectively.

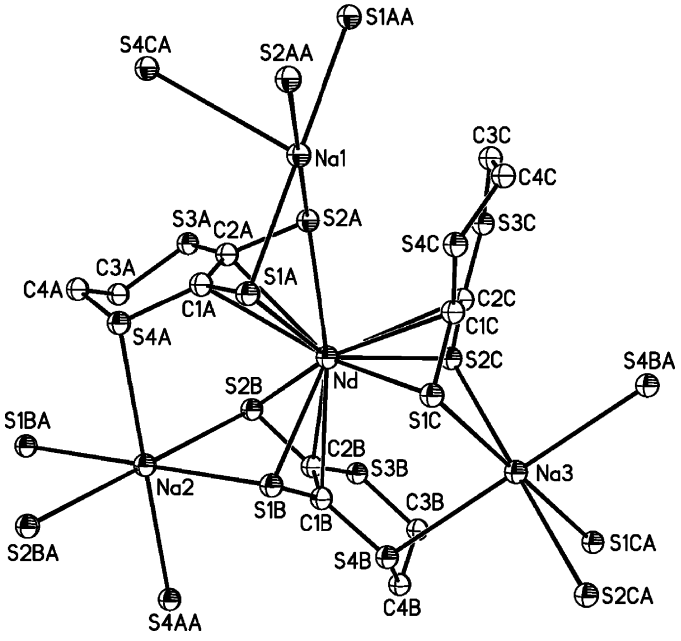

Fig. 28. View of the anionic fragment in $[\{Na(18\text{-crown-}6)(py)_2\}_{0.5}\{Na(18\text{-crown-}6)(py)_{1.5}\}\{Na_{1.5}Nd(dddt)_3\}]_\infty$ with displacement ellipsoids is drawn at the 50% probability level. All H atoms are omitted for clarity [129].

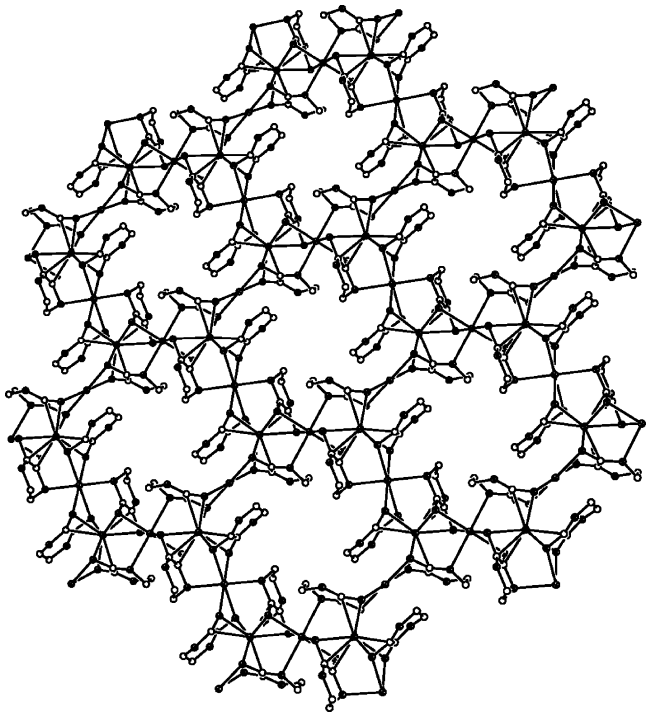

Fig. 29. View of the honeycomb arrangement in compound $[\{Na(18\text{-crown-}6)(py)_2\}_{0.5}\{Na(18\text{-crown-}6)(py)_{1.5}\}\{Na_{1.5}Nd(dddt)_3\}]_\infty$. Counterions and all H atoms have been omitted for clarity [129].

4. Applications of lanthanoid chalcogenolate complexes

Although great effort has been devoted to the synthesis of lanthanide chalcogenolate complexes, their applications are still less explored. In this chapter, we mainly discuss their reactivity and catalytic properties in organic and polymer synthesis. The high electrophilicity and the high Lewis acid character of Ln–ER reagents mostly determine the reactions described here. In other words, because of existence of weak Ln–S bonds, lanthanide thiolate complexes may have unique performance in some chemical reactions (e.g. catalytic reactions) relative to their related precursors. In addition, we briefly describe the very recent development of the luminescent properties of some lanthanide chalcogenolate complexes.

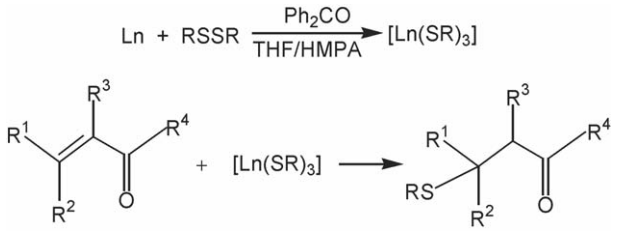

Scheme 25.

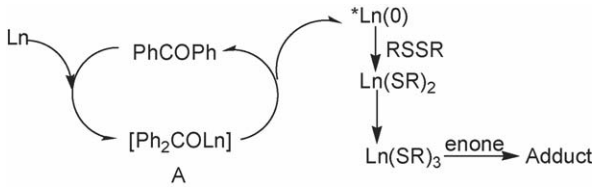

Scheme 26.

4.1. Conjugate addition

Taniguchi et al. found that the reaction of diaryl and -alkyl disulfides with lanthanide metals activated by benzophenone afforded lanthanide(III) thiolate complexes, and that the thiolates thus formed in situ, reacted with enones to give conjugate addition complexes (Scheme 25) [6]. Diaryl disulfides smoothly reacted with lanthanoid metals to produce the corresponding 3-sulfenylcyclohexanones in high yields. The reaction system with dialkyl disulfides gave lower yields. In addition, both cyclic and acyclic enones gave rise to the corresponding adducts. Doubly substituted enones on β-carbon were less reactive and formed the Michael adducts in lower yields due to the steric hindrance. The possible mechanism for the benzophenone-catalyzed reaction of diaryl and -alkyl disulfides with Ln is shown in Scheme 26. Lanthanoid metal reacted with benzophenone to produce the Ln ketyl intermediate (A). The activated lanthanoid metal [Ln(0)] thus formed, would react smoothly with disulfides to yield a divalent lanthanoid thiolate intermediate, which would be further oxidized to a trivalent thiolate complex in the presence of excess disulfides. Thus, the Ln(III) thiolate complex formed served as a sulfenylating reagent. The assignment of the +3 oxidation state of Ln in the thiolate complex was also supported by the fact that no pinacols, but the reduction products, were formed when benzaldehyde, acetophenone and cyclohexanone were treated with the thiolate complex.

4.2. Epoxide opening reaction

As shown in Scheme 27, Yb metal, activated by MeI, can react with diaryl disulfides, diselenides, or di-tellurides, giving Yb(III) chalcogenolate complexes [7]. The resulting complexes were able to transfer arylsulfanyl, -selenanyl, and -telluranyl groups, respectively, to epoxides in a facile ring opening reaction. The cyclic epoxide was opened efficiently to give an anti-β-hydroxy sulfide or selenide in excellent yield. In the case of dialkyl disulfide, a similar reaction with 1,2-epoxybutane afforded the expected sulfide in a lower yield.

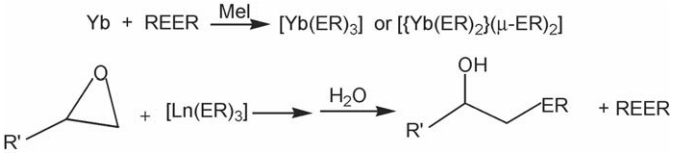

Scheme 27.

4.3. Insertion reaction

Some unsaturated organic molecules could be inserted into a Ln–S bond. For example, insertion of phenyl isocyanate (PhNCO) or phenyl isothiocyanate (PhNCS) into the Ln–S bond of $[(C_5H_4CH_3)_2Nd(\mu\text{-}SPh)(THF)]_2$ generated a bimetallic complex $[(C_5H_4CH_3)_2Nd(\mu\text{-}\eta^2\text{-}OC(SPh)NPh)]_2$ and a monomeric organolanthanide compound $(C_5H_4CH_3)_2Nd[\mu\text{-}\eta^2\text{-}SC(SPh)NPh](THF)$, respectively (Eqs. (55) and (56)) [8]. Insertion of ketene RPhCCO (R = Ph, Et) into the Ln–S σ-bond of $[Cp_2Ln(\mu\text{-}SEt)]_2$ formed the $\mu\text{-}\eta^1\text{:}\eta^2$-thiolate-substituted enolate-bridged complexes $[Cp_2Ln(\mu\text{-}\eta^1\text{:}\eta^2\text{-}OC(SEt)=CPhR)]_2$ (R = Ph, Ln = Yb, Er, Sm, Y; R = Et, Ln = Er) (Eq. (57)) [9]. Treatment of $Cp_2Yb[SC_6H_4(H_2N)\text{-}4](THF)$ with PhNCO gave rise to a simple insertion product $[Cp_2Yb\{\mu\text{-}\eta^1\text{:}\eta^3\text{-}OC(SC_6H_4(H_2N)\text{-}4)NPh\}]_2$ (Eq. (58)), while $[Cp_2Yb(SC_6H_4(H_2N)\text{-}2)]_2$ reacted with PhNCO under the same conditions to form the unexpected complex $[Cp_2Yb(\mu\text{-}\eta^1\text{:}\eta^3\text{-}OSNC_7H_4)]_2$ (Eq. (59)) [10]. CO_2 can be inserted into the Sm–S and Sm–Se bonds of $[(C_5Me_5)_2Sm(\mu\text{-}EPh)]_2$ (E = S, Se) to form the complexes, $[(C_5Me_5)_2Sm(\mu\text{-}O_2CEPh)]_2$ (Eq. (60)). $[(C_5Me_5)_2Sm(\mu\text{-}O_2\text{–}CSePh)]_2$ decarboxylates in THF to form the mononuclear $(C_5Me_5)_2Sm(SePh)(THF)$ (Eq. (60)) [12]:

$$[(C_5H_4CH_3)_2Nd(\mu\text{-}SPh)(THF)]_2 \xrightarrow{2PNCO} [(C_5H_4CH_3)_2Nd(\mu\text{-}\eta^2\text{-}OC(SPh)NPh)]_2 \quad (55)$$

$$[(C_5H_4CH_3)_2Nd(\mu\text{-}SPh)(THF)]_2 \xrightarrow{2PNCS} 2(C_5H_4CH_3)_2Nd(\eta^2\text{-}SC(SPh)NPh)(THF)] \quad (56)$$

$$[Cp_2Ln(\mu\text{-}SEt)]_2 \xrightarrow{PhRC=C=O} [Cp_2Ln(\mu\text{-}\eta^1 : \eta^2\text{-}OC(SEt)=CPhR)]_2$$
$$(R = Ph,\quad Ln = Yb, Er, Sm, Y;\quad R = Et,\quad Ln = Er) \quad (57)$$

$$[Cp_2Yb(SC_6H_4(H_2N)\text{-}4)]_2 + PhNCO \rightarrow \{Cp_2Yb[\mu\text{-}\eta^1\text{: }\eta^3\text{-}OC(SC_6H_4(H_2N)\text{-}4)NPh]\}_2 \quad (58)$$

$$[Cp_2Yb(SC_6H_4(H_2N)\text{-}2)]_2 + PhNCO \rightarrow [Cp_2Yb(\mu\text{-}\eta^1\text{: }\eta^3\text{-}OSNC_7H_4)]_2 \quad (59)$$

$$[(Me_5C_5)_2Sm(\mu\text{-}EPh)]_2 + CO_2 \rightarrow [(Me_5C_5)_2Sm(\mu\text{-}O_2CEPh)]_2 \quad (E = S, Se) \quad (60)$$

$$[(Me_5C_5)_2Sm(\mu\text{-}O_2CEPh)]_2 \xrightarrow{THF} (Me_5C_5)_2Sm(EPh)(THF) \quad (61)$$

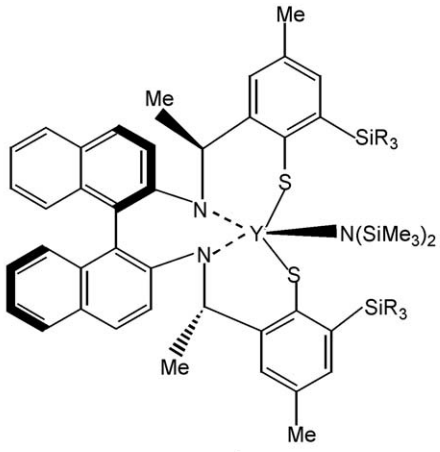

cat.

(R_3 = Me_3, Et_3, Me_2Ph)

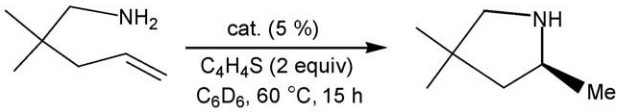

Scheme 28.

4.4. Catalytic enantioselective intramolecular alkene hydroamination reaction

The axially chiral bis(thiolato) complexes of yttrium(III) (Scheme 28) are excellent catalysts for the asymmetric intramolecular hydroamination of representative aminoalkenes, which could provide cyclic amines with ee's ranging from 69 to 89% [25]. The results, coupled with the high activities and diastereoselectivities observed for bis(thiophosphinicamidate) and bis(thioenamide) complexes in aminoalkene cyclizations [28], provided compelling evidence that anionic sulfur-based motifs could serve as superior ligand environments for oxophilic early metals.

4.5. Polymerization of olefin

Lanthanoid benzenethiolate complexes $Ln(SPh)_3(HMPA)_3$ (Ln = Sm, Eu, Yb), $[\{Ln(HMPA)_3\}_2(\mu\text{-}SPh)_3][SPh]$ (Ln = Sm, Yb) and $[Ln(SC_6H_2Pr^i_3\text{-}2,4,6)(\mu\text{-}SC_6H_2Pr^i_3\text{-}2,4,6)(THF)_3]_2$ (Ln = Sm, Yb) [30] catalyze the polymerization of MMA to give syndiotactic polymers, the tacticities (rr up to 82%) of which were comparable to those of PMMA obtained at 0 °C by $(Me_5C_5)_2LnR$ (Ln = Sm, Yb, Lu and Y; R = H, Me) (rr = 82–84%) [166]. Addition of strongly coordinating HMPA/THF ligands changed the stereospecificity of $(py)_3Sm(SC_6H_2Pr^i_3\text{-}2,4,6)_3$ in toluene from isospecific to syndiospecific.

Generally, the stereoregularity of polymers increases with decreasing polymerization temperature. However, these Ln/arenethiolate complexes did not polymerize MMA at −78 °C. Relative to those $(Me_5C_5)_2LnR$ (Ln = Sm, Yb, Lu and Y; R = H, Me), the observed lower activity of these complexes might be attributed to the larger bond disruption enthalpy

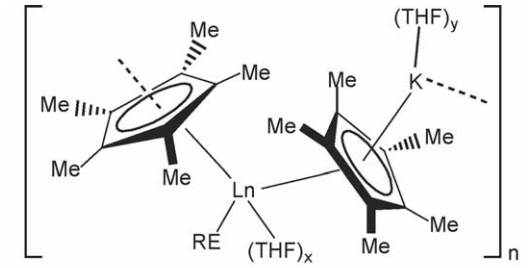

ER = $SC_6H_2Pr^i_3$-2,4,6; $OC_6H_2Bu^t_2$-2,6-Me-4; $N(SiMe_3)_2$

Scheme 29.

of the Sm–S bond [D(Sm–SPr^n) = 73.4 kcal/mol] than that of the Sm–C bond [D(Sm–$CH(SiMe_3)_2$) = 47.0 kcal/mol] [93]. The polymerization of MMA at −78 °C with $Yb(SPh)_3(HMPA)_3$/3MeAl(DBMP)$_2$ afforded PMMA with the highest syndiotacticity (rr = 87%), the highest molecular weight ($M_n = 1.01 \times 10^5$), and the narrowest molecular weight distribution ($M_w/M_n = 1.17$) among the PMMA polymerized by lanthanoid thiolate catalyst systems.

The organosamarium thiolate polymer $[(C_5Me_5)Sm(SC_6H_2Pr^i_3\text{-}2,4,6)(\mu\text{-}C_5Me_5)K(THF)]_n$ (Scheme 29) [31] showed high activity for the polymerization of ethylene at 25 °C under 1 atm, yielding linear polyethylene ($M_w/M_n = 1.79$) with M_n up to 58×10^4. When the polymerization of styrene was carried out at room temperature, a high yield could be achieved within less than 1 h, affording atactic polystyrenes with $M_n = 17.1 \times 10^4$ and $M_w/M_n = 1.45$. This complex also showed good activity and selectivity for copolymerization reactions in the presence of both ethylene and styrene, affording styrene–ethylene copolymers with M_n above 1×10^5 and $1.66 < M_w/M_n < 2.49$. The high selectivity for this copolymerization reaction could reach up to as high as 96%. Among these complexes $[(C_5Me_5)Sm(THF)_x(ER)(\mu\text{-}C_5Me_5)K(THF)_y]_n$, the thiolate ligand $SC_6H_2Pr^i_3$-2,4,6 species showed the highest selectivity for the block copolymerization of styrene and ethylene, while the aryloxide $OC_6H_2Bu^t_2$-2,6-Me-4 derivative and the silylamide $(SiMe_3)_2N$ compound gave the highest activity for the polymerization of ethylene and that of styrene, respectively.

4.6. Homopolymerization of ε-caprolactone or DTC, and copolymerization of DTC with ε-caprolactone

Complexes $[(MeC_5H_4)_2Sm(\mu\text{-}SPh)(THF)]_2$, $Sm(SPh)_3(HMPA)_3$, and $[\{Sm(HMPA)_3\}_2(\mu\text{-}SPh)_3][SPh]$ [35] exhibited high activity for the ring opening polymerization (ROP) of 2,2-dimethyltrimethylene carbonate (DTC) at 60 °C. The molecular weight distributions of poly(DTC) range from 1.52 to 1.95 with $M_n = 3.2 \times 10^4$ to 12.5×10^4. These lanthanide thiolates exhibited the same catalytic activity as lanthanide aryloxides and alkoxides [167–170]. The ^{1}H NMR spectrum for poly(DTC) revealed only two single peaks at 3.94 and 1.00 ppm with the intensity ratio of 2:3 and no peak at 3.1–3.3 ppm was observed, which indicated that CO_2 elimination followed by the formation of ether units did not occur in this polymerization

system. DSC curves of poly(DTC) with two heating cycles indicated that two peaks appeared at the first heating cycle at 87.0 and 120.6 °C, with only one peak at 122.0 °C at the second heating cycle.

Compounds $[(MeC_5H_4)_2Sm(\mu\text{-}SPh)(THF)]_2$ and $[\{Sm(HMPA)_3\}_2(\mu\text{-}SPh)_3][SPh]$ are also efficient initiators for the copolymerization of DTC and ε-caprolactone (ε-CL) to produce copolymer in an almost quantitative yield with relatively broad molecular weight distributions (M_w/M_n = 1.69–2.38) at 60 °C. ^{1}H NMR spectra revealed that the composition of the copolymers is consistent with that of the feed. The GPC profiles of the copolymer showed it to be unimodal, suggesting the presence of only one active center in the growing chain. The ^{1}H NMR spectrum of poly(DTC-*co*-ε-CL) showed four sets of signals at δ 3.75–4.25 ppm, assigned to the hydrogen atoms of the OCH_2 group having four chemical environments. DSC curves of poly(DTC-*co*-ε-CL), poly(DTC), and poly(ε-CL) were recorded, respectively, and only one T_m peak at 49.5 °C was detected in the case of poly(DTC-*co*-ε-CL), while the T_m peak was at 120.6 °C for poly(DTC) and at 63.1 °C for poly(ε-CL), which was also reliable evidence for a random copolymer.

The amidolanthanide thiolate complexes $[\{(Me_3Si)_2N\}_2(\mu\text{-}SPh)Pr(\mu\text{-}SPh)Li(THF)_2]_\infty$, $Li[\{(Me_3Si)_2N\}_4(\mu_4\text{-}Cl)Nd_4(\mu\text{-}SPh)_8]$, and $[\{(Me_3Si)_2N\}_4(\mu_4\text{-}Cl)Sm_4(\mu\text{-}SPh)_4(\mu_3\text{-}Cl)_4Li(THF)]$ [36] and $[\{(TMS)_2N\}_2La(THF)]_2(\mu\text{-}SPh)(\mu\text{-}Cl)]$ $[\{(TMS)_2N\}_2La_5O(SPh)_{10}LiCl_2(THF)_6]$ $[\{(TMS)_2N\}_2(\mu\text{-}SPh)La(\mu\text{-}SPh)Li(THF)_2]_\infty$ [165] initiated the ROP of ε-CL at room temperature to give relatively high molecular weight polymers (M_n > 22000) with narrow molecular weight distributions (M_w/M_n = 1.34–1.63) in high yields. Comparative runs with their precursor and their mono- or di-substituted silylamido complexes of lanthanides [171–174] showed that they initiated faster polymerization and produced poly(ε-CL) with narrower molecular weight distribution. The reason may be ascribed to the clusters [175–177] and the more facile dissociation of SPh^- from the Ln centers.

4.7. Luminescent properties

Recent developments in studies of the optoelectronic properties of the lanthanide chalcogenolate complexes deserve comment. Being extremely air- and moisture- sensitive, the unique optoelectronic properties of lanthanide chalcogenolate complexes have only recently been explored [15,21,87]. For example, the fluorinated thiolate complex $[(DME)_2Er(SC_6F_5)_3]$ showed a 78% quantum yield of emission at 1544 nm. Its high emission intensity was attributed to the absence of high frequency vibrational groups such as C–H and O–H within the Er(III) coordination environment [21]. Very recently Brennan and co-workers reported a set of Ln–Se–M (Ln = Er, Yb, Lu; M = Hg, Cd) clusters $[(py)_8Ln_4M_2Se_2(SePh)_4]$, among which the Er/M compounds were highly emissive materials. The emission lifetimes are 1.41 ms (Er/Cd) and 0.71 ms (Er/Hg), respectively, and the radiative quantum efficiency of the Er/Cd compound was twice as high as that of the Er/Hg compound [87]. In the case of Nd, the oxyselenido cluster $[(THF)_8Nd_8O_2Se_2(SePh)_{16}]$ and the fluorinated thiolate compound $[(DME)_2Nd(SC_6F_5)_3$ were also highly emissive at 1077 and 925 nm, and their emission at 1.83 and 1.35 μm were observed for the first time for a discrete molecular Nd(III) source [15]. These results are important in the rational design of emissive materials with optional performance.

5. Conclusions

The review surveyed different methods for the preparation of the lanthanide chalcogenolate complexes. More than 200 lanthanide chalcogenolate complexes were collected and classified according to the ancillary ligands coordinating to Ln atoms and their Ln nuclearities. The specific structure frameworks were briefly described for different types of lanthanide chalcogenolates. Some lanthanide chalcogenolates could be used as precursors to synthesize organosulfur/selenium/tellurium compounds, organolanthanide compounds, and lanthanide/chalcogenide materials [103–105,117,118]. The weak coordination of a soft basic chalcogen at a hard acidic Ln center might improve the reactivity and catalytic behavior of lanthanide chalcogenolates. Further developments in this area are anticipated to create more efficient catalysts in the polymerization of olefins. In addition, some of lanthanide chalcogenolate clusters have recently been reported to exhibit unique optoelectronic properties [15,21,87]. Such studies are expected to be important and promising topics in the near future.

Acknowledgements

This work was supported by the Distinguished Young Scholar Fund to J.-P. Lang (No. 20525101), the National Natural Science Foundation (No. 20271036), the NSF of Jiangsu Province (No. BK2004205), the State Key Laboratory of Coordination Chemistry, Nanjing University, the Specialized Research Fund for the Doctoral Program of Higher Education (No. 20050285004), and the Key Laboratory of Organic Synthesis of Jiangsu Province (JSK001) in China. The authors highly appreciate the comments from the reviewers and editors.

References

[1] F. Nief, Coord. Chem. Rev. 178–180 (1998) 13.
[2] H. Schumann, K. Herrmann, J. Demtschuk, S.H. Mühle, Z. Anorg. Allg. Chem. 625 (1999) 1107.
[3] J. Magull, A. Mandel, Z. Anorg. Allg. Chem. 620 (1994) 819.
[4] W.J. Evans, M.A. Ansari, J.W. Ziller, S.I. Khan, Organometallics 14 (1995) 3.
[5] A.C. Hillier, S.Y. Liu, A. Sella, M.R.J. Elsegood, Angew. Chem. Int. Ed. 38 (1999) 2745.
[6] Y. Taniguchi, M. Maruo, K. Takaki, Y. Fujiwara, Tetrahedron Lett. 35 (1994) 7789.
[7] J. Dowsland, F. McKerlie, D.J. Procter, Tetrahedron Lett. 41 (2000) 4923.
[8] Q. Shen, H.R. Li, C.S. Yao, Y.M. Yao, L.L. Zhang, K.B. Yu, Organometallics 20 (2001) 3070.
[9] C.M. Zhang, R.T. Liu, X.G. Zhou, Z.X. Chen, L.H. Weng, Y.H. Lin, Organometallics 23 (2004) 3246.
[10] J. Zhang, L.P. Ma, R.F. Cai, L.H. Weng, X.G. Zhou, Organometallics 24 (2005) 738.
[11] J. Gottfriedsen, F.T. Edelmann, Coord. Chem. Rev. 249 (2005) 919.

[12] W.J. Evans, K.A. Miller, J.W. Ziller, Inorg. Chem. 45 (2006) 424.
[13] D.R. Click, B.L. Scott, J.G. Watkin, Chem. Commun. (1999) 633.
[14] D. Jia, W. Jia, D.R. Evans, M.W. Dennis, H. Liu, J. Zhu, W.M. Yen, J. Appl. Phys. 88 (2000) 3402.
[15] S. Banerjee, L. Huebner, M.D. Romanelli, G.A. Kumar, R.E. Riman, T.J. Emge, J.G. Brennan, J. Am. Chem. Soc. 127 (2005) 15900.
[16] D. Pfeiffer, B.J. Ximba, L.M. Liable-Sands, A.L. Rheingold, M.J. Heeg, D.M. Coleman, H.B. Schlegel, T.F. Kuech, C.H. Winter, Inorg. Chem. 38 (1999) 4539.
[17] E. Dowing, L. Hesselink, J. Ralston, R.M. Macfarlane, Science 273 (1986) 1185.
[18] L.S. Griscom, B. Balda, A. Mendioroz, F. Smektala, J. Fernandez, J.L. Adam, J. Non-Cryst. Solids 284 (2001) 268.
[19] G.S. Pomrenke, P.B. Klein, D.W. Langer, Rare Earth Doped Semiconductors: MRS Symposium, vol. 301, Materials Research Society, Pittsburgh, PA, 1993.
[20] A. Goldbach, M.-L. Saboungi, Acc. Chem. Res. 38 (2005) 705.
[21] G.A. Kumar, R.E. Riman, L.A.D. Torres, O.B. Garcia, S. Banerjee, A. Kornienko, J.G. Brennan, Chem. Mater. 17 (2005) 5130.
[22] J.W. Stouwdam, F.C.J.M. Van Veggel, Chem. Phys. Chem. 5 (2004) 743.
[23] T.W. Allen, M.M. Hawkeye, C.J. Haugen, R.G. DeCorby, J.N. McMullin, D. Tonchev, K. Koughia, S.O. Kasap, J. Vac. Sci. Technol. A 22 (2004) 921.
[24] F. Hamano, K. Tanaka, H. Uchiki, Jpn. J. Appl. Phys. 44 (2005) 769.
[25] J.Y. Kim, T. Livinghouse, Org. Lett. 7 (2005) 1737.
[26] S. Arndt, A. Trifonov, T.P. Spaniol, J. Okuda, M. Kitamura, T. Takahashi, J. Organomet. Chem. 647 (2002) 158.
[27] L. Karmazin, M. Mazzanti, J. Pècaut, Chem. Commun. (2002) 654.
[28] Y.K. Kim, T. Livinghouse, Y. Horino, J. Am. Chem. Soc. 125 (2003) 9560.
[29] S.N. Ringelberg, A. Meetsma, B. Hessen, J.H. Teuben, J. Am. Chem. Soc. 121 (1999) 6082.
[30] Y. Nakayama, T. Shibahara, H. Fukumoto, A. Nakamura, K. Mashima, Macromolecules 29 (1996) 8014.
[31] Z.M. Hou, Y.G. Zhang, H. Tezuka, P. Xie, O. Tardif, T. Koizumi, H. Yamazaki, Y. Wakatsuki, J. Am. Chem. Soc. 122 (2000) 10533.
[32] Z.M. Hou, Y. Wakatsuki, J. Alloys Compd. 303–304 (2000) 75.
[33] H. Ma, T.P. Spaniol, J. Okuda, Dalton Trans. (2003) 4770.
[34] P.L. Arnold, L.S. Natrajan, J.J. Hall, S.J. Bird, C. Wilson, J. Organomet. Chem. 647 (2002) 205.
[35] H.R. Li, Y.M. Yao, C.S. Yao, H.T. Sheng, Q. Shen, J. Polym. Sci. Part A Polym. Chem. 43 (2005) 1312.
[36] H.X. Li, Z.G. Ren, Y. Zhang, W.H. Zhang, J.P. Lang, Q. Shen, J. Am. Chem. Soc. 127 (2005) 1122.
[37] A. Recknagel, M. Noltemeyer, D. Stalke, U. Pieper, H.G. Schmidt, F.T. Edelmann, J. Organomet. Chem. 411 (1991) 347.
[38] D.J. Berg, R.A. Andersen, A. Zalkin, Organometallics 7 (1988) 1858.
[39] A. Zalkin, T.J. Henly, R.A. Andersen, Acta Crystallogr. C43 (1987) 233.
[40] M. Weidler, A. Recknagel, F.T. Edelmann, J. Organomet. Chem. 395 (1990) C26.
[41] W.J. Evans, K.A. Miller, D.S. Lee, J.W. Ziller, Inorg. Chem. 44 (2005) 4326.
[42] F.T. Edelmann, M. Rieckhoff, I. Haiduc, I. Silaghi-Dimitrescu, J. Organomet. Chem. 447 (1993) 203.
[43] M. Wedler, M. Noltemeyer, U. Pieper, H.G. Schmidt, D. Stalke, F.T. Edelmann, Angew. Chem. Int. Ed. Engl. 29 (1990) 894.
[44] M. Wedler, A. Recknagel, J.W. Gilje, M. Nottemeyer, F.T. Edelmann, J. Organomet. Chem. 426 (1992) 295.
[45] A.C. Hillier, S.Y. Liu, A. Sella, M.R.J. Elsegood, Inorg. Chem. 39 (2000) 2635.
[46] I. Lopes, A.C. Hillier, S.Y. Liu, Â. Domingos, J. Ascenso, A. Galvão, A. Sella, N. Marques, Inorg. Chem. 40 (2001) 1116.
[47] A.C. Hillier, S.Y. Liu, A. Sella, M.R.J. Elsegood, J. Alloys Compd. 303–304 (2000) 83.
[48] M. Geissinger, J. Magull, Z. Anorg. Allg. Chem. 623 (1997) 755.
[49] H.X. Li, Y. Zhang, Z.G. Ren, M.L. Cheng, J. Wang, J.P. Lang, Chin. J. Chem. 23 (2005) 1499.
[50] D.J. Berg, C.J. Burns, R.A. Andersen, A. Zalkin, Organometallics 8 (1989) 1865.
[51] W.J. Evans, G.W. Rabe, J.W. Ziller, R.J. Doedens, Inorg. Chem. 33 (1994) 2719.
[52] A. Zalkin, D.J. Berg, Acta Crystallogr. C44 (1988) 1488.
[53] W.J. Evans, G.W. Rabe, M.A. Ansari, J.W. Ziller, Angew. Chem. Int. Ed. Engl. 33 (1994) 2110.
[54] W.J. Evans, G.W. Nyce, R.D. Clark, R.J. Doedens, J.W. Ziller, Angew. Chem. Int. Ed. 38 (1999) 1801.
[55] K. Mashima, Y. Nakayama, T. Shibahara, H. Fukumoto, A. Nakamura, Inorg. Chem. 35 (1996) 93.
[56] K. Mashima, Y. Nakayama, H. Fukumoto, N. Kanehisa, Y. Kai, A. Nakamura, J. Chem. Soc. Chem. Commun. (1994) 2523.
[57] K. Mashima, T. Shibahara, Y. Nakayama, A. Nakamura, J. Organomet. Chem. 501 (1995) 263.
[58] K. Mashima, Y. Nakayama, A. Nakamura, N. Kanehisa, Y. Kai, H. Takaya, J. Organomet. Chem. 473 (1994) 85.
[59] K. Mashima, Y. Nakayama, N. Kanehisa, Y. Kai, A. Nakamura, J. Chem. Soc. Chem. Commun. (1993) 1847.
[60] K. Mashima, T. Shibahara, Y. Nakayama, A. Nakamura, J. Organomet. Chem. 559 (1998) 197.
[61] F. Nief, L. Ricard, J. Chem. Soc. Chem. Commun. (1994) 2723.
[62] M. Brewer, D. Khasnis, M. Buretea, M. Berardini, T.J. Emge, J.G. Brennan, Inorg. Chem. 33 (1994) 2743.
[63] D. Freedman, A. Kornienko, T.J. Emge, J.G. Brennan, Inorg. Chem. 39 (2000) 2168.
[64] J. Lee, M. Brewer, M. Berardini, J.G. Brennan, Inorg. Chem. 34 (1995) 3215.
[65] J. Lee, D. Freedman, J.H. Melman, M. Brewer, L. Sun, T.J. Emge, F.H. Long, J.G. Brennan, Inorg. Chem. 37 (1998) 2512.
[66] M. Geissinger, J. Magull, Z. Anorg. Allg. Chem. 621 (1995) 2043.
[67] J.H. Melman, T.J. Emge, J.G. Brennan, Inorg. Chem. 40 (2001) 1078.
[68] J.H. Melman, C. Rohde, T.J. Emge, J.G. Brennan, Inorg. Chem. 41 (2002) 28.
[69] S. Banerjee, T.J. Emge, J.G. Brennan, Inorg. Chem. 43 (2004) 6307.
[70] M. Berardini, J.G. Brennan, Inorg. Chem. 34 (1995) 6179.
[71] M. Berardini, J. Lee, D. Freedman, J. Lee, T.J. Emge, J.G. Brennan, Inorg. Chem. 36 (1997) 5772.
[72] A. Kornienko, D. Freedman, T.J. Emge, J.G. Brennan, Inorg. Chem. 40 (2001) 140.
[73] M. Berardini, T. Emge, J.G. Brennan, J. Am. Chem. Soc. 166 (1994) 6941.
[74] M. Berardini, T.J. Emge, J.G. Brennan, Inorg. Chem. 34 (1995) 5327.
[75] M. Brewer, J. Lee, J.G. Brennan, Inorg. Chem. 34 (1995) 5919.
[76] J. Lee, T.J. Emge, J.G. Brennan, Inorg. Chem. 36 (1997) 5064.
[77] D. Freedman, J.H. Melman, T.J. Emge, J.G. Brennan, Inorg. Chem. 37 (1998) 4162.
[78] M. Fitzgerald, T.J. Emge, J.G. Brennan, Inorg. Chem. 41 (2002) 3528.
[79] A.Y. Kornienko, T.J. Emge, J.G. Brennan, J. Am. Chem. Soc. 123 (2001) 11933.
[80] D. Freedman, T.J. Emge, J.G. Brennan, Inorg. Chem. 41 (2002) 492.
[81] A. Kornienko, L. Huebner, D. Freedman, T.J. Emge, J.G. Brennan, Inorg. Chem. 42 (2003) 8476.
[82] J.H. Melman, T.J. Emge, J.G. Brennan, J. Chem. Soc. Chem. Commun. (1997) 2269.
[83] J.H. Melman, T.J. Emge, J.G. Brennan, Inorg. Chem. 38 (1999) 2117.
[84] D. Freedman, T.J. Emge, J.G. Brennan, Inorg. Chem. 38 (1999) 4400.
[85] D. Freedman, T.J. Emge, J.G. Brennan, J. Am. Chem. Soc. 119 (1997) 11112.
[86] D. Freedman, S. Sayan, T.J. Emge, M. Croft, J.G. Brennan, J. Am. Chem. Soc. 121 (1999) 11713.
[87] A. Kornienko, S. Banerjee, G.A. Kumar, R.E. Riman, T.J. Emge, J.G. Brennan, J. Am. Chem. Soc. 127 (2005) 14008.
[88] H. Schumann, I. Albrecht, E. Hahn, Angew. Chem. Int. Ed. Engl. 24 (1985) 985.

[89] H. Schumann, I. Albrecht, M. Gallagher, E. Hahn, C. Muchmore, J. Pickardt, J. Organomet. Chem. 349 (1988) 103.
[90] S.P. Nolan, D. Stern, T.J. Marks, J. Am. Chem. Soc. 111 (1989) 7844.
[91] Z.Z. Wu, Z.E. Huang, R.F. Cai, X.Z. Zhou, Z. Xu, X.Z. You, X.Y. Huang, J. Organomet. Chem. 506 (1996) 25.
[92] Z.Z. Wu, W.W. Ma, Z.E. Huang, R.F. Cai, Z. Xu, X.Z. You, J. Sun, Polyhedron 15 (1996) 3427.
[93] S.D. Stults, R.A. Andersen, A. Zalkin, Organometallics 9 (1990) 1623.
[94] H.R. Li, Y.M. Yao, Q. Shen, L.H. Weng, Acta Crystallogr. C57 (2001) 887.
[95] P. Poremba, M. Noltemeyer, H.G. Schmidt, F.T. Edelmann, J. Organomet. Chem. 501 (1995) 315.
[96] L.X. Zhang, X.G. Zhou, Z.E. Huang, R.F. Cai, X.Y. Huang, Polyhedron 18 (1999) 1533.
[97] L.X. Zhang, X.G. Zhou, Z.E. Huang, R.F. Cai, L.B. Zhang, D.J. Wu, Chin. J. Struct. Chem. 20 (2001) 40.
[98] C.G. Pernin, J.A. Ibers, Inorg. Chem. 39 (2000) 1222.
[99] C.G. Pernin, J.A. Ibers, Inorg. Chem. 39 (2000) 1216.
[100] K.S. Gharia, M. Singh, S. Mathur, R. Roy, B.S. Sankle, Synth. React. Inorg. Metal Org. Chem. 12 (1982) 337.
[101] H.C. Aspinall, S.A. Cunningham, Inorg. Chem. 37 (1998) 5396.
[102] B. Cetinkaya, P.B. Hitchcock, M.F. Lappert, R.G. Smith, J. Chem. Soc. Chem. Commun. (1992) 932.
[103] D.R. Cary, J. Arnold, Inorg. Chem. 33 (1994) 1791.
[104] D.R. Cary, J. Arnold, J. Am. Chem. Soc. 115 (1993) 2520.
[105] D.R. Cary, G.E. Ball, J. Arnold, J. Am. Chem. Soc. 117 (1995) 3492.
[106] M. Niemeyer, Eur. J. Inorg. Chem. (2001) 1969.
[107] H.C. Aspinall, D.C. Bradley, M.B. Hursthouse, K.D. Sales, N.P.C. Walker, J. Chem. Soc. Chem. Commun. (1985) 1585.
[108] H. Sugiyama, Y. Hayashi, H. Kawaguchi, K. Tatsumi, Inorg. Chem. 37 (1998) 6773.
[109] K. Tatsumi, T. Amemiya, H. Kawaguchi, K. Tani, J. Chem. Soc. Chem. Commun. (1993) 773.
[110] X.Y. Yu, G.X. Jin, N.H. Hu, L.H. Weng, Organomellics 21 (2002) 5540.
[111] X.Y. Yu, G.X. Jin, L.H. Weng, Chin. J. Chem. 20 (2002) 1256.
[112] G.X. Jin, Coord. Chem. Rev. 248 (2004) 587.
[113] I.P. Beletskaya, A.Z. Voskoboynikov, A.K. Shetakova, A.I. Yanovsky, G.K. Fukin, L.N. Zacharov, Y.T. Struchkov, H. Schumann, J. Organomet. Chem. 468 (1994) 121.
[114] S. Kapur, B.L. Kalsotra, R.K. Multani, J. Inorg. Nucl. Chem. 35 (1973) 3966.
[115] S.M. Cendrowski-Guillaume, G.L. Gland, M. Nierlich, M. Ephritikhine, Organometallics 19 (2000) 5654.
[116] N. Froelich, P.B. Hitchcock, J. Hu, M.F. Lappert, J.R. Dilworth, J. Chem. Soc. Dalton Trans. (1996) 1941.
[117] A.R. Strzelecki, C.L. Likar, B.A. Helsel, T. Utz, M.C. Lin, P.A. Bianconi, Inorg. Chem. 33 (1994) 5188.
[118] A.R. Strzelecki, P.A. Timinski, B.A. Helsel, P.A. Bianconi, J. Am. Chem. Soc. 114 (1992) 3159.
[119] M. Berardini, T.J. Emge, J.G. Brennan, J. Chem. Soc. Chem. Commun. (1993) 1537.
[120] M. Berardini, T.J. Emge, J.G. Brennan, J. Am. Chem. Soc. 115 (1993) 8501.
[121] D.V. Khasnis, M. Brewer, J. Lee, T.J. Emge, J.G. Brennan, J. Am. Chem. Soc. 116 (1994) 7129.
[122] H. Gornitzka, F.T. Edelmann, K. Jacob, J. Organomet. Chem. 436 (1992) 325.
[123] R.G. Xiong, J.L. Zuo, X.Z. You, X.Y. Huang, Polyhedron 15 (1996) 3321.
[124] P. Cassoux, L. Valade, H. Kobayashi, A. Kobayashi, R.A. Clark, A.E. Underhill, Coord. Chem. Rev. 110 (1991) 115.
[125] R.M. Olk, B. Olk, W. Dietzsch, R. Kirmse, E. Hoyer, Coord. Chem. Rev. 117 (1992) 99.
[126] Y. Tang, X.M. Gan, M.Y. Tan, X.Q. Zheng, Polyhedron 17 (1998) 429.
[127] C. Baux, C. Daiguebonne, O. Guillou, K. Boubekeur, R. Carlier, L. Sorace, A. Caneschi, J. Alloys Compd. 344 (2002) 114.
[128] M. Roger, L. Belkhiri, P. Thuéry, T. Arliguie, A. Fourmigué, A. Boucekkine, M. Ephritikhine, Organometallics 24 (2005) 4940.
[129] M. Roger, T. Arliguie, P. Thuéry, M. Fourmigué, M. Ephritikhine, Inorg. Chem. 44 (2005) 584.
[130] V. Monga, B.O. Patrick, C. Orvig, Inorg. Chem. 44 (2005) 2666.
[131] Y.R. Li, C.F. Pi, J. Zhang, X.G. Zhou, Z.X. Chen, L.H. Weng, Organometallics 24 (2005) 1982.
[132] W.E. Piers, D.J. Parks, L.R. MacGillivray, M.J. Zaworotko, Organometallics 13 (1994) 4547.
[133] W.E. Piers, L.R. MacGillivray, M. Zaworotko, Organometallics 12 (1993) 4723.
[134] W.E. Piewrs, J. Chem. Soc. Chem. Commun. (1994) 309.
[135] I.P. Beletskaya, A.Z. Voskoboynikov, A.K. Shestakova, H. Schumann, J. Organomet. Chem. 463 (1993) C1.
[136] W.E. Piers, G. Ferguson, J.F. Gallagher, Inorg. Chem. 33 (1994) 3784.
[137] L.K. Knight, W.E. Piers, R. McDonald, Chem. Eur. J. 6 (2000) 4322.
[138] G.X. Jin, Y.X. Cheng, Y.H. Lin, Organometallics 18 (1999) 947.
[139] Y.X. Cheng, G.X. Jin, Qi Shen, Y.H. Lin, J. Organomet. Chem. 631 (2001) 94.
[140] A. Kornienko, T.J. Emge, G.A. Kumar, R.E. Riman, J.G. Brennan, J. Am. Chem. Soc. 127 (2005) 3501.
[141] L. Huebner, A. Kornienko, T.J. Emge, J.G. Brennan, Inorg. Chem. 44 (2005) 5118.
[142] C.G. Pernin, J.A. Ibers, Inorg. Chem. 36 (1997) 3802.
[143] A. Kornienko, J.H. Melman, G. Hall, T.J. Emge, J.G. Brennan, Inorg. Chem. 41 (2002) 121.
[144] J.H. Melman, M. Fitzgerald, D. Freedman, T.J. Emge, J.G. Brennan, J. Am. Chem. Soc. 121 (1999) 10247.
[145] W.E. Piers, D.J.H. Emslie, Coord. Chem. Rev. 233–234 (2002) 131.
[146] F. Edelmann, Coord. Chem. Rev. 137 (1994) 403.
[147] Z.P. Lu, G.P.A. Yap, D.S. Richeson, Organometallics 20 (2001) 706.
[148] G.R. Giesbrecht, G.D. Whitener, J. Arnold, J. Chem. Soc. Dalton Trans. (2001) 923.
[149] S. Bambirra, A. Meetsma, B. Hessen, J.H. Teuben, Organometallics 20 (2001) 782.
[150] Y.J. Luo, Y.M. Yao, Q. Shen, Macromolecules 35 (2002) 8670.
[151] N. Marques, A. Sella, J. Takats, Chem. Rev. 102 (2002) 2137.
[152] K.W. Bagnall, J. Edwards, J.G.H. du Preez, R.F. Warren, J. Chem. Soc. Dalton Trans. (1975) 140.
[153] M.A. Subhan, T. Suzuki, S. Kaizaki, J. Chem. Soc. Dalton Trans. (2001) 492.
[154] I. Santos, N. Marques, New J. Chem. 19 (1995) 551.
[155] X.W. Zhang, G.R. Loppnow, R. McDonald, J. Takats, J. Am. Chem. Soc. 117 (1995) 7828.
[156] L. Bourget-Merle, M.F. Lappert, J.R. Severn, Chem. Rev. 102 (2002) 3031.
[157] O. Eisentein, P.B. Hitchcock, A.V. Khvostov, M.F. Lappert, L. Maron, L. Perrin, A.V. Protchenko, J. Am. Chem. Soc. 125 (2003) 10790.
[158] P.G. Hayes, W.E. Piers, R. McDonald, J. Am. Chem. Soc. 124 (2002) 2132.
[159] F.T. Edelmann, D.M.M. Freckmann, H. Schmann, Chem. Rev. 102 (2002) 1851.
[160] G.B. Deacon, C.M. Forsyth, P.C. Junk, B.W. Skelton, A.H. White, Chem. Eur. J. 5 (1999) 1452.
[161] F.G.N. Cloke, Chem. Soc. Rev. 22 (1993) 17.
[162] G.B. Deacon, Q. Shen, J. Organomet. Chem. 506 (1996) 1.
[163] M.N. Bochkarev, Chem. Rev. 102 (2002) 2089.
[164] M.L. Cheng, J.P. Lang, Unpublished results.
[165] L.H. Li, M.L. Cheng, Z.G. Ren, W.H. Zhang, J.P. Lang, Q. Shen, Inorg. Chem. 45 (2006) 1885.
[166] H. Yasuda, H. Yamamoto, M. Yamashita, K. Yokota, A. Nakamura, S. Miyake, Y. Kai, N. Kanehisa, Macromolecules 26 (1993) 7134.
[167] J. Ling, W.P. Zhu, Z.Q. Shen, Macromolecules 37 (2004) 758.
[168] A.P. Pego, Z.Y. Zhong, P.J. Dijkstra, D.W. Grijpma, J. Feijen, Macromol. Chem. Phys. 204 (2003) 747.
[169] M. Schappacher, T. Fabre, A.F. Mingotaud, A. Soum, Biomaterials 22 (2001) 2849.

[170] V. Onfroy, M. Schappacher, A. Soum, International Symposium on Ionic Polymerization, Paris, France, 1997, p. 246.
[171] W.J. Evans, H. Katsumata, Macromolecules 27 (1994) 2330.
[172] S. Agarwal, M. Karl, S. Anfang, K. Dehnicke, A. Greiner, Polym. Prepr. (Am. Chem. Soc. Div. Polym. Chem.) 39 (1998) 361.
[173] Z.M. Hou, Y. Wakatsuki, Coord. Chem. Rev. 231 (2002) 1.
[174] H.X. Li, Q.F. Xu, J.X. Chen, M.L. Cheng, Y. Zhang, W.H. Zhang, J.P. Lang, Q. Shen, J. Organomet. Chem. 689 (2004) 3438.
[175] W.M. Stevels, M.J.K. Ankoné, P.J. Dijkstra, J. Feijen, Macromol. Chem. Phys. 196 (1995) 1153.
[176] W.M. Stevels, M.J.K. Ankoné, P.J. Dijkstra, J. Feijen, Macromolecules 29 (1996) 8296.
[177] E. Martin, P. Dubois, R. Jérôme, Macromolecules 33 (2000) 1530.